

3.3 10-m Wind Speed Projections

In general, mean 10-m wind speeds are projected to decrease slightly (or show no change) over all regions except the Arctic and the Southern Hemisphere oceans surrounding Antarctica. This general trend is evident for annual (Figures 3.17 and 3.18), DJF (Figures 3.19 and 3.20) and JJA (Figures 3.21 and 3.22) projections. The trend is enhanced for the 2071–2100 period and the higher SSPs (e.g. Figures 3.18c and d). For JJA, small increases in wind speed are evident over extended regions of the Southern Hemisphere oceans (e.g. Figures 3.21 and 3.22).

The mean global annual 10-m wind speed anomalies (relative to 1981–2010) for all five historical simulations (1850–2014) and 20 SSPs (2015–2100) are presented

in Figure 3.23. The bold lines represent the ensemble means. All ensemble members show a small steady decrease in 10-m wind speed from around 2010. Although a small divergence between the SSPs is evident from around 2070, the differences are small. By the end of the century, the global mean 10-m wind speed is projected to decrease by approximately 0.05 m/s (1%), 0.1 m/s (1.5%), 0.15 m/s (2.2%) and 0.2 m/s (3%) for SSP1–2.6, SSP2–4.5, SSP3–7.0 and SSP5–8.5, respectively. It should be noted that, although there is a consistent downwards trend in wind speed on a global scale, the numbers are small, ranging from 1% to 3%. Figure 3.24 shows the standard deviation of each SSP ensemble of climate projections; there is a high level of agreement between ensembles, particularly over land.

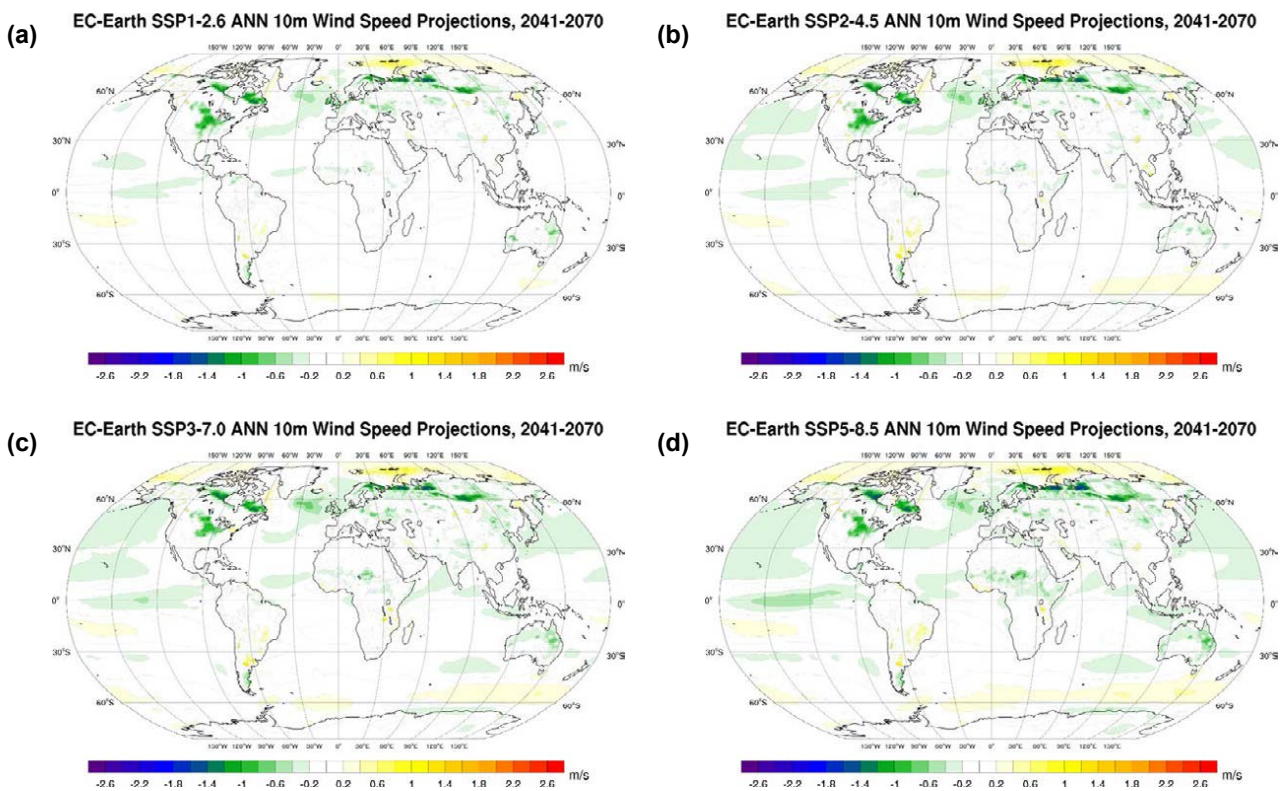


Figure 3.17. EC-Earth annual mean 10-m wind speed projections (2041–2070 vs 1981–2010, m/s difference): (a) SSP1–2.6, (b) SSP2–4.5, (c) SSP3–7.0 and (d) SSP5–8.5. In each case, an average is taken of the ensemble members r6i1p1f1, r9i1p1f1, r11i1p1f1, r13i1p1f1 and r15i1p1f1.

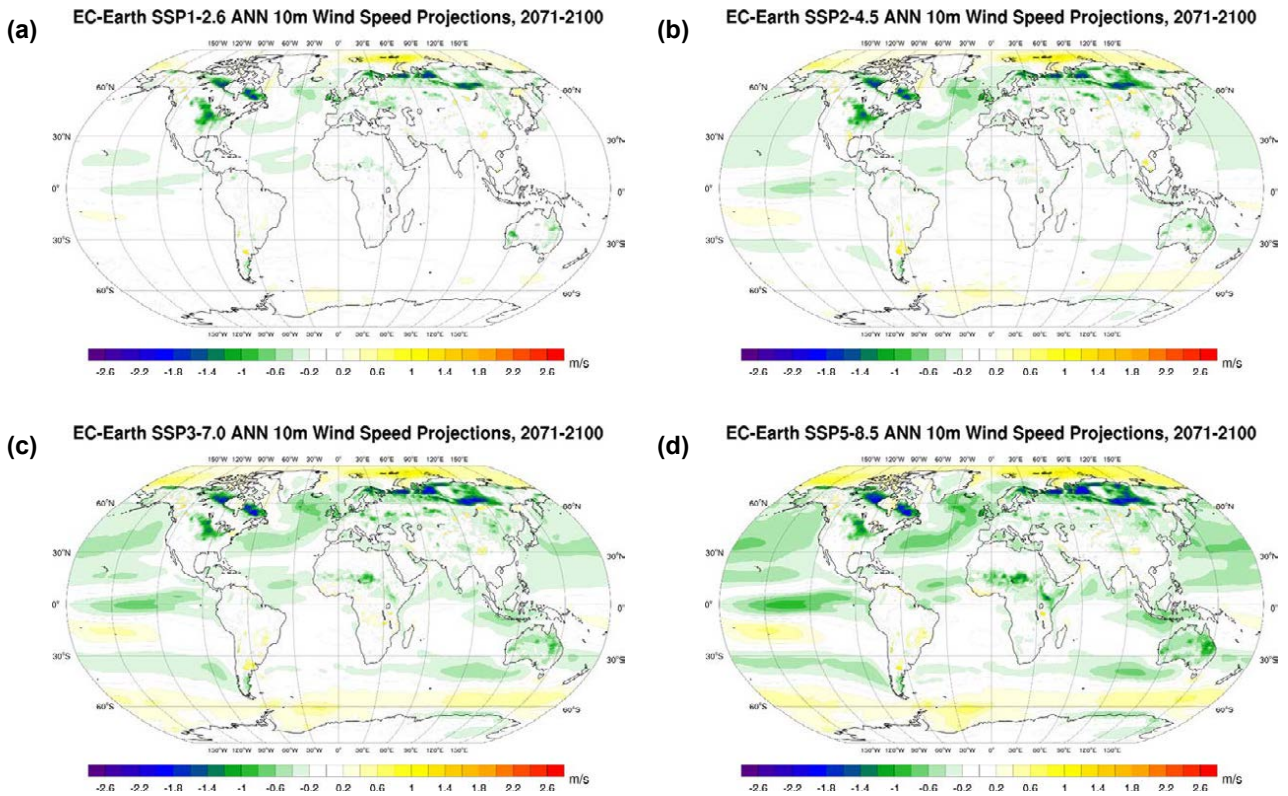


Figure 3.18. EC-Earth annual mean 10-m wind speed projections (2071–2100 vs 1981–2010, m/s difference): (a) SSP1–2.6, (b) SSP2–4.5, (c) SSP3–7.0 and (d) SSP5–8.5. In each case, an average is taken of the ensemble members r6i1p1f1, r9i1p1f1, r11i1p1f1, r13i1p1f1 and r15i1p1f1.

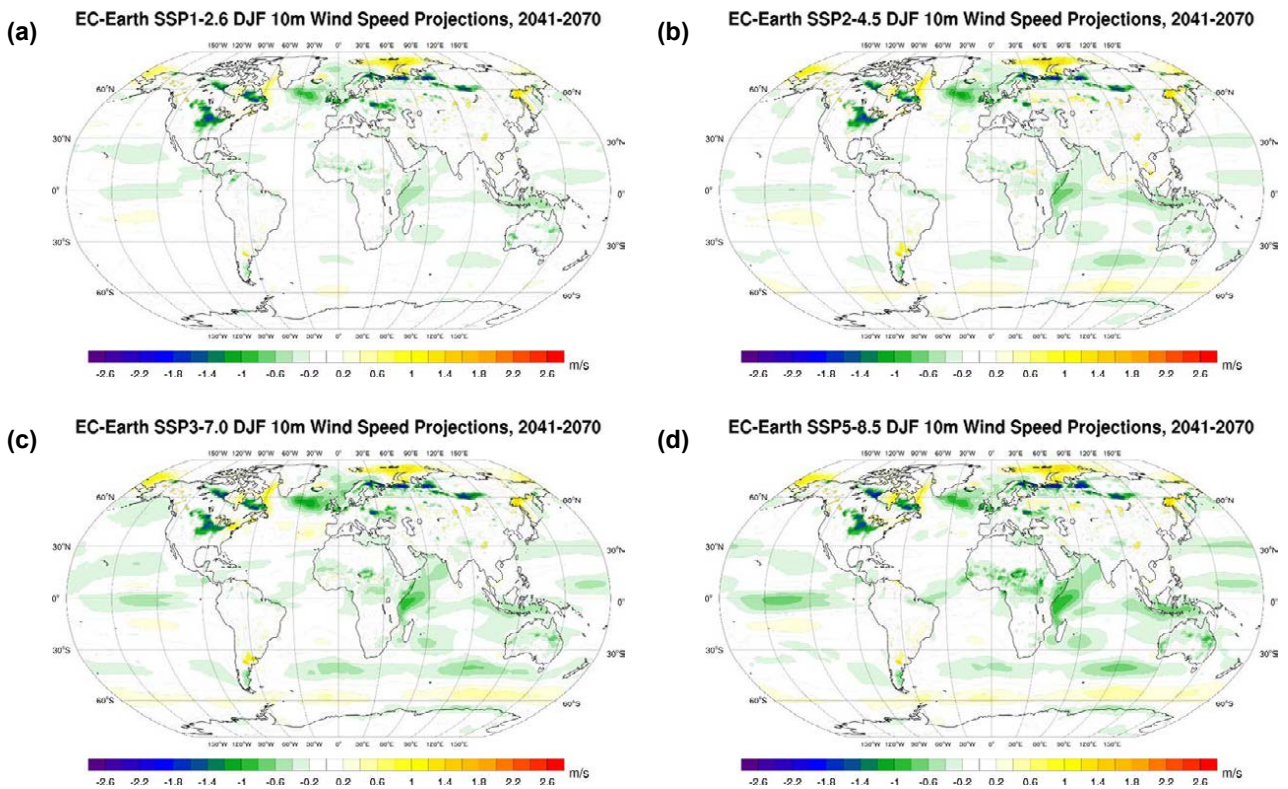


Figure 3.19. EC-Earth DJF mean 10-m wind speed projections (2041–2070 vs 1981–2010, m/s difference): (a) SSP1–2.6, (b) SSP2–4.5, (c) SSP3–7.0 and (d) SSP5–8.5. In each case, an average is taken of the ensemble members r6i1p1f1, r9i1p1f1, r11i1p1f1, r13i1p1f1 and r15i1p1f1.

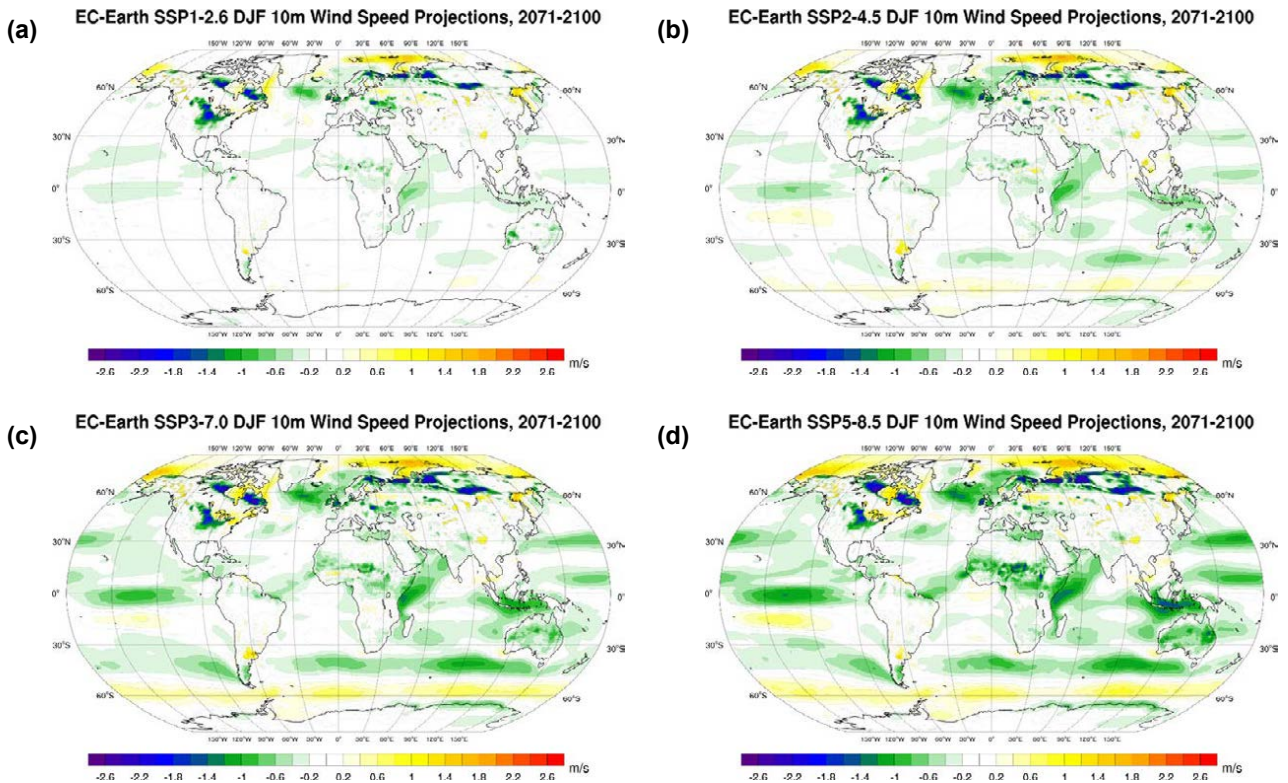


Figure 3.20. EC-Earth DJF mean 10-m wind speed projections (2071–2100 vs 1981–2010, m/s difference): (a) SSP1–2.6, (b) SSP2–4.5, (c) SSP3–7.0 and (d) SSP5–8.5. In each case, an average is taken of the ensemble members r6i1p1f1, r9i1p1f1, r11i1p1f1, r13i1p1f1 and r15i1p1f1.

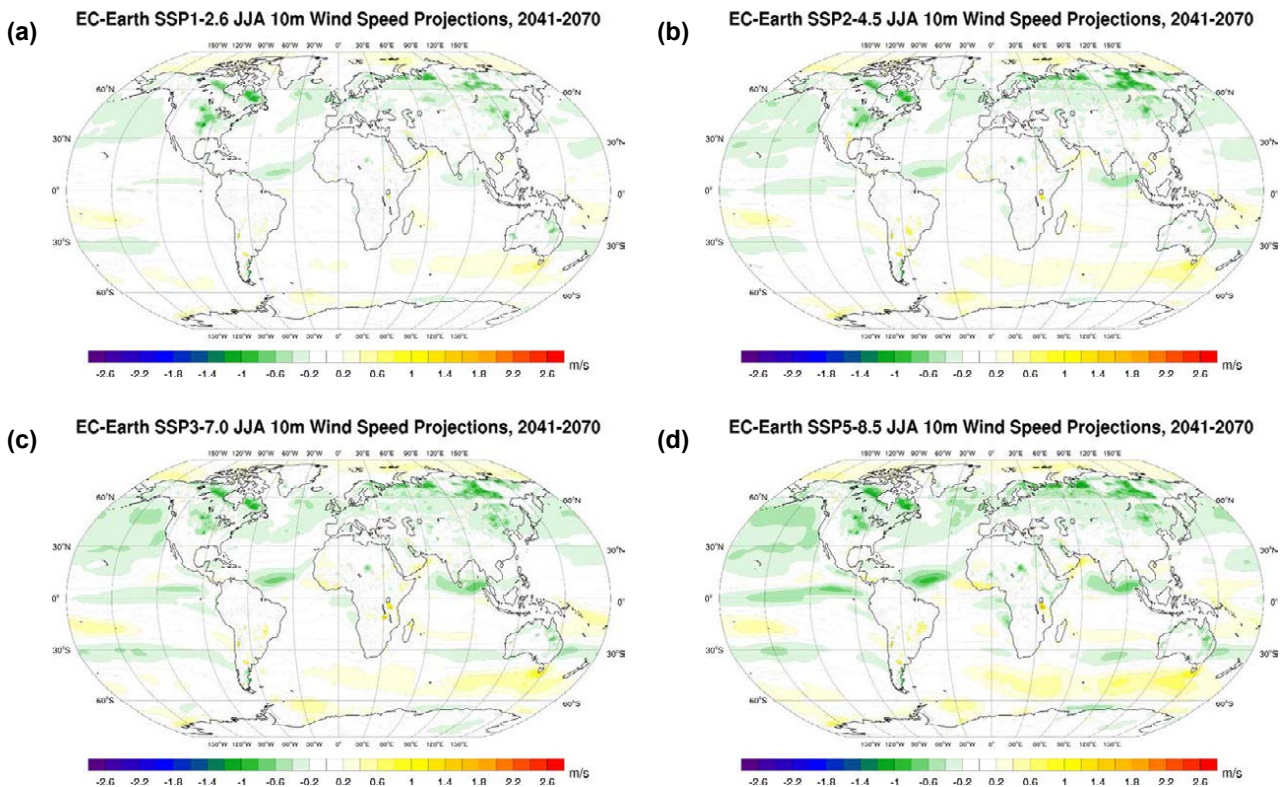


Figure 3.21. EC-Earth JJA mean 10-m wind speed projections (2041–2070 vs 1981–2010, m/s difference): (a) SSP1–2.6, (b) SSP2–4.5, (c) SSP3–7.0 and (d) SSP5–8.5. In each case, an average is taken of the ensemble members r6i1p1f1, r9i1p1f1, r11i1p1f1, r13i1p1f1 and r15i1p1f1.

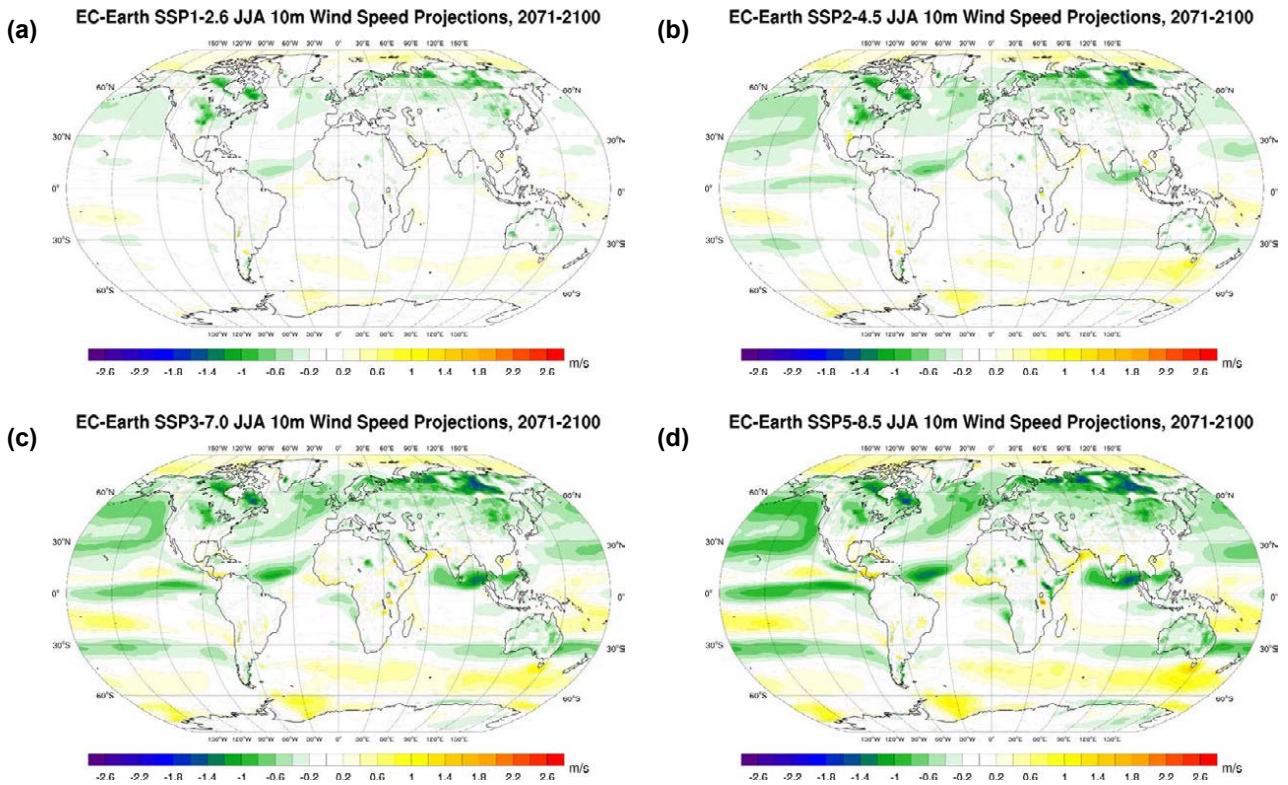


Figure 3.22. EC-Earth JJA mean 10m wind speed projections (2071–2100 vs 1981–2010, m/s difference): (a) SSP1–2.6, (b) SSP2–4.5, (c) SSP3–7.0 and (d) SSP5–8.5. In each case, an average is taken of the ensemble members r6i1p1f1, r9i1p1f1, r11i1p1f1, r13i1p1f1 and r15i1p1f1.

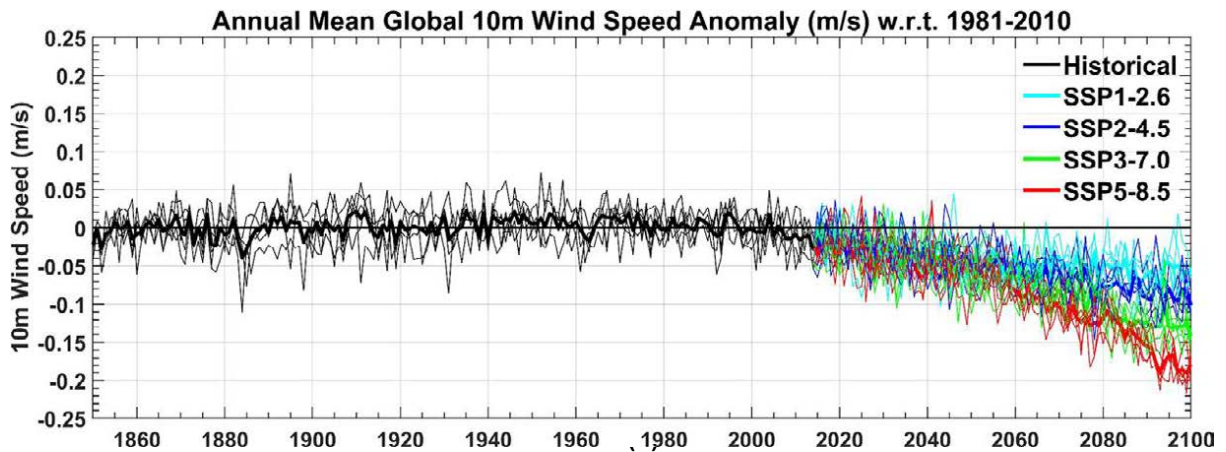


Figure 3.23. Global annual mean 10-m wind speed anomalies with respect to the 30-year period 1981–2010: EC-Earth ensemble members r6i1p1f1, r9i1p1f1, r11i1p1f1, r13i1p1f1 and r15i1p1f1. The bold lines represent the ensemble means.

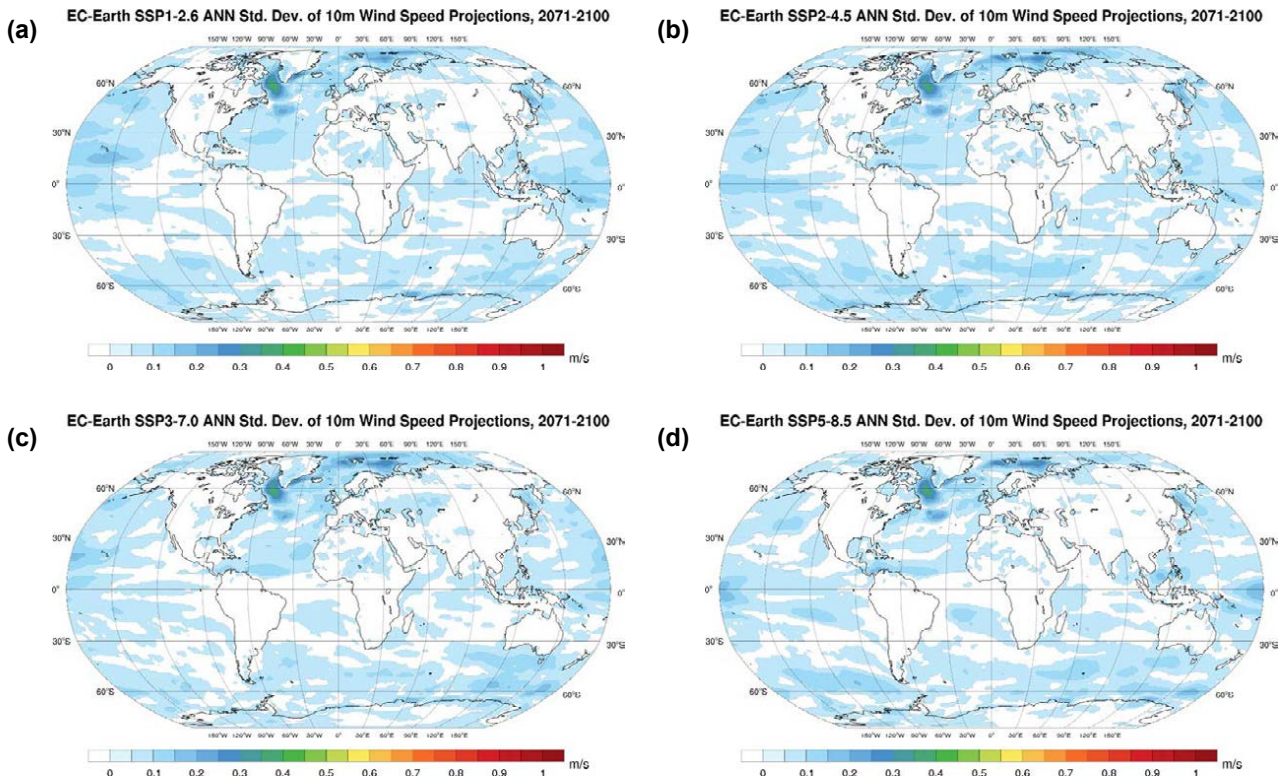


Figure 3.24. Standard deviation of the ensemble of annual mean 10-m wind speed projections (2071–2100): (a) SSP1–2.6, (b) SSP2–4.5, (c) SSP3–7.0 and (d) SSP5–8.5.

3.4 Mean Sea Level Pressure Projections

Figures 3.25 and 3.26 present the spatial distribution of annual projections of MSLP for each of the four SSPs for the 2041–2070 and 2071–2100 periods, respectively. The general trend is for a small increase (or no change) in MSLP in all regions except the Arctic, Antarctic, North African and East European regions. The trend is enhanced for the 2071–2100 period and the higher SSPs (e.g. Figure 3.26c and d).

The MSLP projections for DJF (Figures 3.27 and 3.28) show decreases over Antarctica, North Africa and most of the northern-most latitudes. During DJF, MSLP is projected to decrease (increase) in the North Atlantic Ocean south (north) of Ireland. These results suggest a weakening of both the subpolar low and the subtropical high and a trend towards a more negative North Atlantic Oscillation during future winters. Future work will fully investigate this issue by analysing the full ensemble of CMIP6 simulations. Elsewhere,

increases in MSLP are projected over the majority of the oceans. MSLP projections for JJA (Figures 3.29 and 3.30) follow a similar (but enhanced) trend to the annual projections.

The mean global annual MSLP anomalies (relative to 1981–2010) for all five historical simulations (1850–2014) and 20 SSPs (2015–2100) are presented in Figure 3.31. The bold lines represent the ensemble means. All ensemble members show a steady increase in MSLP from around 2015, with a noticeable divergence between the SSPs around 2060. By the year 2100, the global mean MSLP is projected to increase by approximately 0.15, 0.3, 0.6 and 0.7 hPa for SSP1–2.6, SSP2–4.5, SSP3–7.0 and SSP5–8.5, respectively. The spread between ensemble members is small. This is reflected in Figure 3.32, which shows the standard deviation of each SSP ensemble of climate projections; there is a high level of agreement between ensemble members for all regions except regions in the high latitudes.

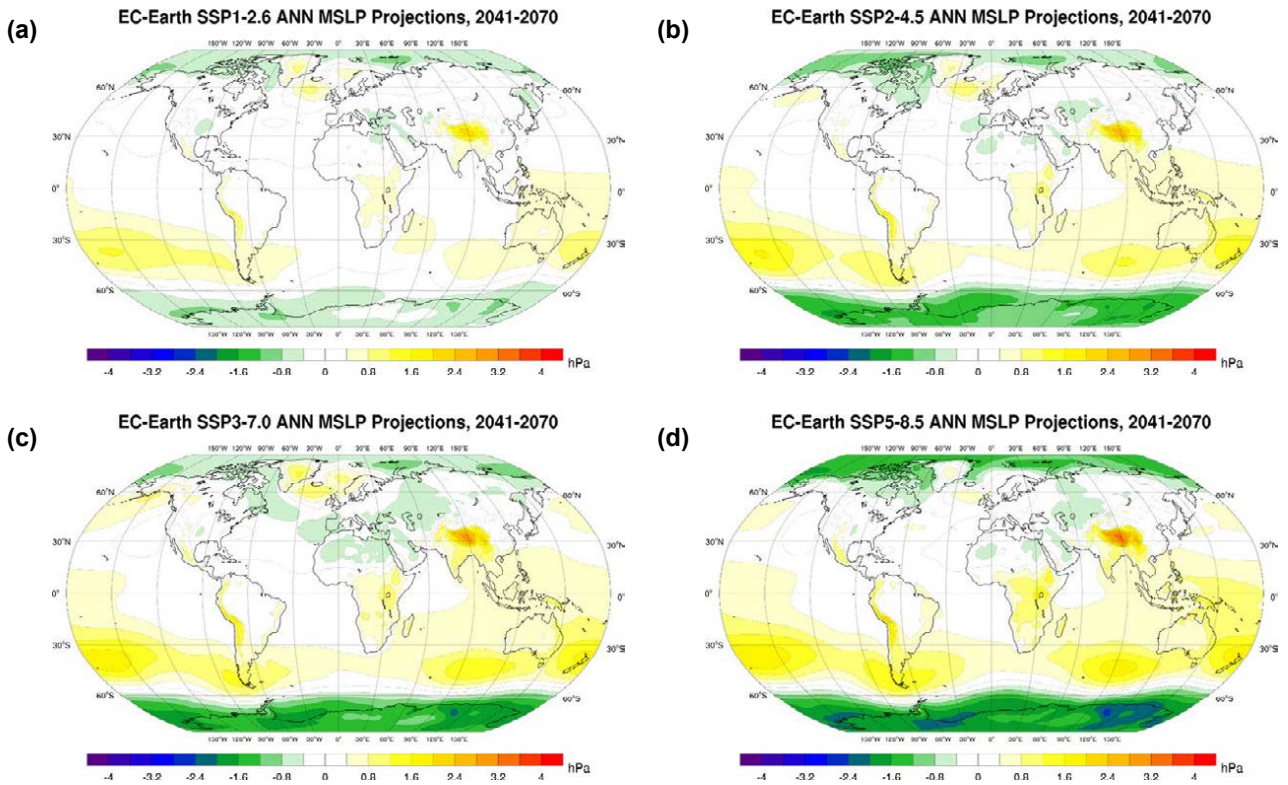


Figure 3.25. EC-Earth annual MSLP projections (2041–2070 vs 1981–2010, hPa difference): (a) SSP1–2.6, (b) SSP2–4.5, (c) SSP3–7.0 and (d) SSP5–8.5. In each case, an average is taken of the ensemble members r6i1p1f1, r9i1p1f1, r11i1p1f1, r13i1p1f1 and r15i1p1f1.

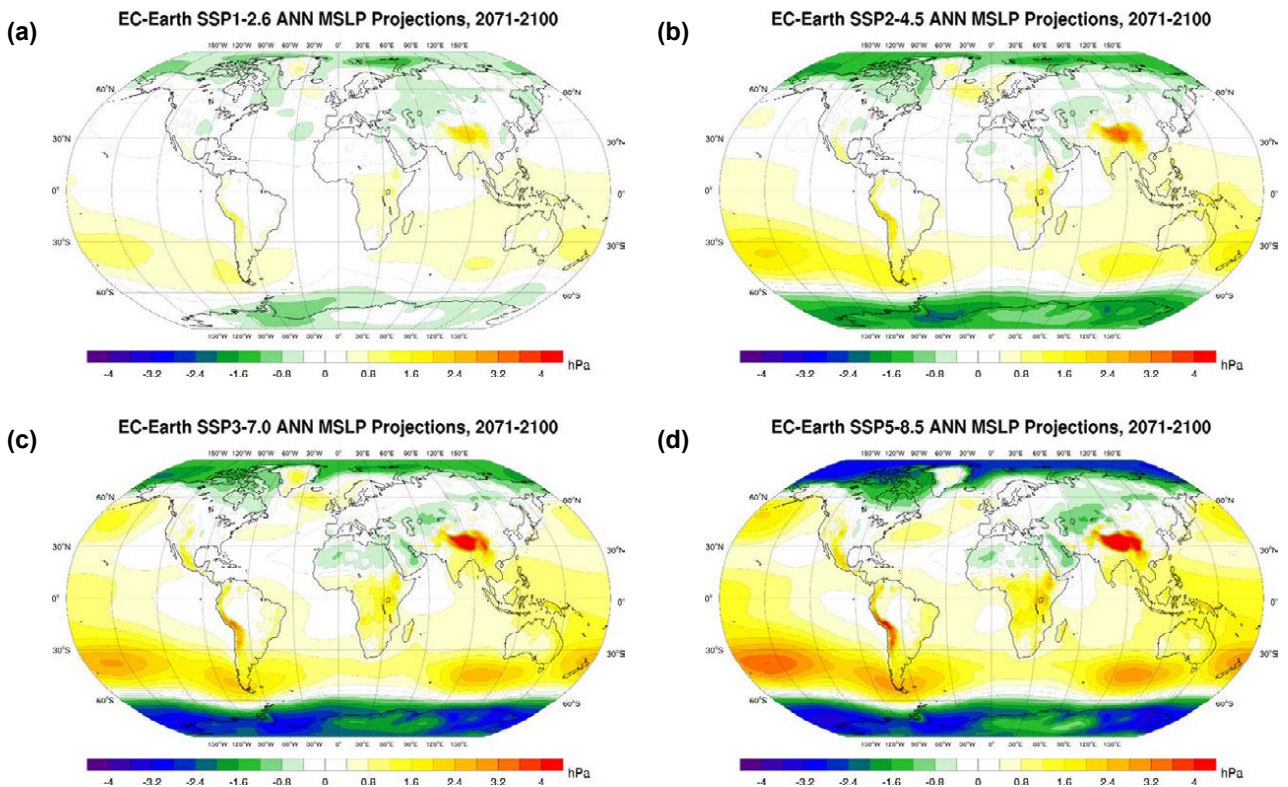


Figure 3.26. EC-Earth annual MSLP projections (2071–2100 vs 1981–2010, hPa difference): (a) SSP1–2.6, (b) SSP2–4.5, (c) SSP3–7.0 and (d) SSP5–8.5. In each case, an average is taken of the ensemble members r6i1p1f1, r9i1p1f1, r11i1p1f1, r13i1p1f1 and r15i1p1f1.

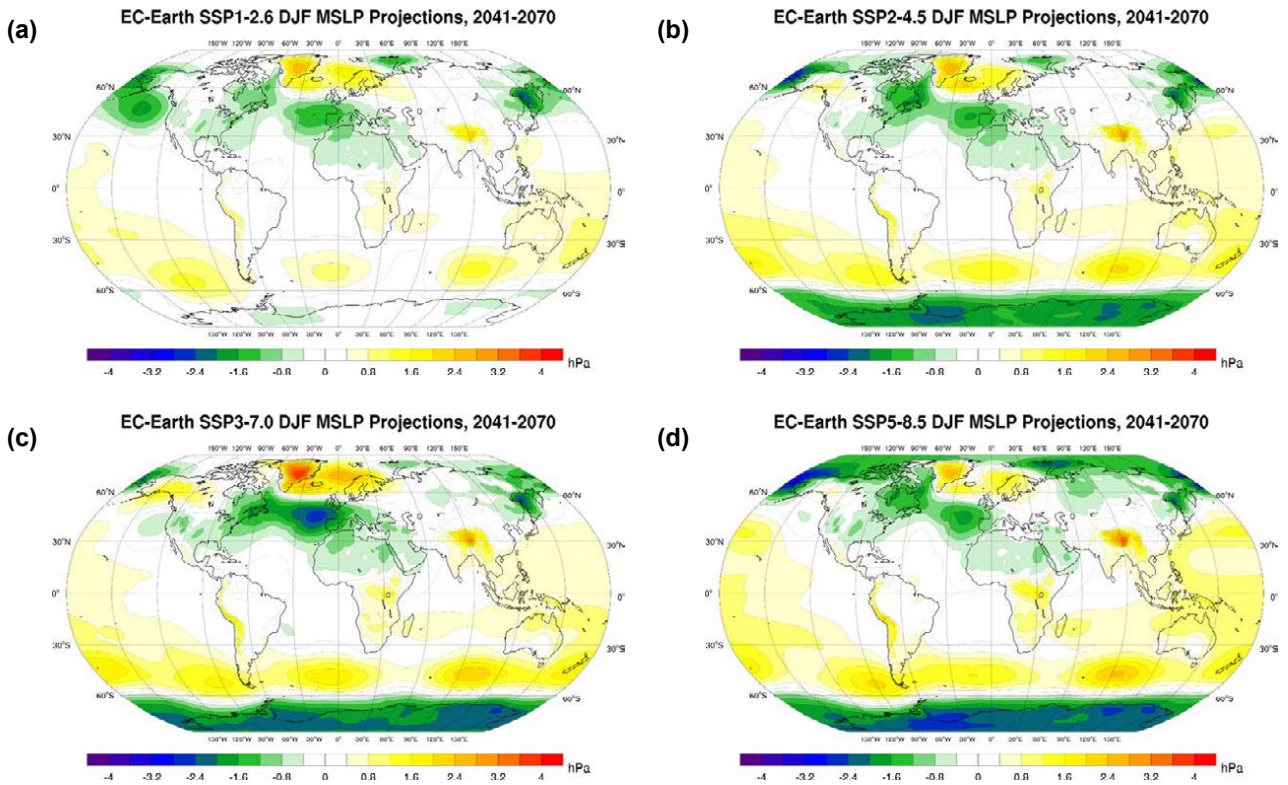


Figure 3.27. EC-Earth DJF MSLP projections (2041–2070 vs 1981–2010, hPa difference): (a) SSP1–2.6, (b) SSP2–4.5, (c) SSP3–7.0 and (d) SSP5–8.5. In each case, an average is taken of the ensemble members r6i1p1f1, r9i1p1f1, r11i1p1f1, r13i1p1f1 and r15i1p1f1.

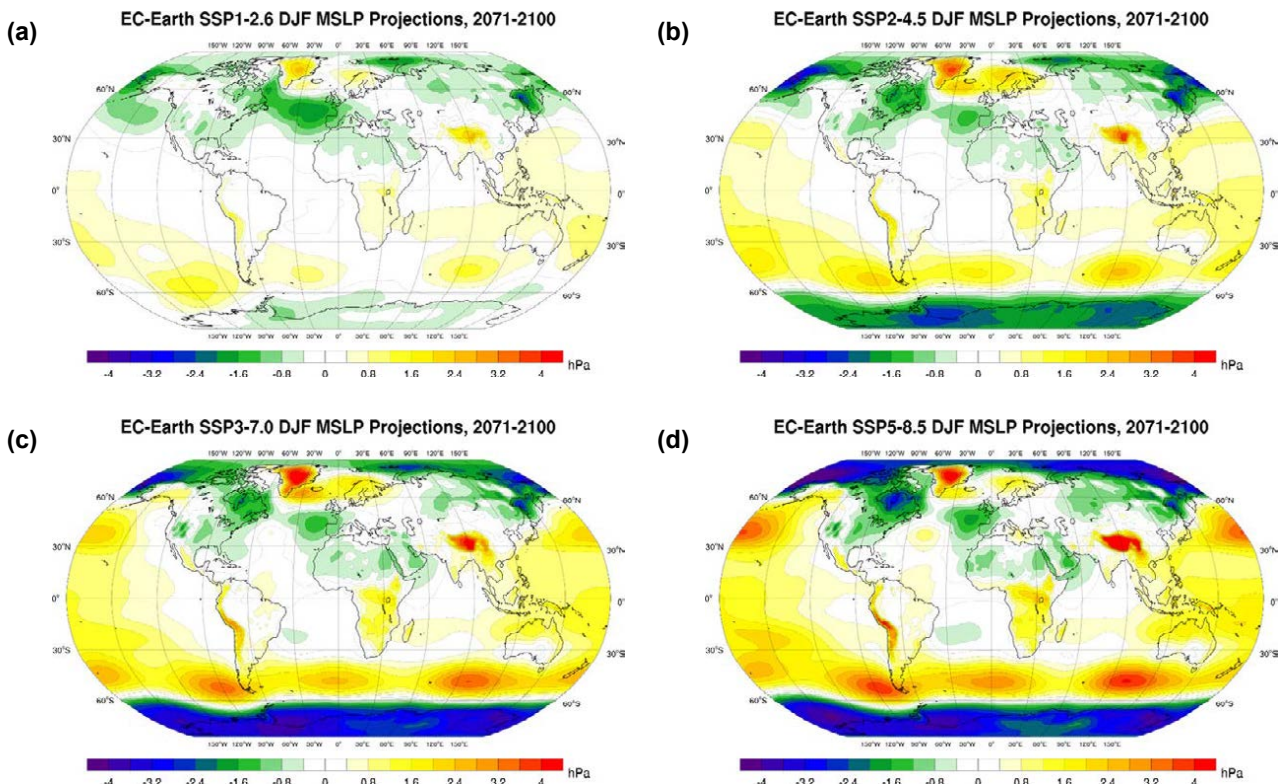


Figure 3.28. EC-Earth DJF MSLP projections (2071–2100 vs 1981–2010, hPa difference): (a) SSP1–2.6, (b) SSP2–4.5, (c) SSP3–7.0 and (d) SSP5–8.5. In each case, an average is taken of the ensemble members r6i1p1f1, r9i1p1f1, r11i1p1f1, r13i1p1f1 and r15i1p1f1.

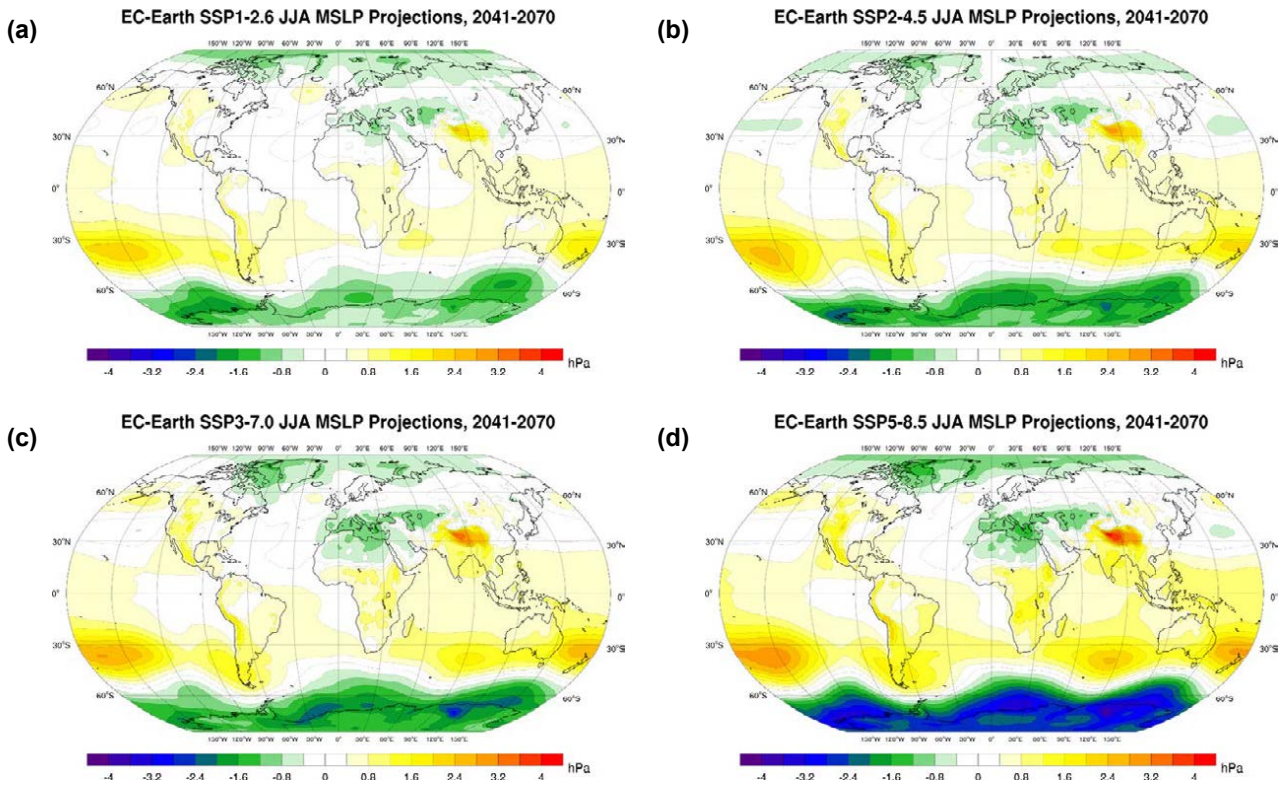


Figure 3.29. EC-Earth JJA MSLP projections (2041–2070 vs 1981–2010, hPa difference): (a) SSP1–2.6, (b) SSP2–4.5, (c) SSP3–7.0 and (d) SSP5–8.5. In each case, an average is taken of the ensemble members r6i1p1f1, r9i1p1f1, r11i1p1f1, r13i1p1f1 and r15i1p1f1.

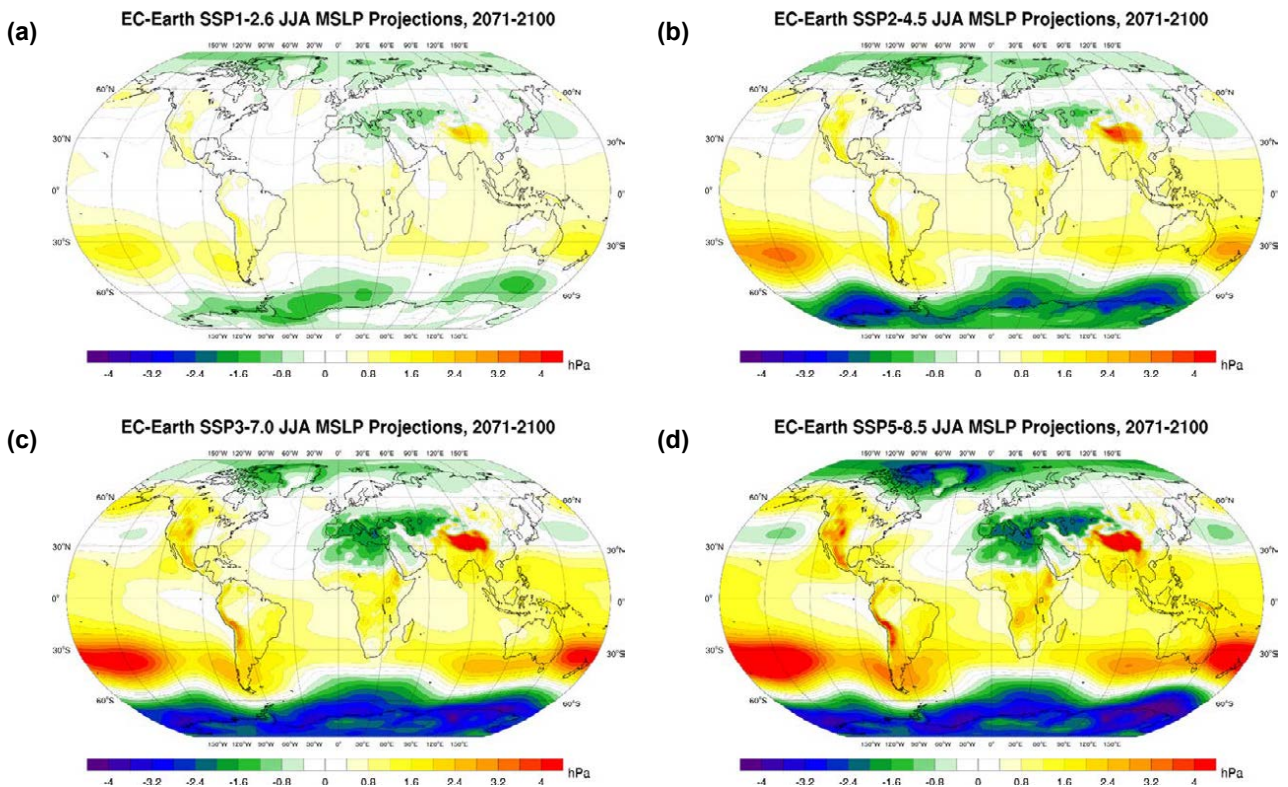


Figure 3.30. EC-Earth JJA MSLP projections (2071–2100 vs 1981–2010, hPa difference): (a) SSP1–2.6, (b) SSP2–4.5, (c) SSP3–7.0 and (d) SSP5–8.5. In each case, an average is taken of the ensemble members r6i1p1f1, r9i1p1f1, r11i1p1f1, r13i1p1f1 and r15i1p1f1.

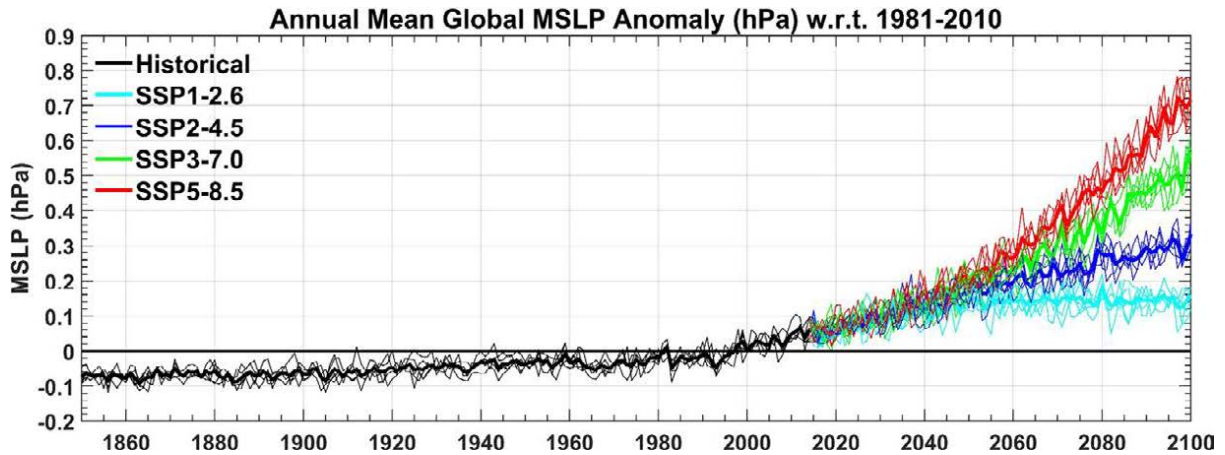


Figure 3.31. Global annual MSLP anomalies with respect to the 30-year period 1981–2010: EC-Earth ensemble members r6i1p1f1, r9i1p1f1, r11i1p1f1, r13i1p1f1 and r15i1p1f1. The bold lines represent the ensemble means.

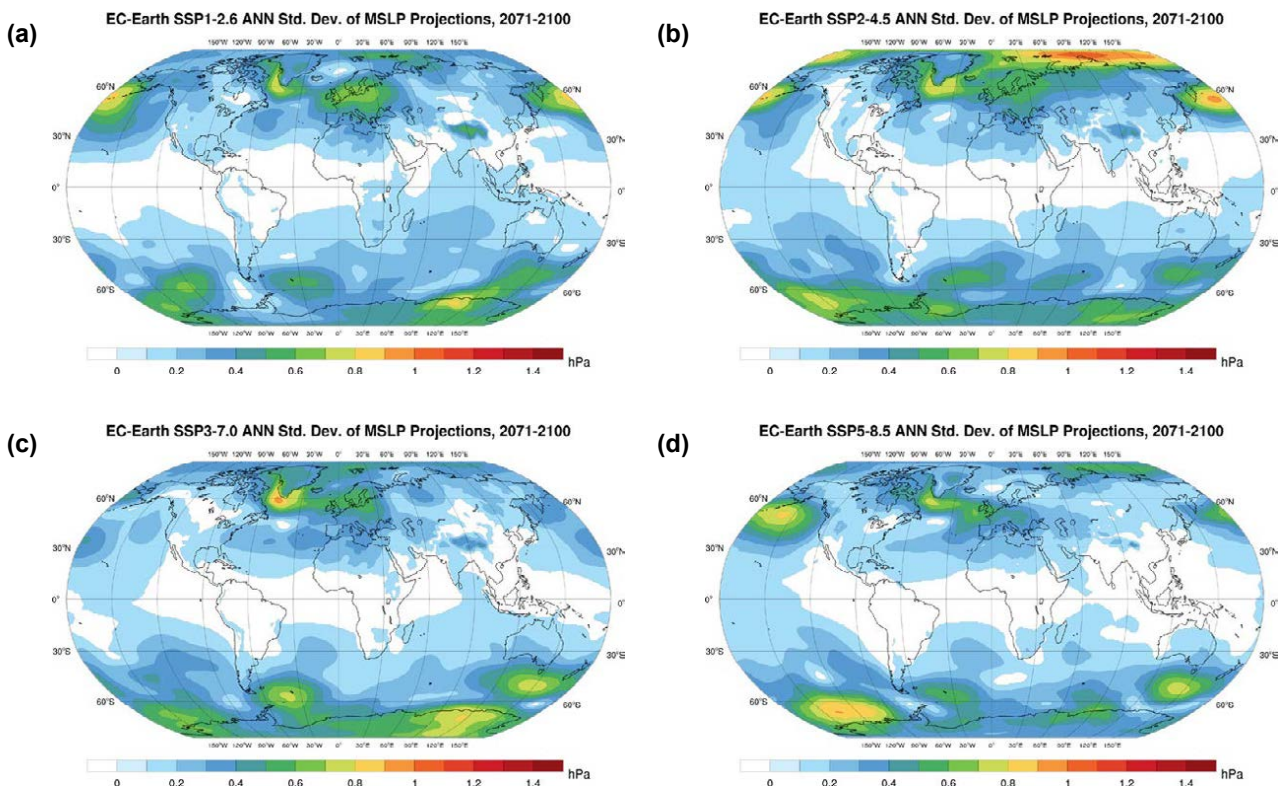


Figure 3.32. Standard deviation of the ensemble of annual MSLP projections (2071–2100): (a) SSP1–2.6, (b) SSP2–4.5, (c) SSP3–7.0 and (d) SSP5–8.5.

3.5 Total Cloud Cover Projections

In general, mean total cloud cover is projected to decrease slightly (or exhibit no change) over all regions except Central Africa, the Arabian Peninsula, India, the eastern equatorial Pacific and the equatorial Atlantic regions, where small increases are projected. This general trend is evident for annual (Figures 3.33

and 3.34) and DJF (Figures 3.35 and 3.36) projections. For DJF, a general small increase is also noted over Eurasia (e.g. Figure 3.36d). For JJA, the trend is similar except that cloud cover is projected to decrease over all of Eurasia and larger decreases are projected over the North Atlantic (Figures 3.37 and 3.38). The trends are enhanced for the 2071–2100 period and the higher SSPs (e.g. Figure 3.38c and d).

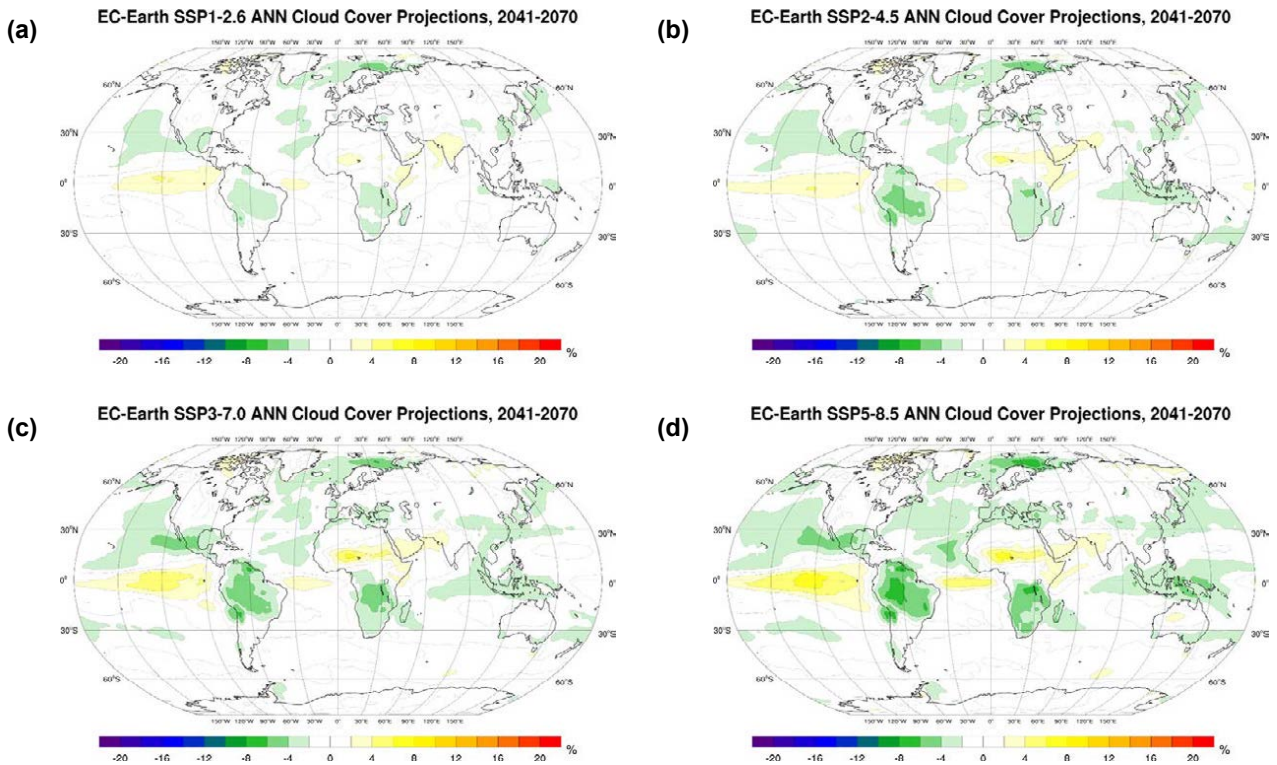


Figure 3.33. EC-Earth annual total cloud cover projections (2041–2070 vs 1981–2010, % difference): (a) SSP1–2.6, (b) SSP2–4.5, (c) SSP3–7.0 and (d) SSP5–8.5. In each case, an average is taken of the ensemble members r6i1p1f1, r9i1p1f1, r11i1p1f1, r13i1p1f1 and r15i1p1f1. The anomalies (%) are calculated as “future (%) minus past (%)” as opposed to a percentage change.

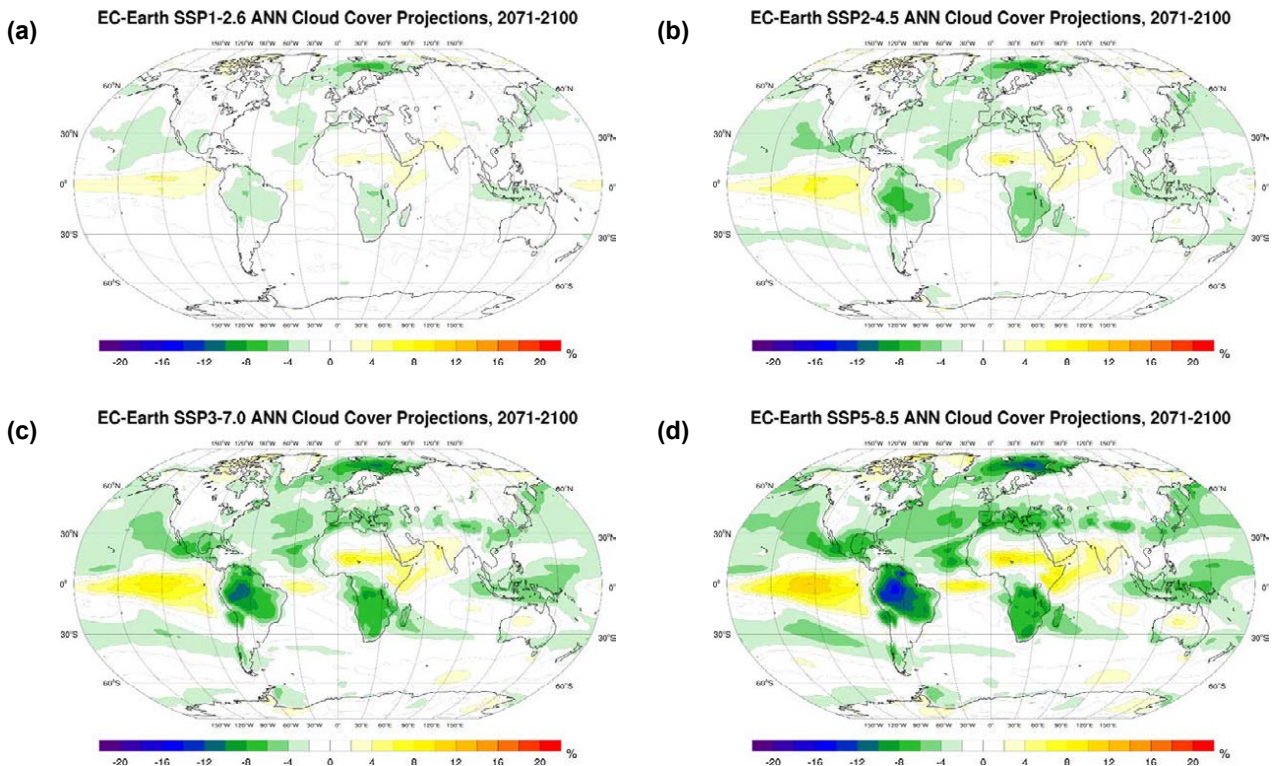


Figure 3.34. EC-Earth annual total cloud cover projections (2071–2100 vs 1981–2010, % difference): (a) SSP1–2.6, (b) SSP2–4.5, (c) SSP3–7.0 and (d) SSP5–8.5. In each case, an average is taken of the ensemble members r6i1p1f1, r9i1p1f1, r11i1p1f1, r13i1p1f1 and r15i1p1f1. The anomalies (%) are calculated as “future (%) minus past (%)” as opposed to a percentage change.

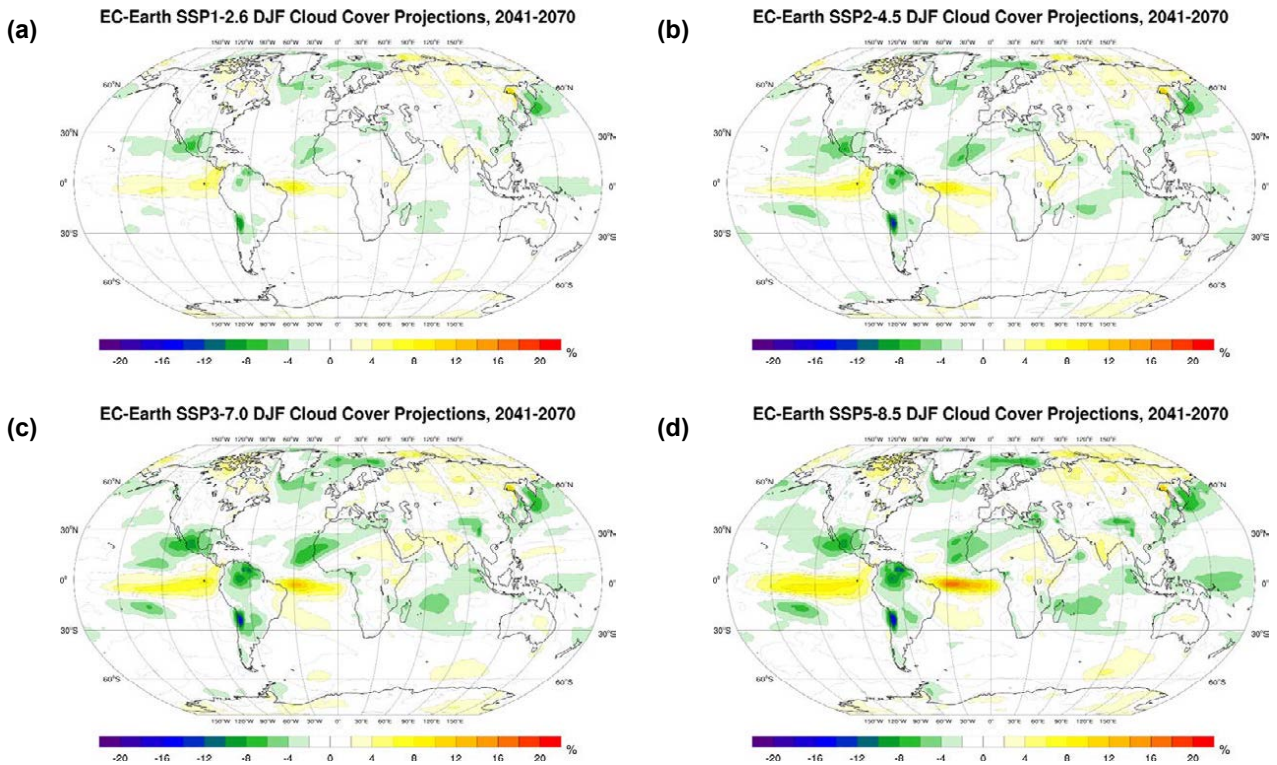


Figure 3.35. EC-Earth DJF total cloud cover projections (2041–2070 vs 1981–2010, % difference): (a) SSP1–2.6, (b) SSP2–4.5, (c) SSP3–7.0 and (d) SSP5–8.5. In each case, an average is taken of the ensemble members r6i1p1f1, r9i1p1f1, r11i1p1f1, r13i1p1f1 and r15i1p1f1. The anomalies (%) are calculated as “future (%) minus past (%)” as opposed to a percentage change.

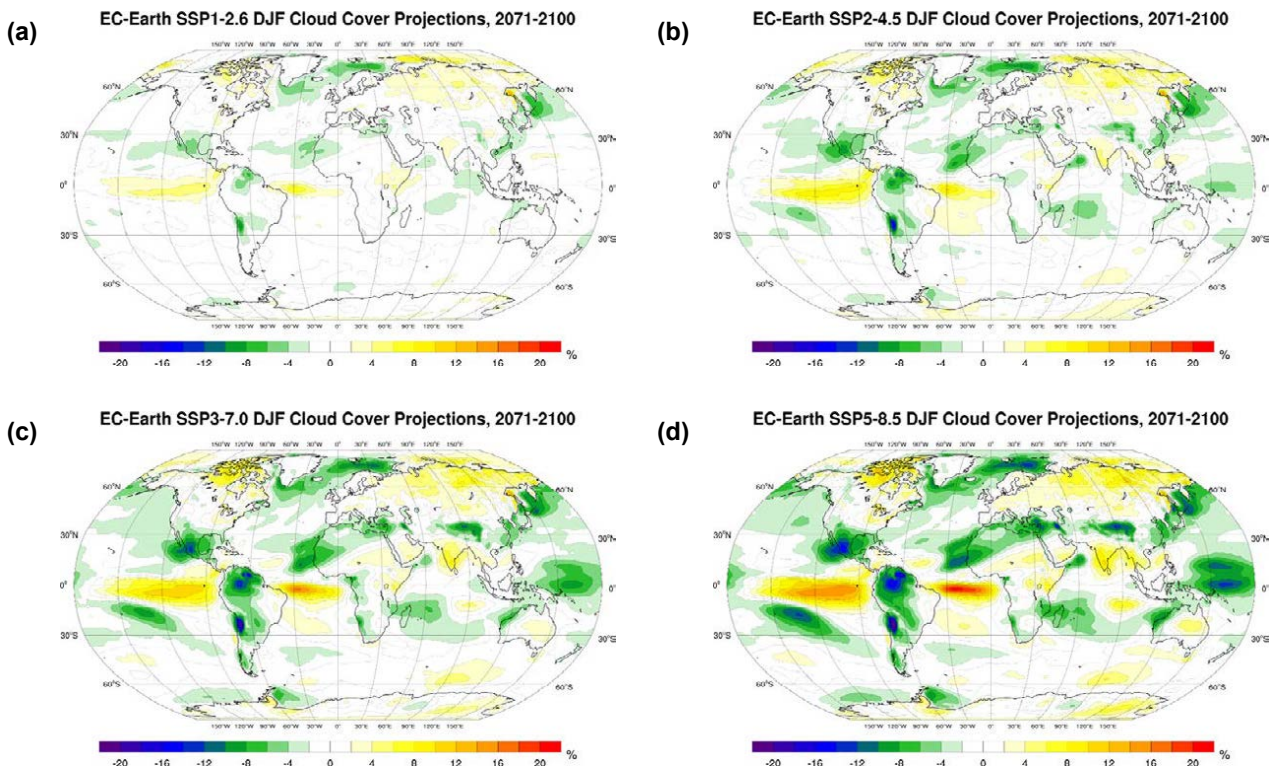


Figure 3.36. EC-Earth DJF total cloud cover projections (2071–2100 vs 1981–2010, % difference): (a) SSP1–2.6, (b) SSP2–4.5, (c) SSP3–7.0 and (d) SSP5–8.5. In each case, an average is taken of the ensemble members r6i1p1f1, r9i1p1f1, r11i1p1f1, r13i1p1f1 and r15i1p1f1. The anomalies (%) are calculated as “future (%) minus past (%)” as opposed to a percentage change.

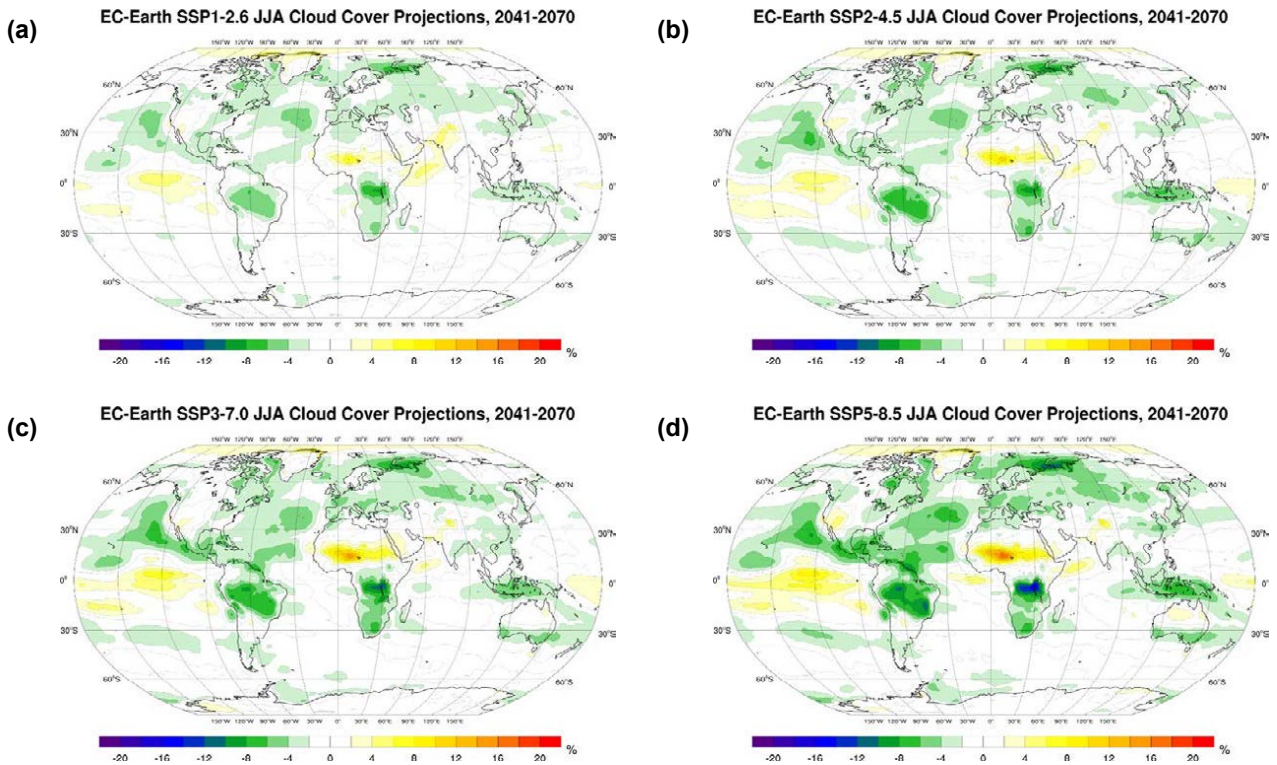


Figure 3.37. EC-Earth JJA total cloud cover projections (2041–2070 vs 1981–2010, % difference): (a) SSP1–2.6, (b) SSP2–4.5, (c) SSP3–7.0 and (d) SSP5–8.5. In each case, an average is taken of the ensemble members r6i1p1f1, r9i1p1f1, r11i1p1f1, r13i1p1f1 and r15i1p1f1. The anomalies (%) are calculated as “future (%) minus past (%)” as opposed to a percentage change.

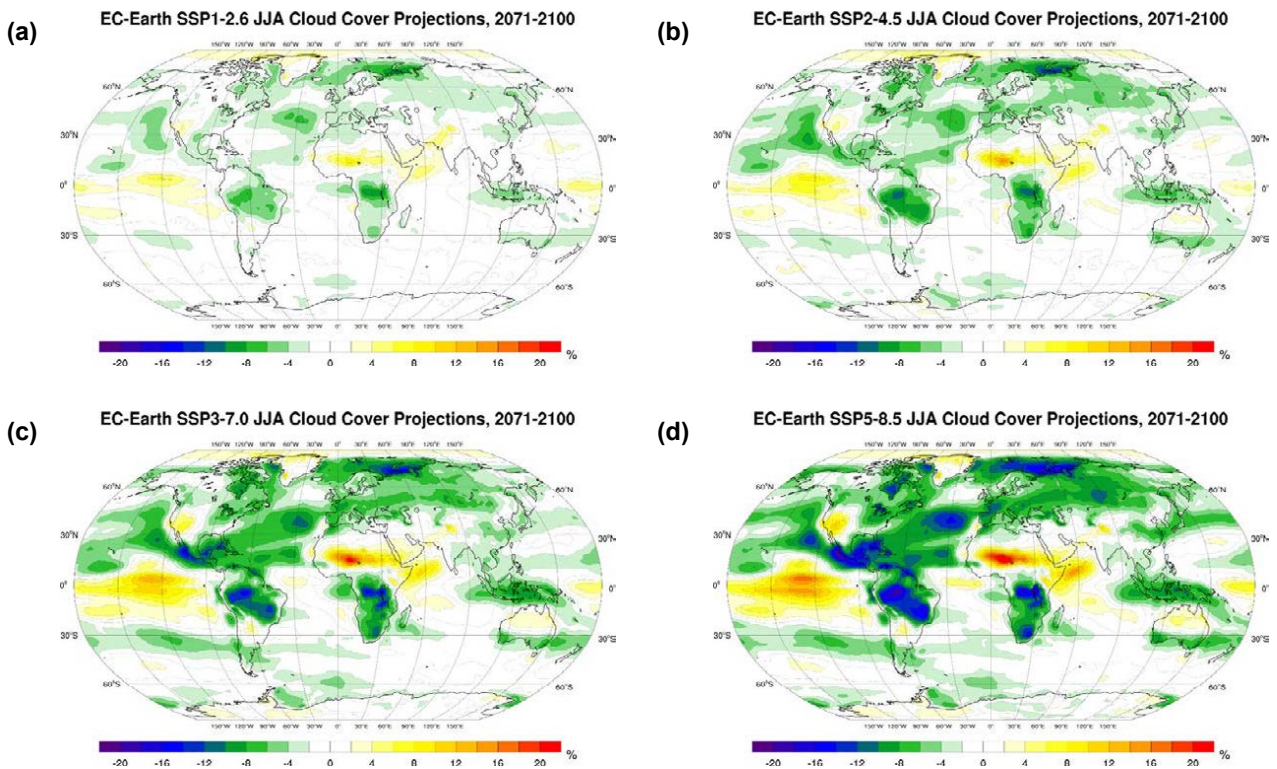


Figure 3.38. EC-Earth JJA total cloud cover projections (2071–2100 vs 1981–2010, % difference): (a) SSP1–2.6, (b) SSP2–4.5, (c) SSP3–7.0 and (d) SSP5–8.5. In each case, an average is taken of the ensemble members r6i1p1f1, r9i1p1f1, r11i1p1f1, r13i1p1f1 and r15i1p1f1. The anomalies (%) are calculated as “future (%) minus past (%)” as opposed to a percentage change.

The mean global annual total cloud cover anomalies (relative to 1981–2010) for all five historical simulations (1850–2014) and 20 SSPs (2015–2100) are presented in Figure 3.39. The bold lines represent the ensemble means. All ensemble members show a small steady decrease in total cloud cover from around 2000. Although a small divergence between the SSPs is evident from around 2060, the differences are small. By the end of the century, global mean total cloud cover is projected to decrease by approximately 0.5%, 1%, 1.5% and 2% for SSP1–2.6, SSP2–4.5, SSP3–7.0 and SSP5–8.5, respectively.

Figure 3.40, which presents the standard deviation of each SSP ensemble of climate projections, shows high agreement between ensemble members. The North Atlantic and tropical Pacific regions exhibit the largest disagreements. In these regions, the annual cloud projections (see Figure 3.34) should be viewed with caution as the magnitude of change is less than (or equal to) the spread (standard deviation) between ensemble member projections (Figure 3.40).

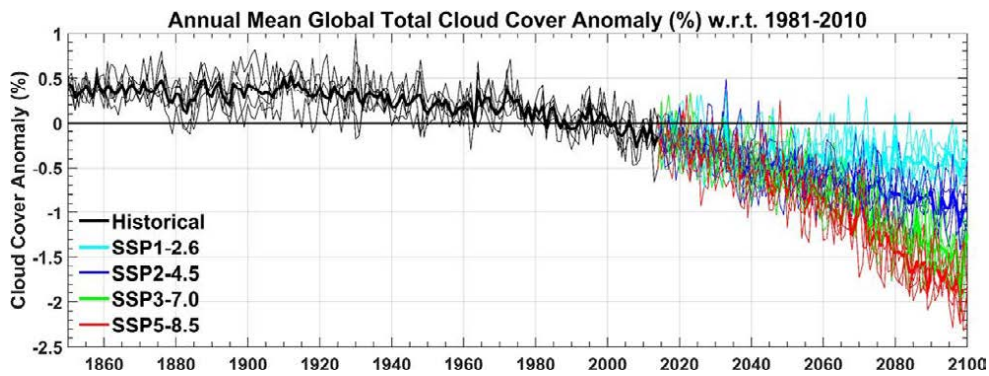


Figure 3.39. Global annual total cloud cover anomalies (%) with respect to the 30-year period 1981–2010: EC-Earth ensemble members r6i1p1f1, r9i1p1f1, r11i1p1f1, r13i1p1f1 and r15i1p1f1. The bold lines represent the ensemble means. The anomalies (%) are calculated as “future (%) minus past (%)” as opposed to a percentage change.

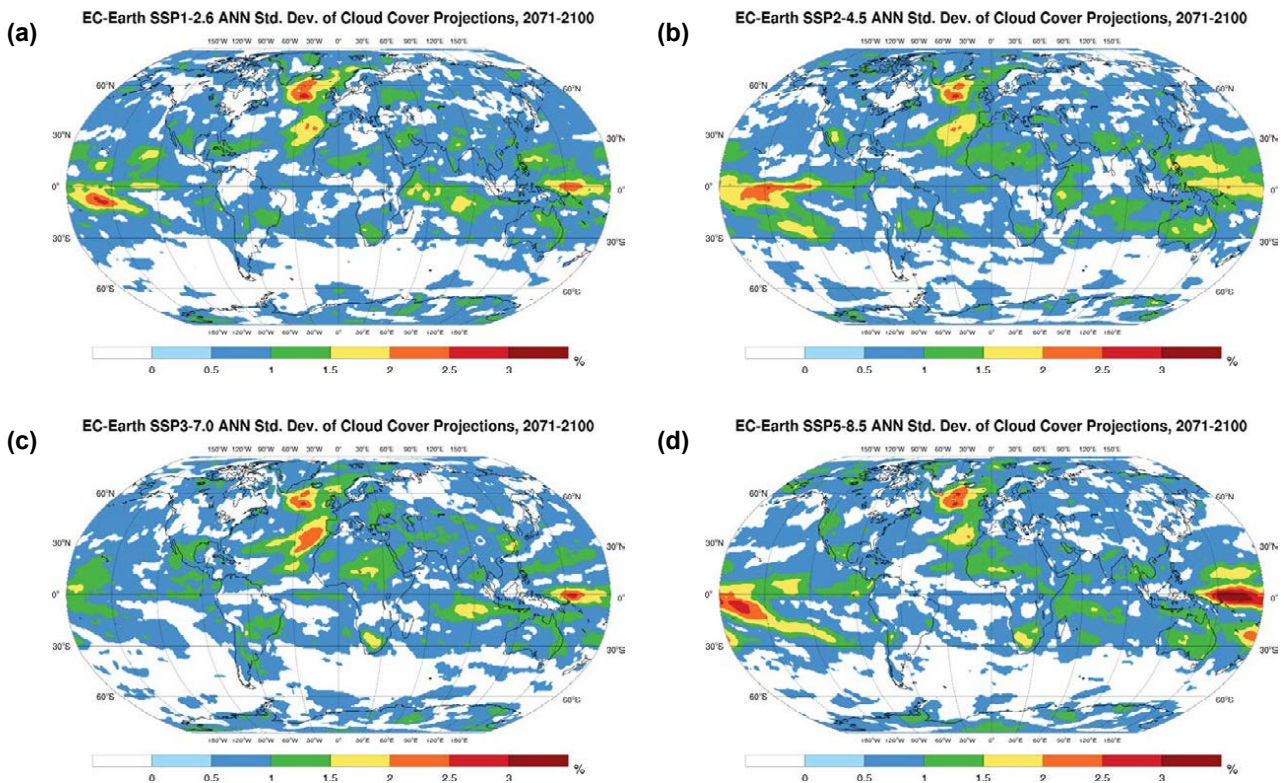


Figure 3.40. Standard deviation of the ensemble of annual total cloud cover projections (2071–2100): (a) SSP1–2.6, (b) SSP2–4.5, (c) SSP3–7.0 and (d) SSP5–8.5.

3.6 Snowfall Projections

Figures 3.41 and 3.42 present the spatial distribution of annual projections of snowfall for each of the four SSPs for the 2041–2070 and 2071–2100 periods, respectively. The general trend is for large decreases in snowfall for all regions except Antarctica, northern Russia and Greenland. The DJF projections (Figures 3.43 and 3.44) are similar except that the trends are greatly enhanced in the Northern Hemisphere and the increase in snowfall extends over the Arctic. For JJA, snowfall is projected to decrease in all regions except for central Greenland and Antarctica (Figures 3.45 and 3.46). In general, the snowfall trends are enhanced for the 2071–2100 period and the higher SSPs.

The mean global annual snowfall anomalies (% change relative to 1981–2010) for all five historical simulations (1850–2014) and 20 SSPs (2015–2100) are presented in Figure 3.47a. The bold lines represent the ensemble means. All ensemble members show a steady decrease in snowfall from around 2020. By the end of the century, global mean

snowfall is projected to decrease by approximately 3%, 7%, 8% and 10% for SSP1–2.6, SSP2–4.5, SSP3–7.0 and SSP5–8.5, respectively. The Northern Hemisphere annual snowfall anomalies, presented in Figure 3.47b, are substantially larger, with end-of-century projected decreases ranging from 7% (SSP1–2.6) to 18% (SSP5–8.5). The Southern Hemisphere annual snowfall anomalies (Figure 3.47c) exhibit no trend.

Figure 3.48 shows the standard deviation of each SSP ensemble of climate projections; there is a high level of agreement between ensemble members for all regions except the north-west Atlantic. An analysis of the individual ensemble members shows that the disagreement in the North Atlantic region is the result of a difference between two groups – the r6i1p1f1 and r11i1p1f1 ensemble members project larger decreases in snowfall than the r9i1p1f1, r13i1p1f1 and r15i1p1f1 ensemble members. Note that this result is similar (and probably related) to the spread of 2-m temperature projections discussed in section 3.1. Future work will fully address this issue by extending the analysis to include the full ensemble of EC-Earth CMIP6 simulations produced by the consortium.

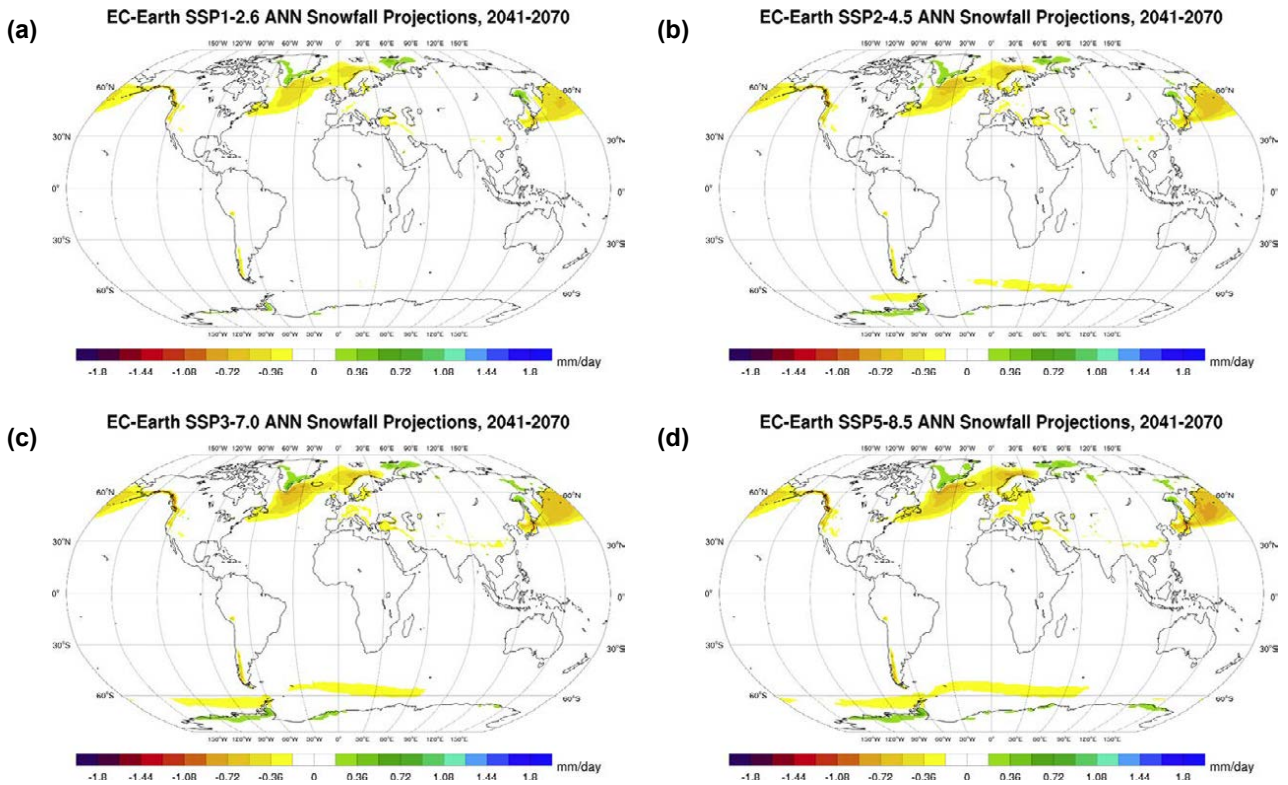


Figure 3.41. EC-Earth annual snowfall projections (2041–2070 vs 1981–2010, mm/day difference): (a) SSP1–2.6, (b) SSP2–4.5, (c) SSP3–7.0 and (d) SSP5–8.5. In each case, an average is taken of the ensemble members r6i1p1f1, r9i1p1f1, r11i1p1f1, r13i1p1f1 and r15i1p1f1.

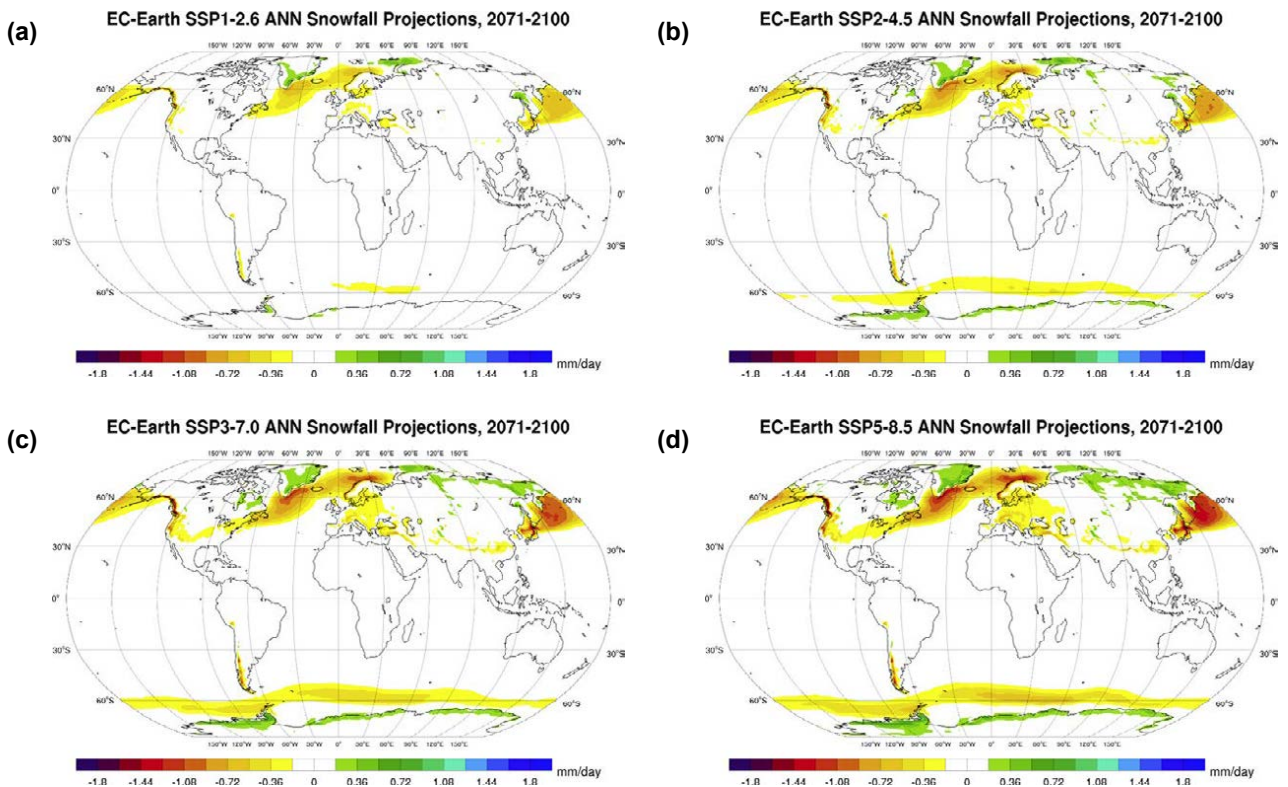


Figure 3.42. EC-Earth annual snowfall projections (2071–2100 vs 1981–2010, mm/day difference): (a) SSP1–2.6, (b) SSP2–4.5, (c) SSP3–7.0 and (d) SSP5–8.5. In each case, an average is taken of the ensemble members r6i1p1f1, r9i1p1f1, r11i1p1f1, r13i1p1f1 and r15i1p1f1.

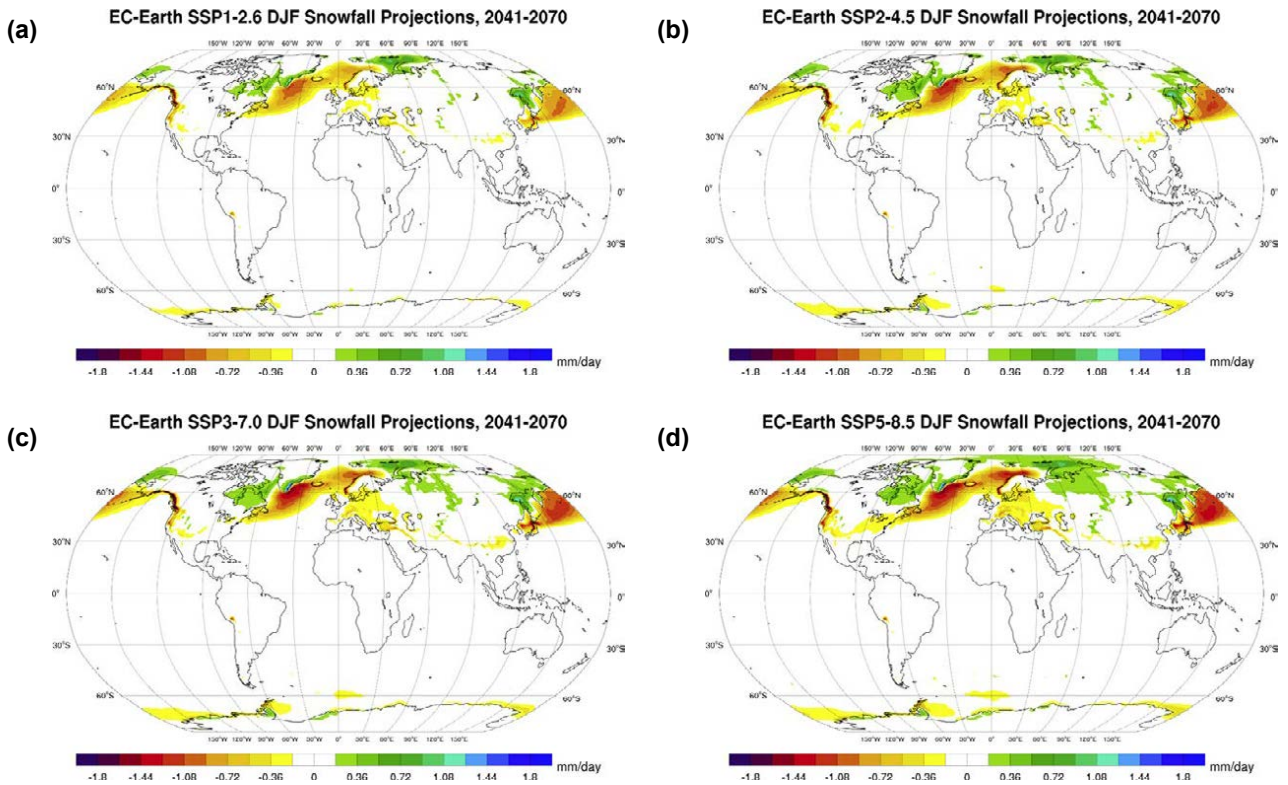


Figure 3.43. EC-Earth DJF snowfall projections (2041–2070 vs 1981–2010, mm/day difference): (a) SSP1–2.6, (b) SSP2–4.5, (c) SSP3–7.0 and (d) SSP5–8.5. In each case, an average is taken of the ensemble members r6i1p1f1, r9i1p1f1, r11i1p1f1, r13i1p1f1 and r15i1p1f1.

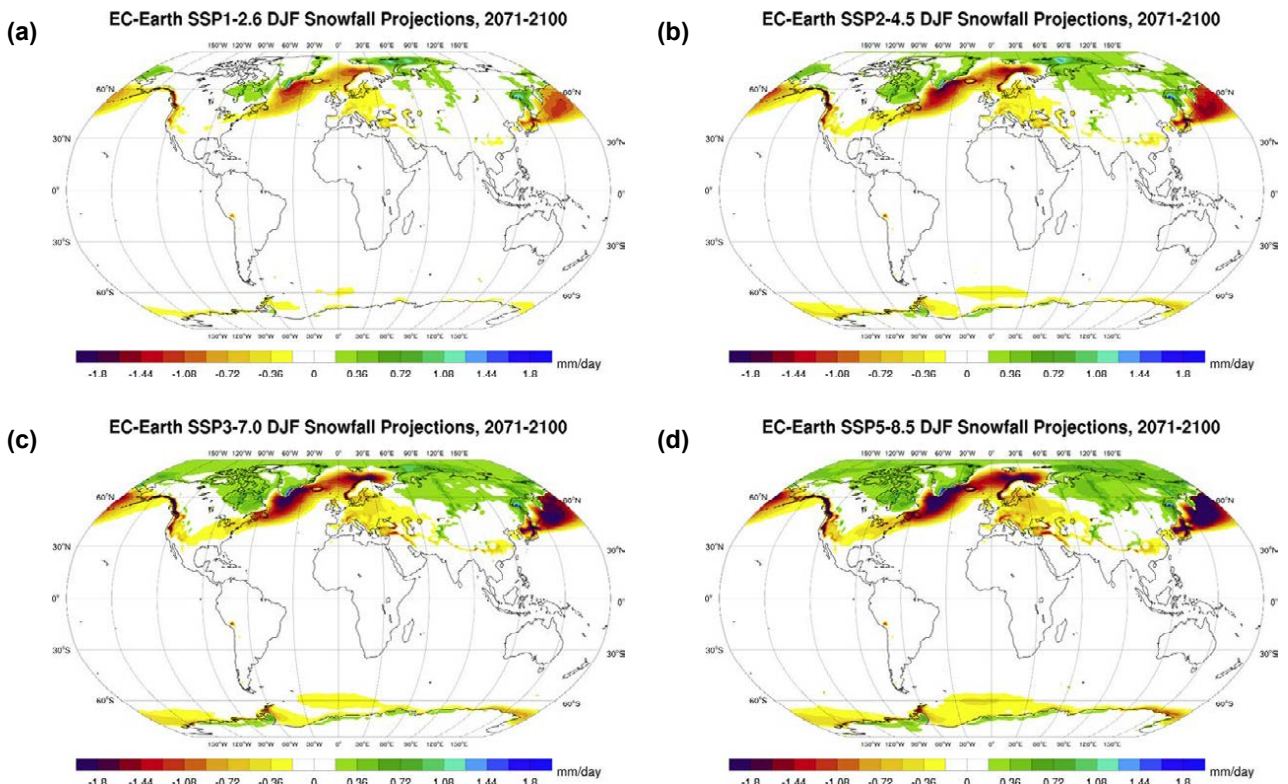


Figure 3.44. EC-Earth DJF snowfall projections (2071–2100 vs 1981–2010, mm/day difference): (a) SSP1–2.6, (b) SSP2–4.5, (c) SSP3–7.0 and (d) SSP5–8.5. In each case, an average is taken of the ensemble members r6i1p1f1, r9i1p1f1, r11i1p1f1, r13i1p1f1 and r15i1p1f1.

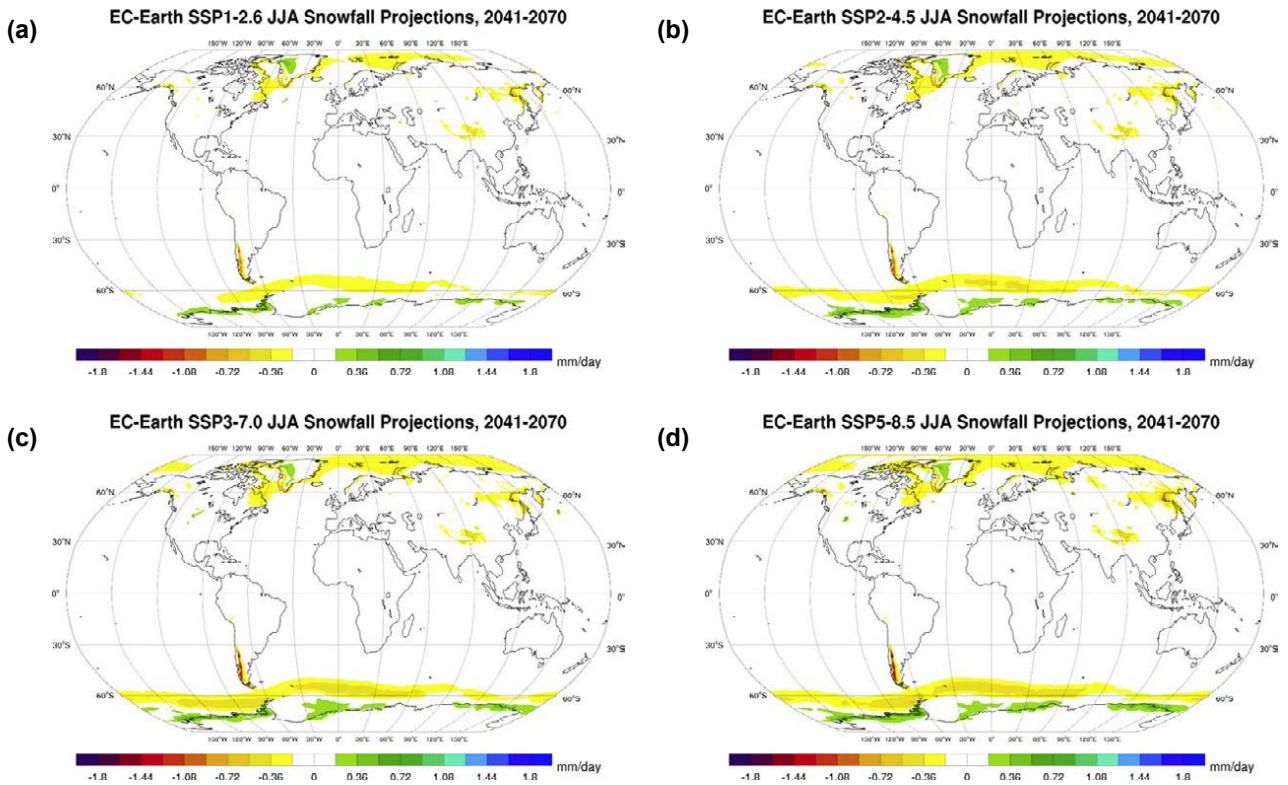


Figure 3.45. EC-Earth JJA snowfall projections (2041–2070 vs 1981–2010, mm/day difference): (a) SSP1–2.6, (b) SSP2–4.5, (c) SSP3–7.0 and (d) SSP5–8.5. In each case, an average is taken of the ensemble members r6i1p1f1, r9i1p1f1, r11i1p1f1, r13i1p1f1 and r15i1p1f1.

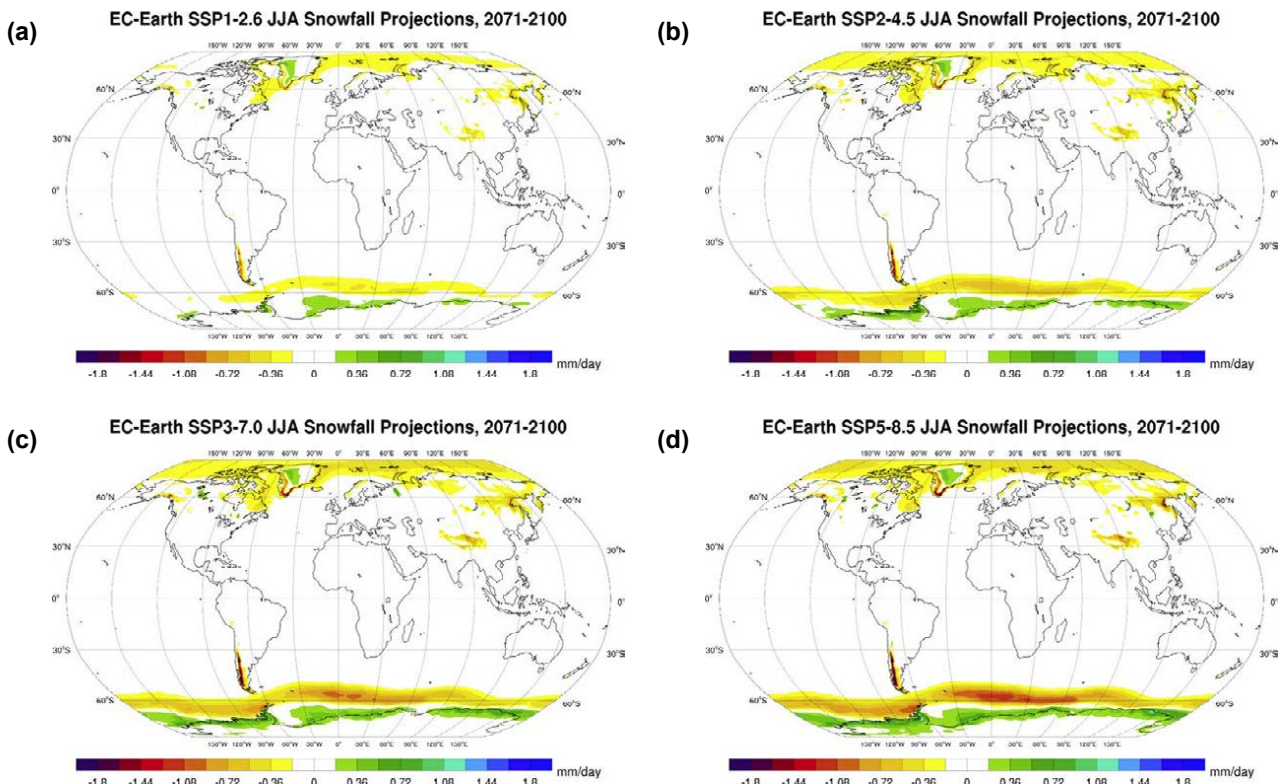


Figure 3.46. EC-Earth JJA snowfall projections (2071–2100 vs 1981–2010, mm/day difference): (a) SSP1–2.6, (b) SSP2–4.5, (c) SSP3–7.0 and (d) SSP5–8.5. In each case, an average is taken of the ensemble members r6i1p1f1, r9i1p1f1, r11i1p1f1, r13i1p1f1 and r15i1p1f1.

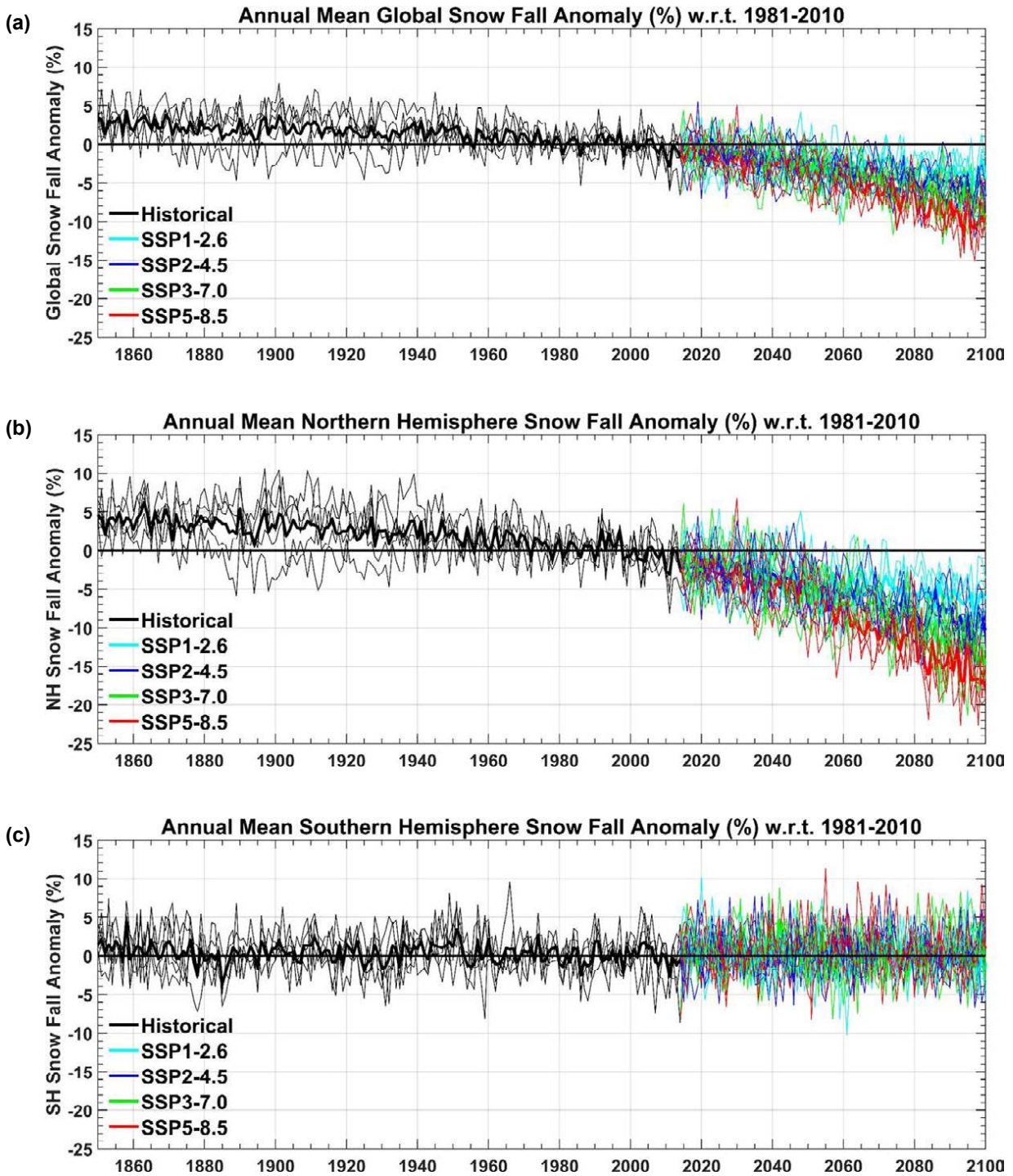


Figure 3.47. Annual snowfall anomalies (%) with respect to the 30-year period 1981–2010: EC-Earth ensemble members r6i1p1f1, r9i1p1f1, r11i1p1f1, r13i1p1f1 and r15i1p1f1 – (a) global, (b) Northern Hemisphere and (c) Southern Hemisphere. The bold lines represent the ensemble means.

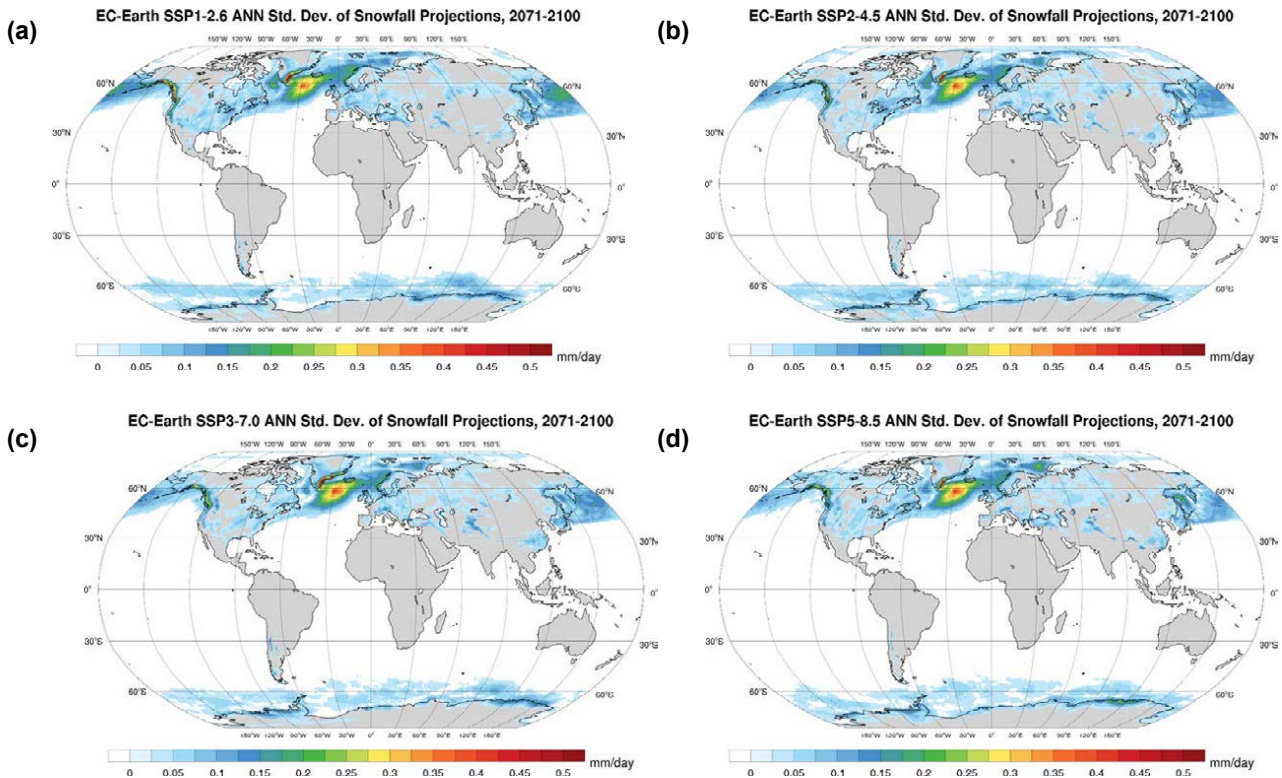


Figure 3.48. Standard deviation of the ensemble of annual snowfall projections (2071–2100): (a) SSP1–2.6, (b) SSP2–4.5, (c) SSP3–7.0 and (d) SSP5–8.5.

3.7 Sea Surface Temperature Projections

Figures 3.49 and 3.50 present the spatial distribution of annual SST projections for each of the four SSPs for 2041–2070 and 2071–2100, respectively. The largest increases in temperatures are noted over the northern latitudes, in particular over the Arctic region. Projections for DJF (Figures 3.51 and 3.52) follow a similar trend to the annual projections except that increases in SST over the Southern (Northern) Hemisphere are enhanced (diminished). The projections for JJA (Figures 3.53 and 3.54) also follow a similar trend to the annual projections except that increases in SST over the northern latitudes are enhanced. In all plots, a “dipole” feature is noted in the North Atlantic, where SST projections are enhanced (diminished) north (south) of Iceland. Projections of SST range from -1°C for the region south of Iceland for DJF 2041–2070 SSP1–2.6 (Figure 3.51a) to $+10^{\circ}\text{C}$ over the Arctic region for JJA 2071–2100 SSP5–8.5 (Figure 3.54d).

The mean global annual SST anomalies (relative to 1981–2010) for all five historical simulations (1850–2014) and 20 SSPs (2015–2100) are presented in Figure 3.55. The bold lines represent

the ensemble means. All ensemble members show a steady increase in temperature from around 2000 with a noticeable divergence between the SSPs from around 2050. By the year 2100, the global mean SST is projected to increase by approximately 1°C , 2°C , 3°C and 4°C for SSP1–2.6, SSP2–4.5, SSP3–7.0 and SSP5–8.5, respectively. The small spread between the individual ensemble members demonstrates a high level of agreement and adds a measure of confidence to the projections. This is confirmed in Figure 3.56, which shows the standard deviation of each SSP ensemble of climate projections; a high level of agreement between ensembles is noted for all regions except those south of Greenland and north of Iceland. An analysis of the individual ensemble members showed that the disagreement over the region south of Greenland is the result of a difference between two groups – the r6i1p1f1 and r11i1p1f1 ensemble members project larger increases in SST than the r9i1p1f1, r13i1p1f1 and r15i1p1f1 ensemble members. This result is similar (and very probably related) to the spread of 2-m temperature projections discussed in section 3.1. Future work will fully address this issue by extending the analysis to include the full ensemble of EC-Earth CMIP6 simulations produced by the consortium.

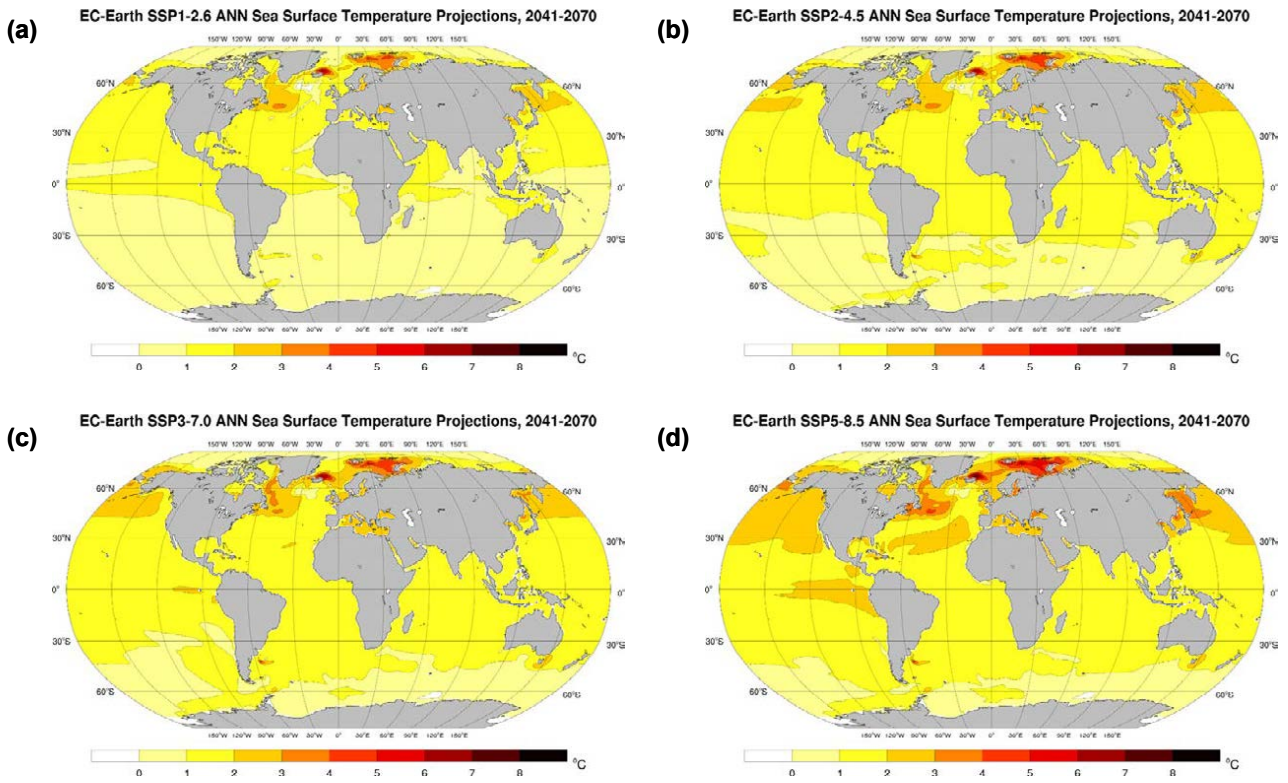


Figure 3.49. EC-Earth annual SST projections (2041–2070 vs 1981–2010, °C change): (a) SSP1–2.6, (b) SSP2–4.5, (c) SSP3–7.0 and (d) SSP5–8.5. In each case, an average is taken of the ensemble members r6i1p1f1, r9i1p1f1, r11i1p1f1, r13i1p1f1 and r15i1p1f1.

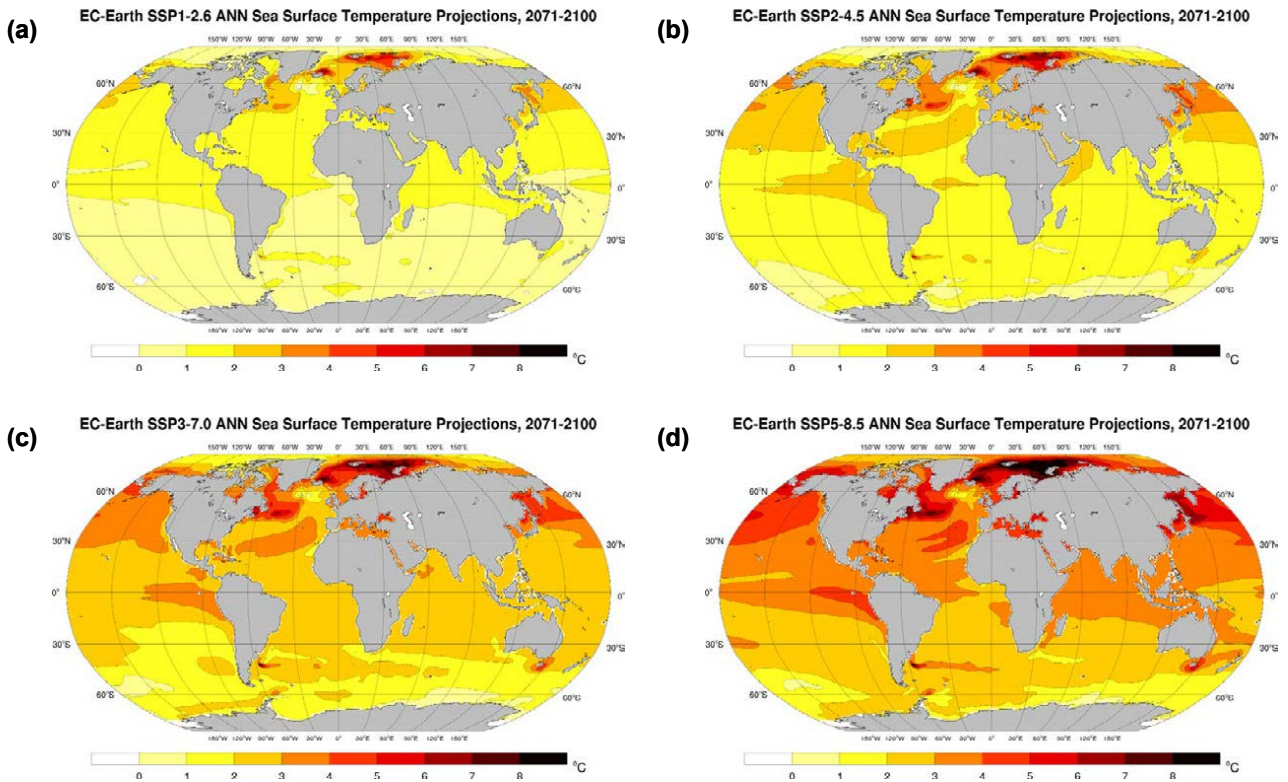


Figure 3.50. EC-Earth annual SST projections (2071–2100 vs 1981–2010, °C change): (a) SSP1–2.6, (b) SSP2–4.5, (c) SSP3–7.0 and (d) SSP5–8.5. In each case, an average is taken of the ensemble members r6i1p1f1, r9i1p1f1, r11i1p1f1, r13i1p1f1 and r15i1p1f1

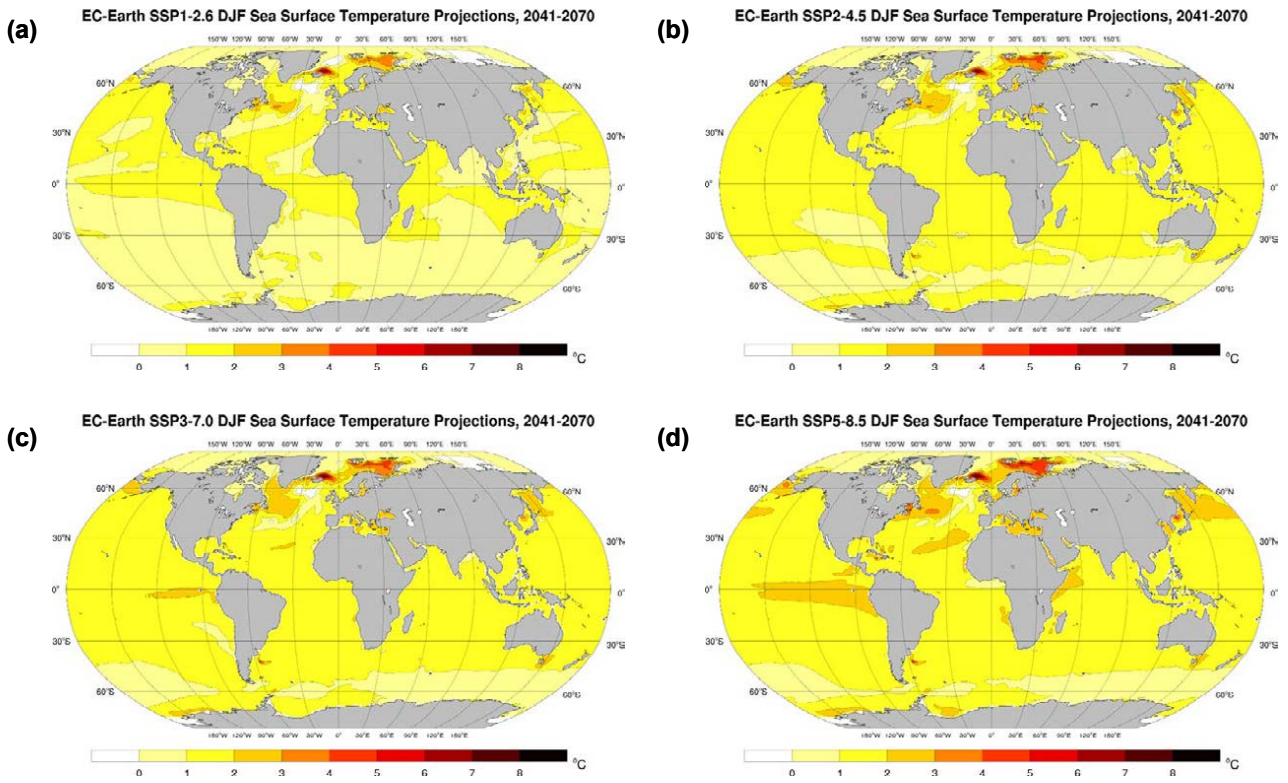


Figure 3.51. EC-Earth DJF SST projections (2041–2070 vs 1981–2010, °C change): (a) SSP1–2.6, (b) SSP2–4.5, (c) SSP3–7.0 and (d) SSP5–8.5. In each case, an average is taken of the ensemble members r6i1p1f1, r9i1p1f1, r11i1p1f1, r13i1p1f1 and r15i1p1f1.

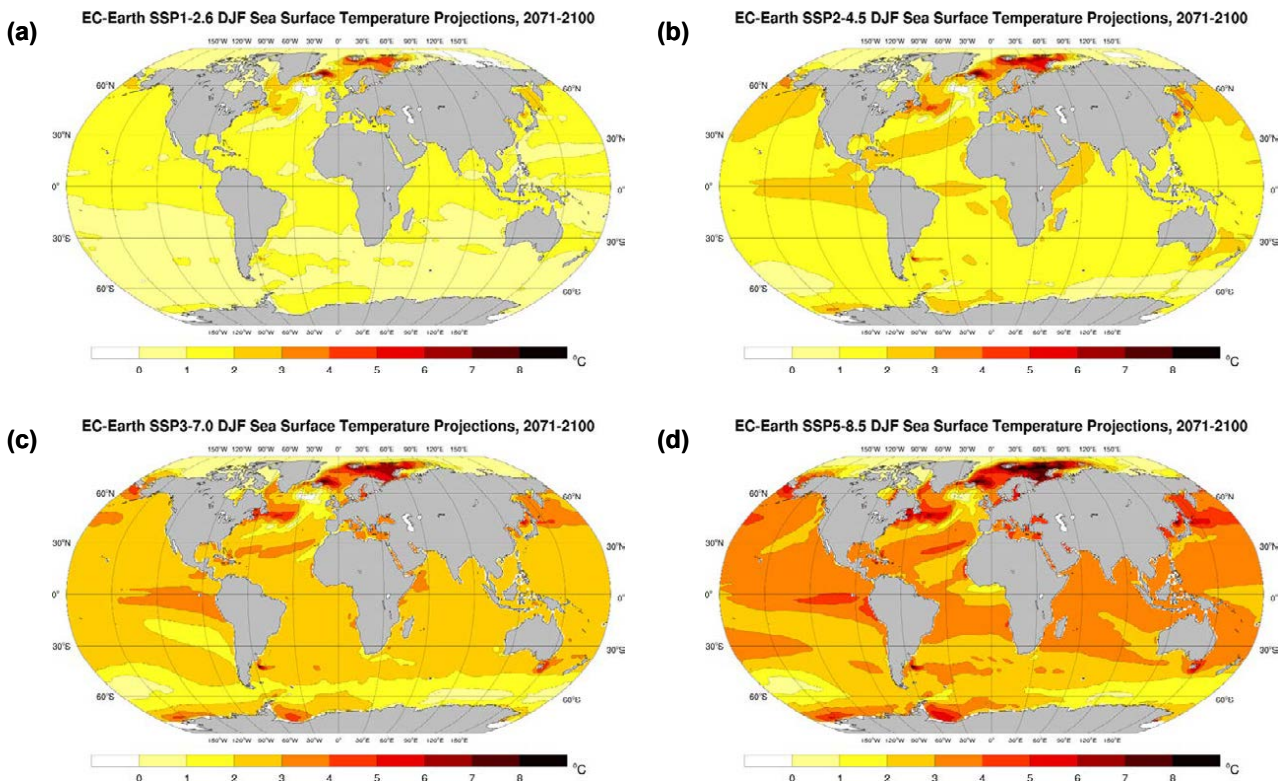


Figure 3.52. EC-Earth DJF SST projections (2071–2100 vs 1981–2010, °C change): (a) SSP1–2.6, (b) SSP2–4.5, (c) SSP3–7.0 and (d) SSP5–8.5. In each case, an average is taken of the ensemble members r6i1p1f1, r9i1p1f1, r11i1p1f1, r13i1p1f1 and r15i1p1f1.

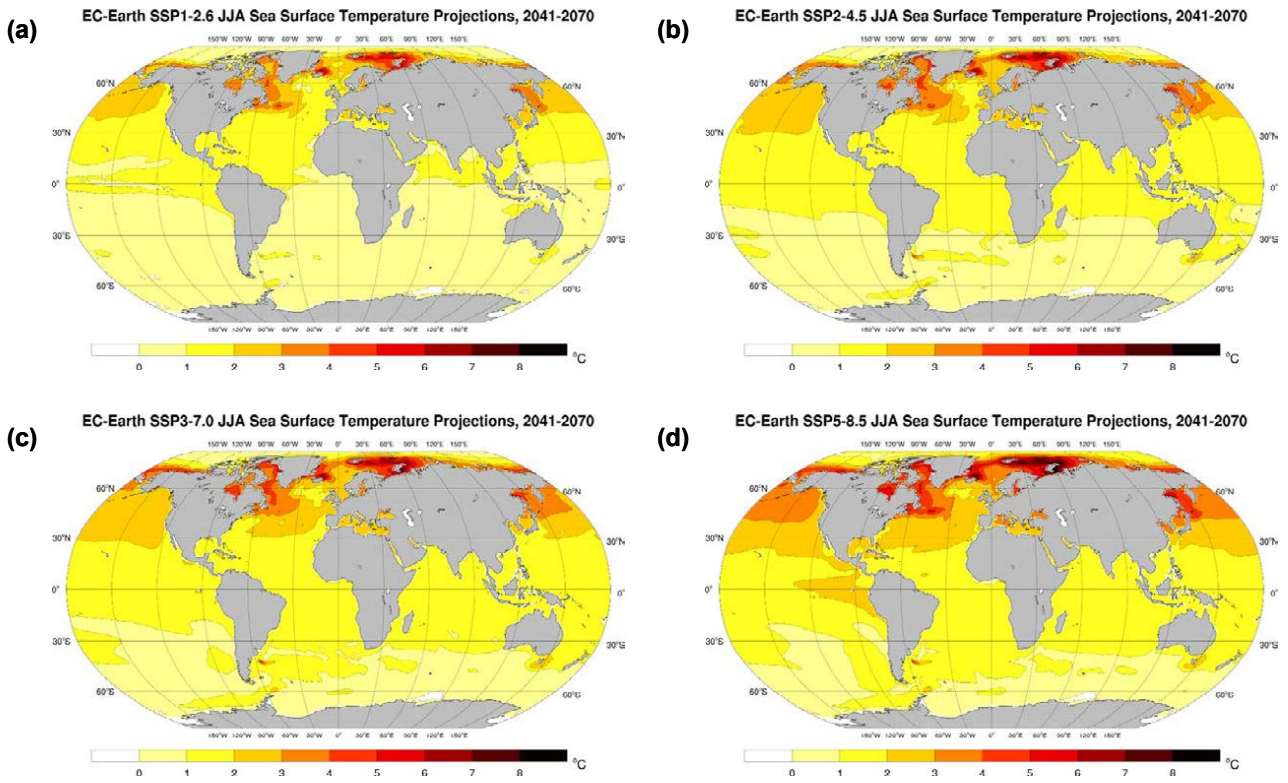


Figure 3.53. EC-Earth JJA SST projections (2041–2070 vs 1981–2010, °C change); (a) SSP1–2.6, (b) SSP2–4.5, (c) SSP3–7.0 and (d) SSP5–8.5. In each case, an average is taken of the ensemble members r6i1p1f1, r9i1p1f1, r11i1p1f1, r13i1p1f1 and r15i1p1f1.

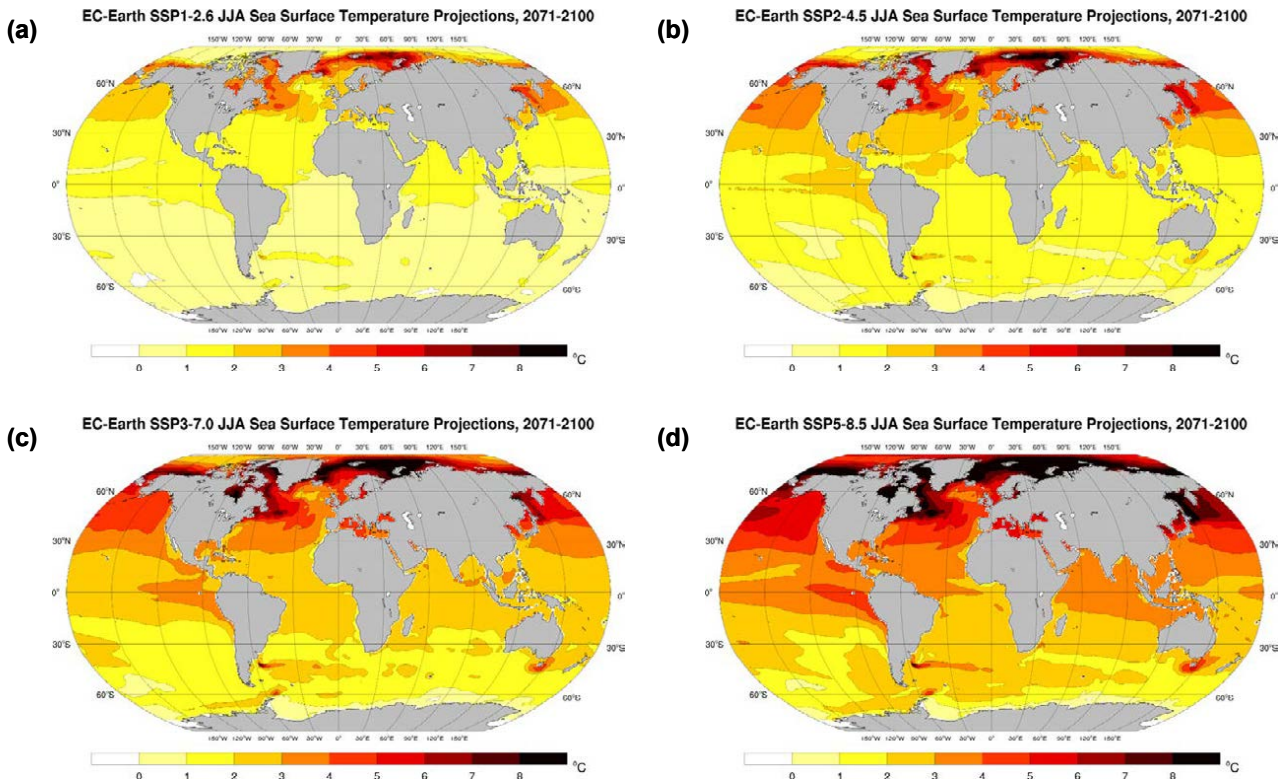


Figure 3.54. EC-Earth JJA SST projections (2071–2100 vs 1981–2010, °C change): (a) SSP1–2.6, (b) SSP2–4.5, (c) SSP3–7.0 and (d) SSP5–8.5. In each case, an average is taken of the ensemble members r6i1p1f1, r9i1p1f1, r11i1p1f1, r13i1p1f1 and r15i1p1f1.

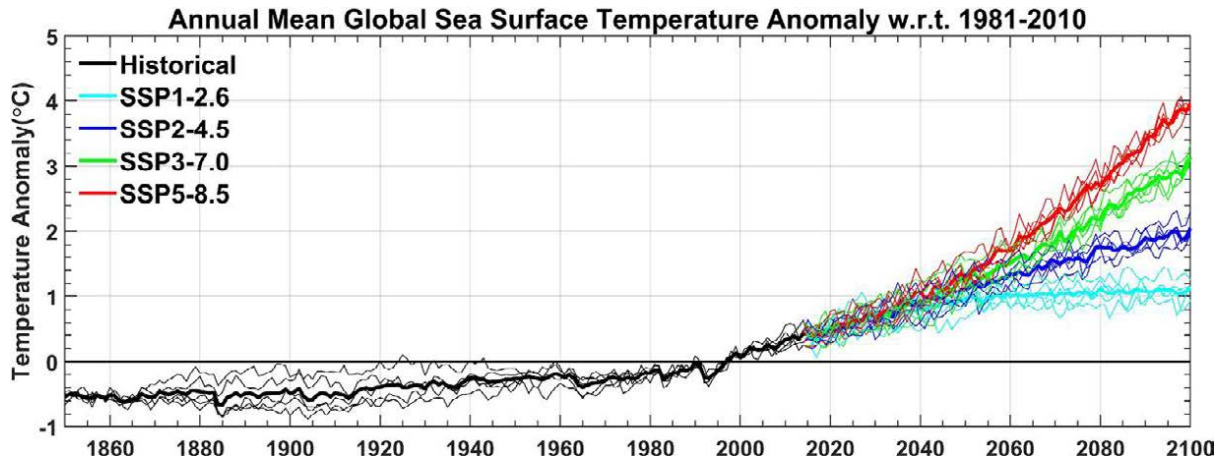


Figure 3.55. Global annual SST anomalies with respect to the 30-year period 1981–2010: EC-Earth ensemble members r6i1p1f1, r9i1p1f1, r11i1p1f1, r13i1p1f1 and r15i1p1f1. The bold lines represent the ensemble mean.

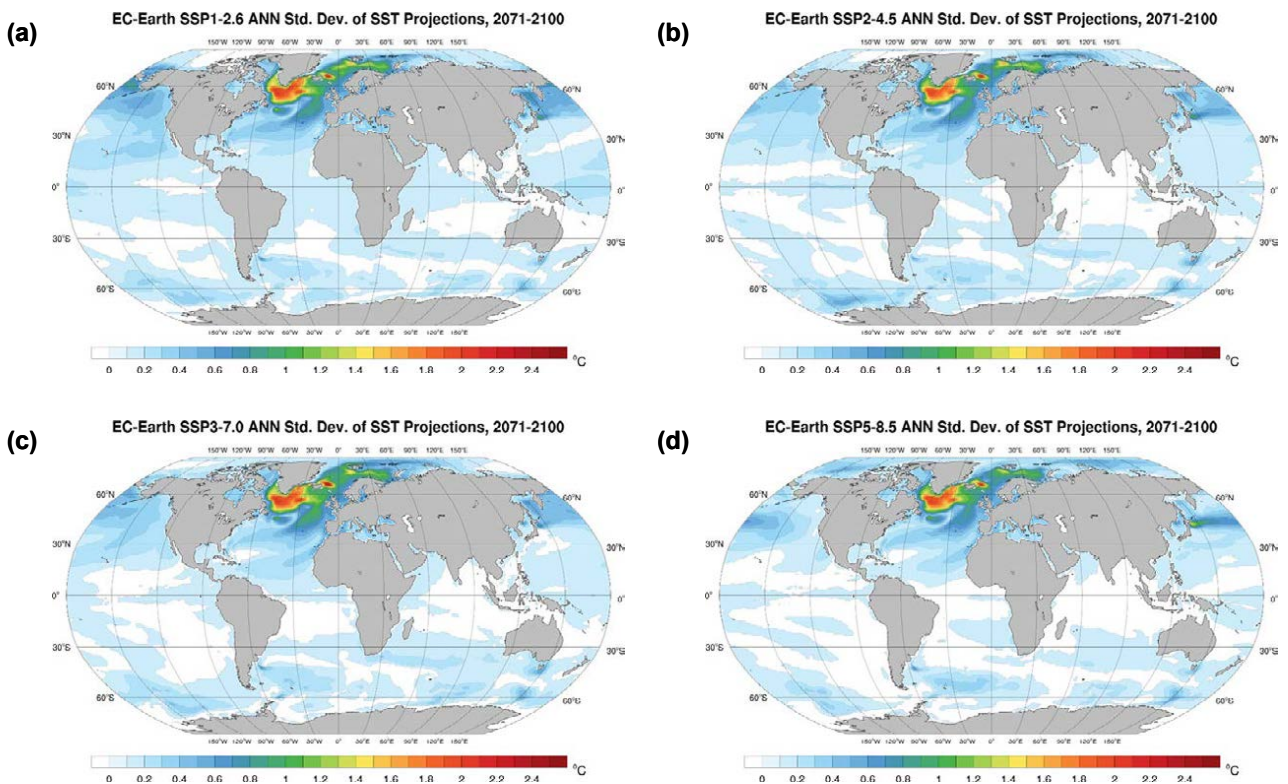


Figure 3.56. Standard deviation of the ensemble of annual SST projections (2071–2100): (a) SSP1–2.6, (b) SSP2–4.5, (c) SSP3–7.0 and (d) SSP5–8.5.

3.8 Sea Ice Projections

3.8.1 Northern Hemisphere sea ice projections

Figure 3.57 presents the Northern Hemisphere annual mean sea ice fraction for the historical ensemble (1981–2010) and each of the four SSPs (2041–2070). The projected annual anomalies (%) for 2041–2070 are presented in Figure 3.58. The corresponding data for 2071–2100 are presented in Figures 3.59 and 3.60. The results show large projected decreases in sea ice in terms of both extent and fraction.

The corresponding results for the Northern Hemisphere March sea ice fraction are presented in Figure 3.61 (sea ice fraction; historical ensemble

1981–2010 and 2041–2070), Figure 3.62 (sea ice anomalies; 2041–2070), Figure 3.63 (sea ice fraction; 2071–2100) and Figure 3.64 (sea ice anomalies; 2071–2100). Although substantial decreases are projected for the March Northern Hemisphere sea ice extent, the changes are smaller than those in the annual (and September) projections.

The projected changes for the Northern Hemisphere September sea ice fraction are substantial.

Figures 3.65 and 3.66 show large decreases for all SSPs, with the Arctic projected to be nearly ice free under SSP3–7.0 and SSP5–8.5 by 2041–2070.

For the period 2071–2100 all SSPs except SSP1–2.6 (Figure 3.67) project an ice-free Arctic during September.

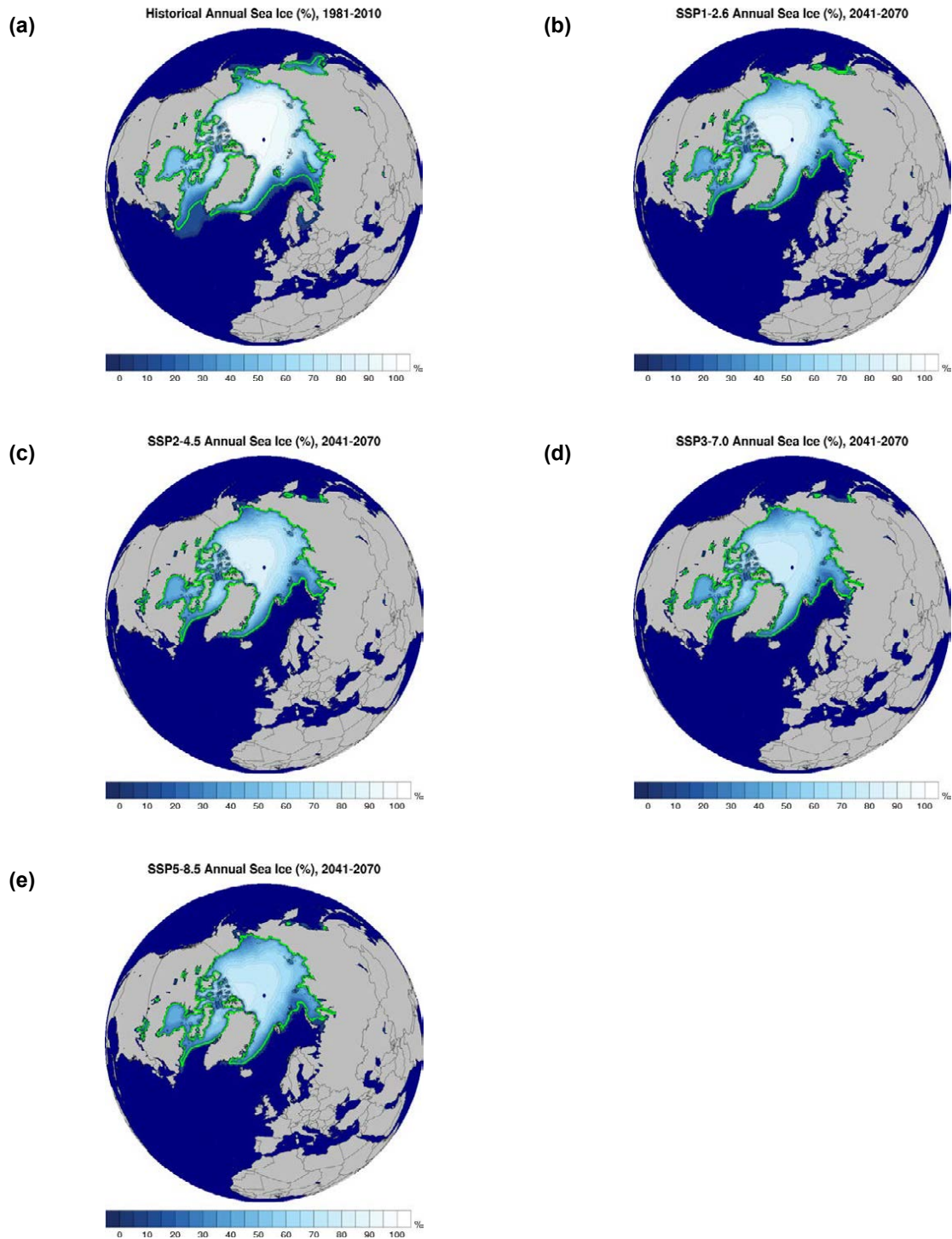


Figure 3.57. Annual mean Northern Hemisphere sea ice fraction (%): (a) historical ensemble for the period 1981–2010 and (b) SSP1–2.6, (c) SSP2–4.5, (d) SSP3–7.0 and (e) SSP5–8.5 for the period 2041–2070. In each case, an average is taken of the ensemble members r6i1p1f1, r9i1p1f1, r11i1p1f1, r13i1p1f1 and r15i1p1f1. The green line shows the 15% contour line of the sea ice fraction.

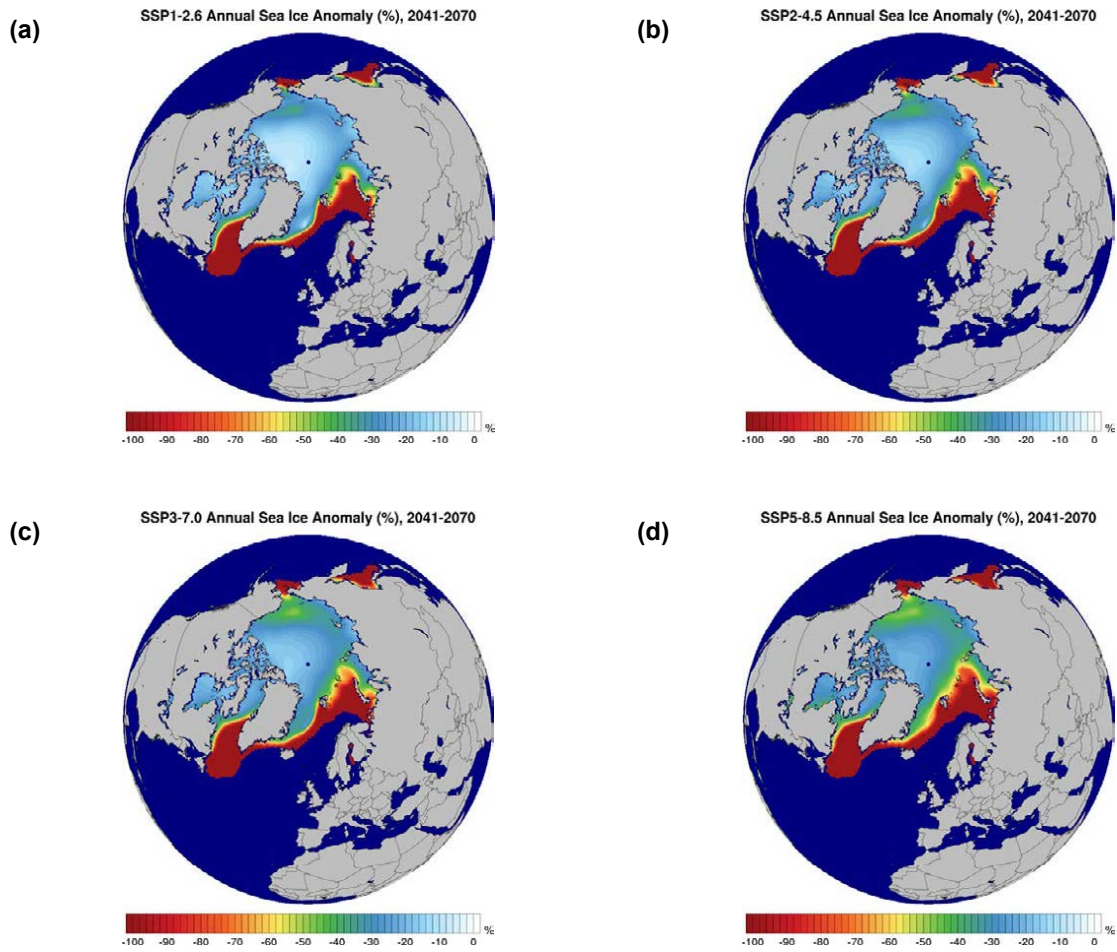


Figure 3.58. Annual Northern Hemisphere sea ice projections (% change) (2041–2070 vs 1981–2010): (a) SSP1–2.6, (b) SSP2–4.5, (c) SSP3–7.0 and (d) SSP5–8.5. In each case, an average is taken of the ensemble members r6i1p1f1, r9i1p1f1, r11i1p1f1, r13i1p1f1 and r15i1p1f1.

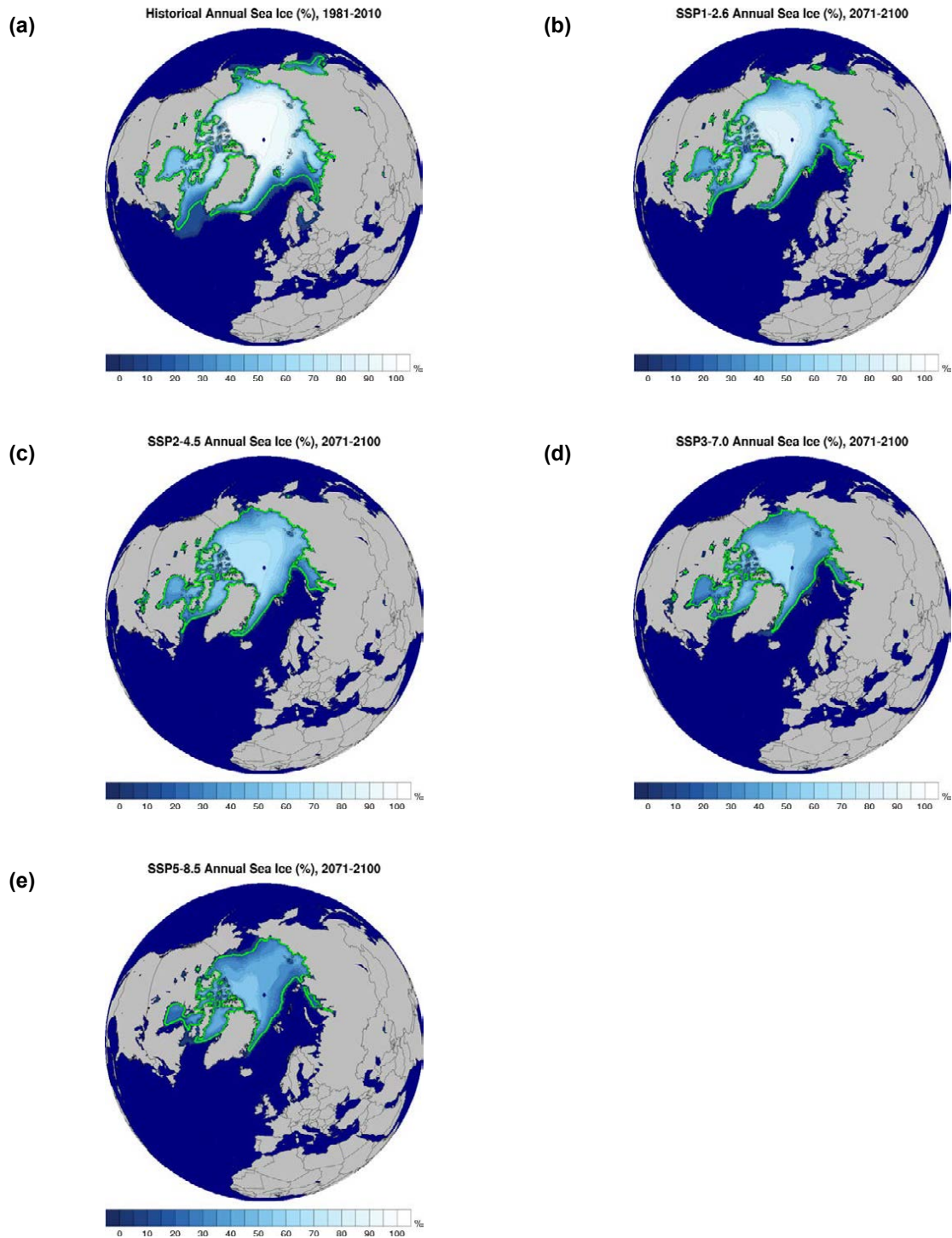


Figure 3.59. Annual mean Northern Hemisphere sea ice fraction (%): (a) historical ensemble for the period 1981–2010 and (b) SSP1–2.6, (c) SSP2–4.5, (d) SSP3–7.0 and (e) SSP5–8.5 for the period 2071–2100. In each case, an average is taken of the ensemble members r6i1p1f1, r9i1p1f1, r11i1p1f1, r13i1p1f1 and r15i1p1f1. The green line shows the 15% contour line of the sea ice fraction.

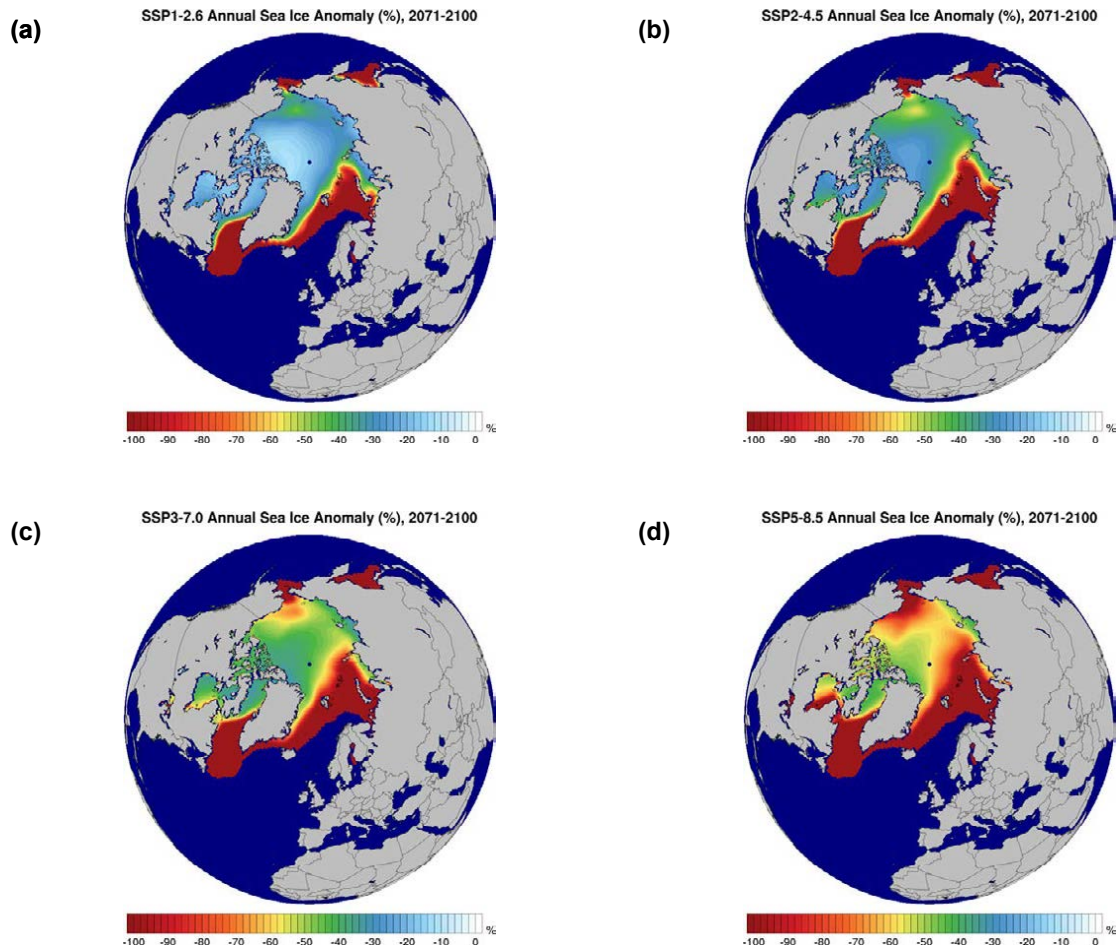


Figure 3.60. Annual Northern Hemisphere sea ice projections (% change) (2071–2100 vs 1981–2010): (a) SSP1–2.6, (b) SSP2–4.5, (c) SSP3–7.0 and (d) SSP5–8.5. In each case, an average is taken of the ensemble members r6i1p1f1, r9i1p1f1, r11i1p1f1, r13i1p1f1 and r15i1p1f1.

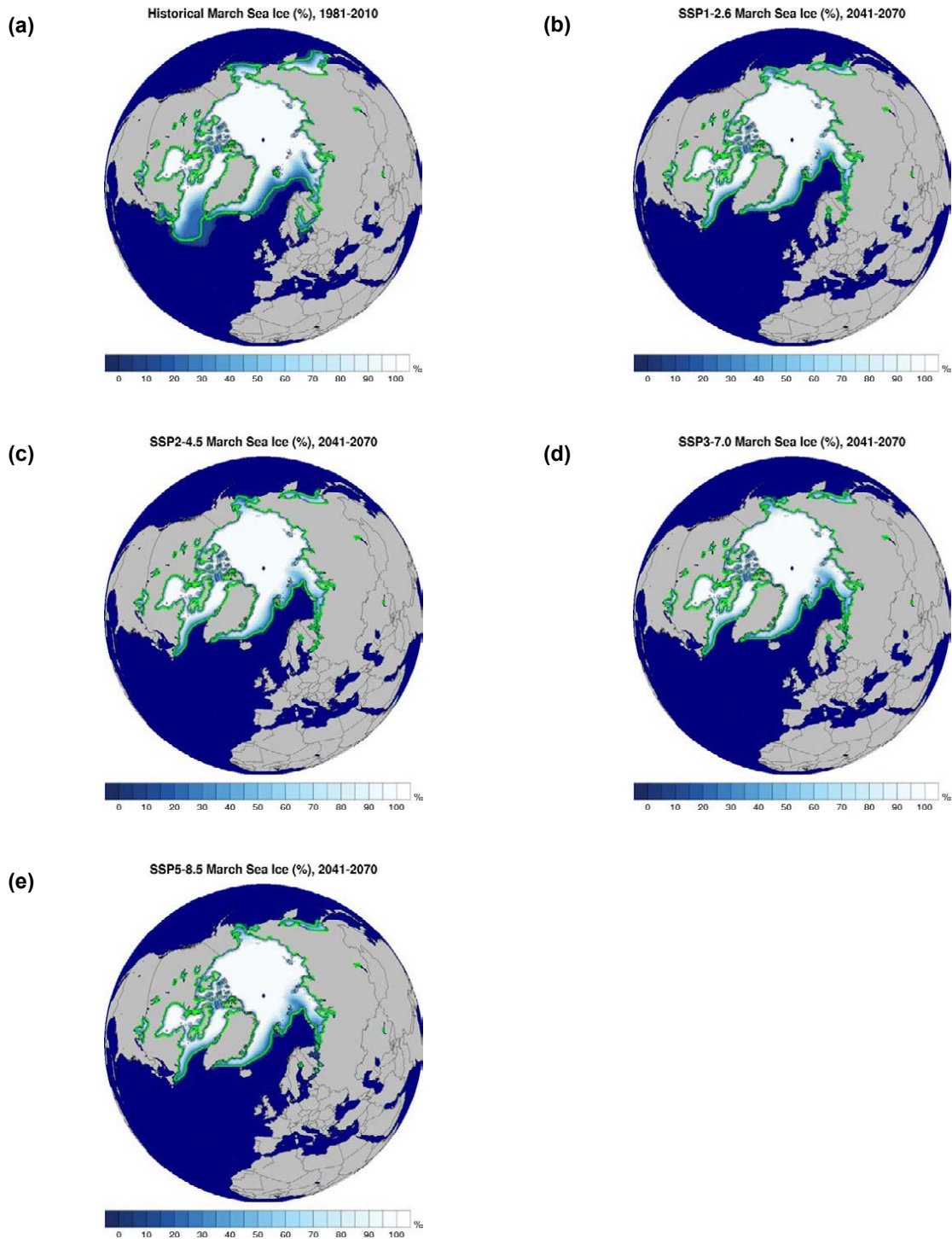


Figure 3.61. Mean Northern Hemisphere March sea ice fraction (%): (a) historical ensemble for the period 1981–2010 and (b) SSP1–2.6, (c) SSP2–4.5, (d) SSP3–7.0 and (e) SSP5–8.5 for the period 2041–2070. In each case, an average is taken of the ensemble members r6i1p1f1, r9i1p1f1, r11i1p1f1, r13i1p1f1 and r15i1p1f1. The green line shows the 15% contour line of the sea ice fraction.

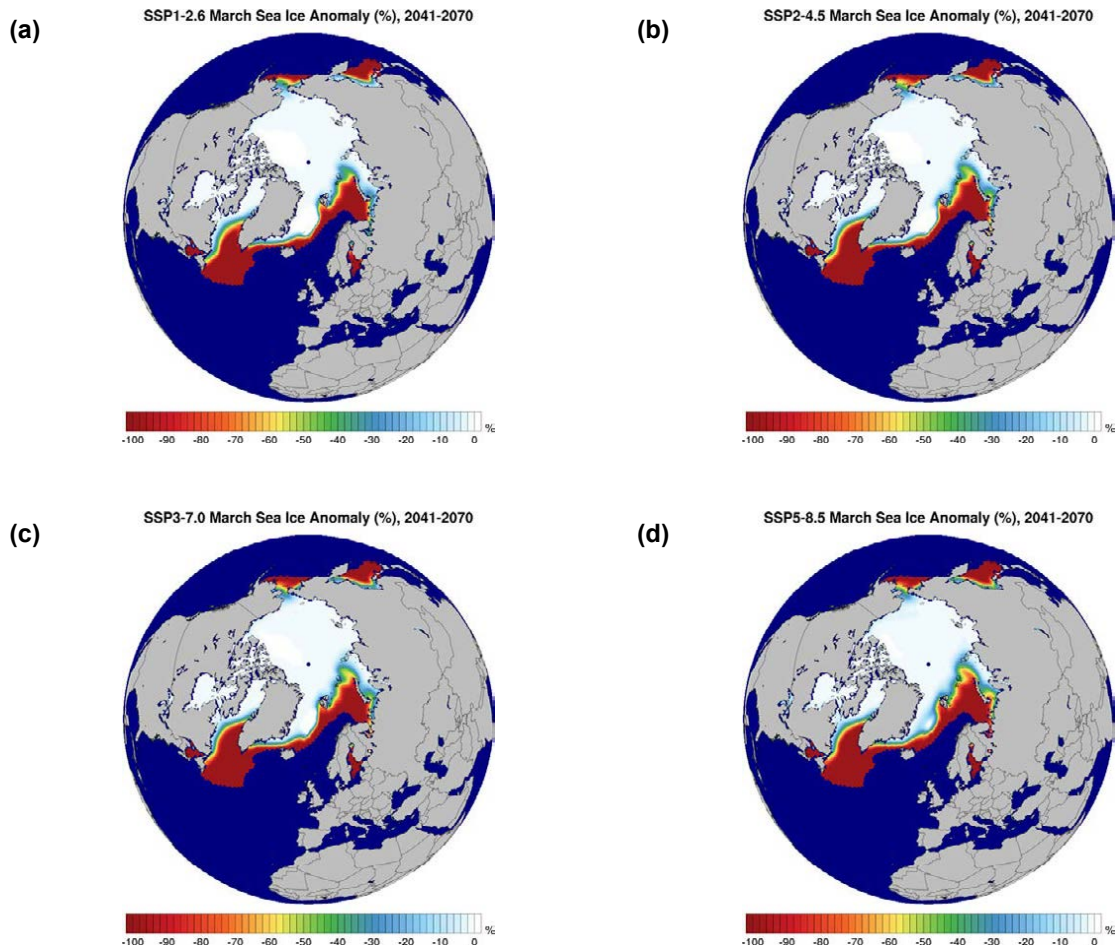


Figure 3.62. Northern Hemisphere March sea ice projections (% change) (2041–2070 vs 1981–2010): (a) SSP1–2.6, (b) SSP2–4.5, (c) SSP3–7.0 and (d) SSP5–8.5. In each case, an average is taken of the ensemble members r6i1p1f1, r9i1p1f1, r11i1p1f1, r13i1p1f1 and r15i1p1f1.

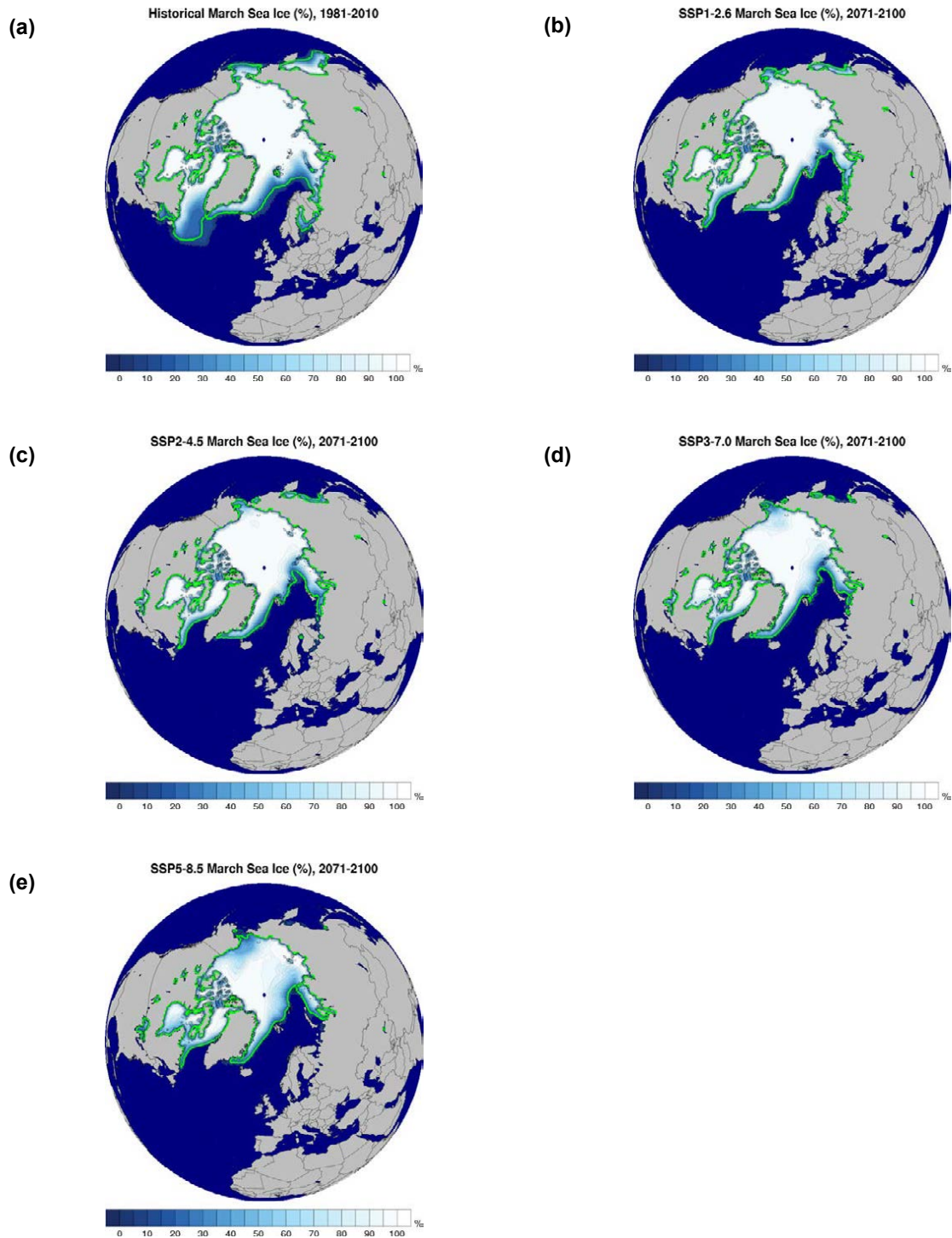


Figure 3.63. Mean Northern Hemisphere March sea ice fraction (%): (a) historical ensemble for the period 1981–2010 and (b) SSP1–2.6, (c) SSP2–4.5, (d) SSP3–7.0 and (e) SSP5–8.5 for the period 2071–2100. In each case, an average is taken of the ensemble members r6i1p1f1, r9i1p1f1, r11i1p1f1, r13i1p1f1 and r15i1p1f1. The green line shows the 15% contour line of the sea ice fraction.

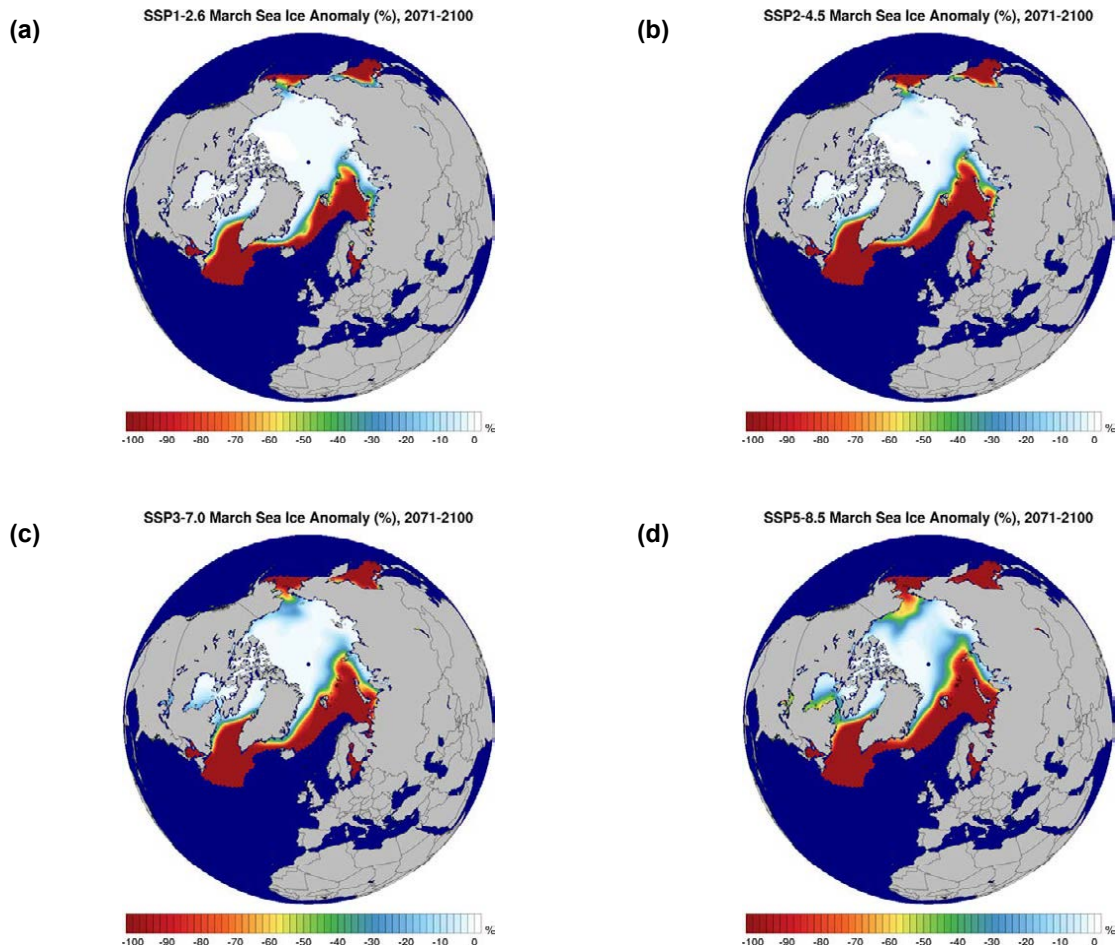


Figure 3.64. Northern Hemisphere March sea ice projections (% change) (2071–2100 vs 1981–2010): (a) SSP1–2.6, (b) SSP2–4.5, (c) SSP3–7.0 and (d) SSP5–8.5. In each case, an average is taken of the ensemble members r6i1p1f1, r9i1p1f1, r11i1p1f1, r13i1p1f1 and r15i1p1f1.

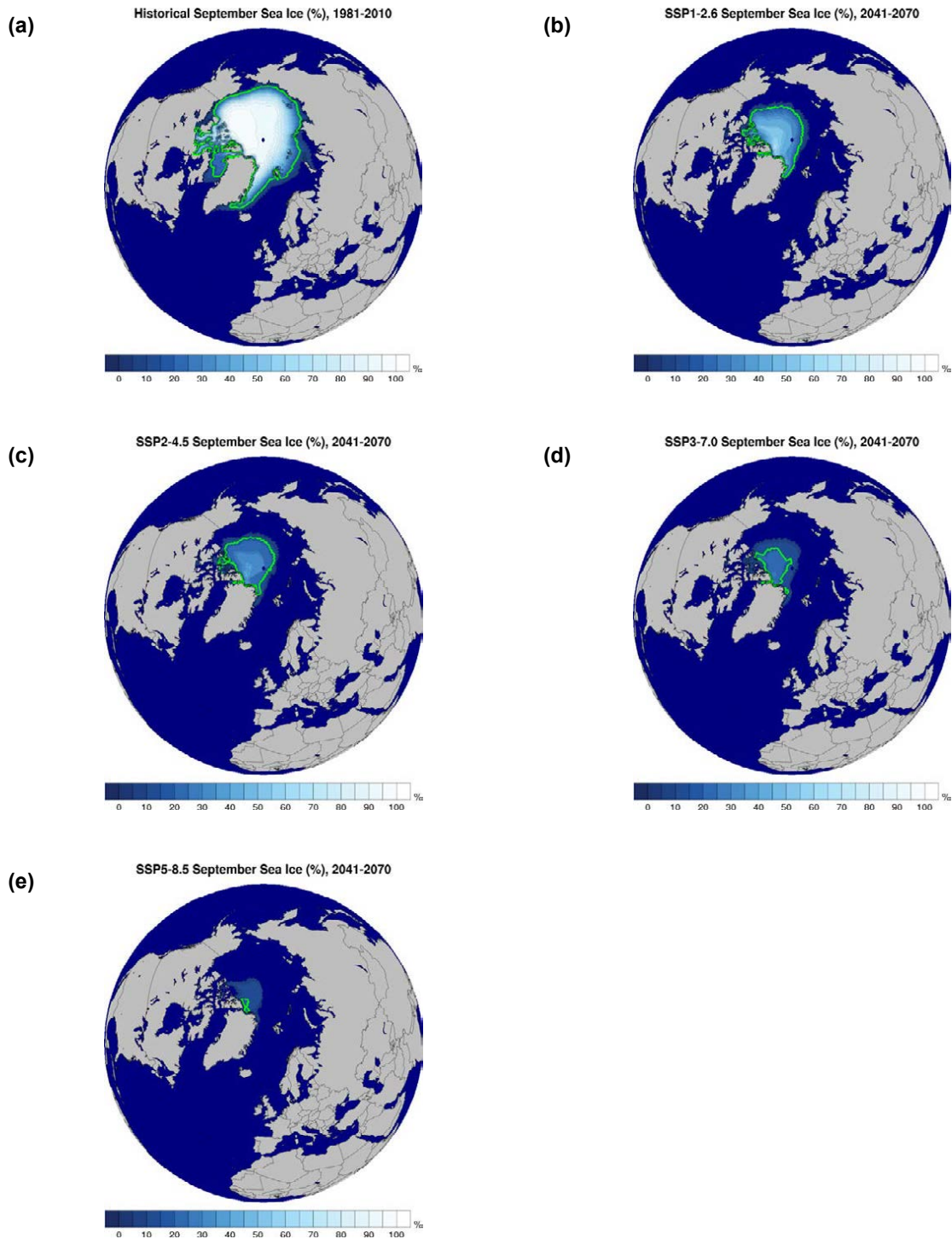


Figure 3.65. Mean Northern Hemisphere September sea ice fraction (%): (a) historical ensemble for the period 1981–2010 and (b) SSP1–2.6, (c) SSP2–4.5, (d) SSP3–7.0 and (e) SSP5–8.5 for the period 2041–2070. In each case, an average is taken of the ensemble members r6i1p1f1, r9i1p1f1, r11i1p1f1, r13i1p1f1 and r15i1p1f1. The green line shows the 15% contour line of the sea ice fraction.

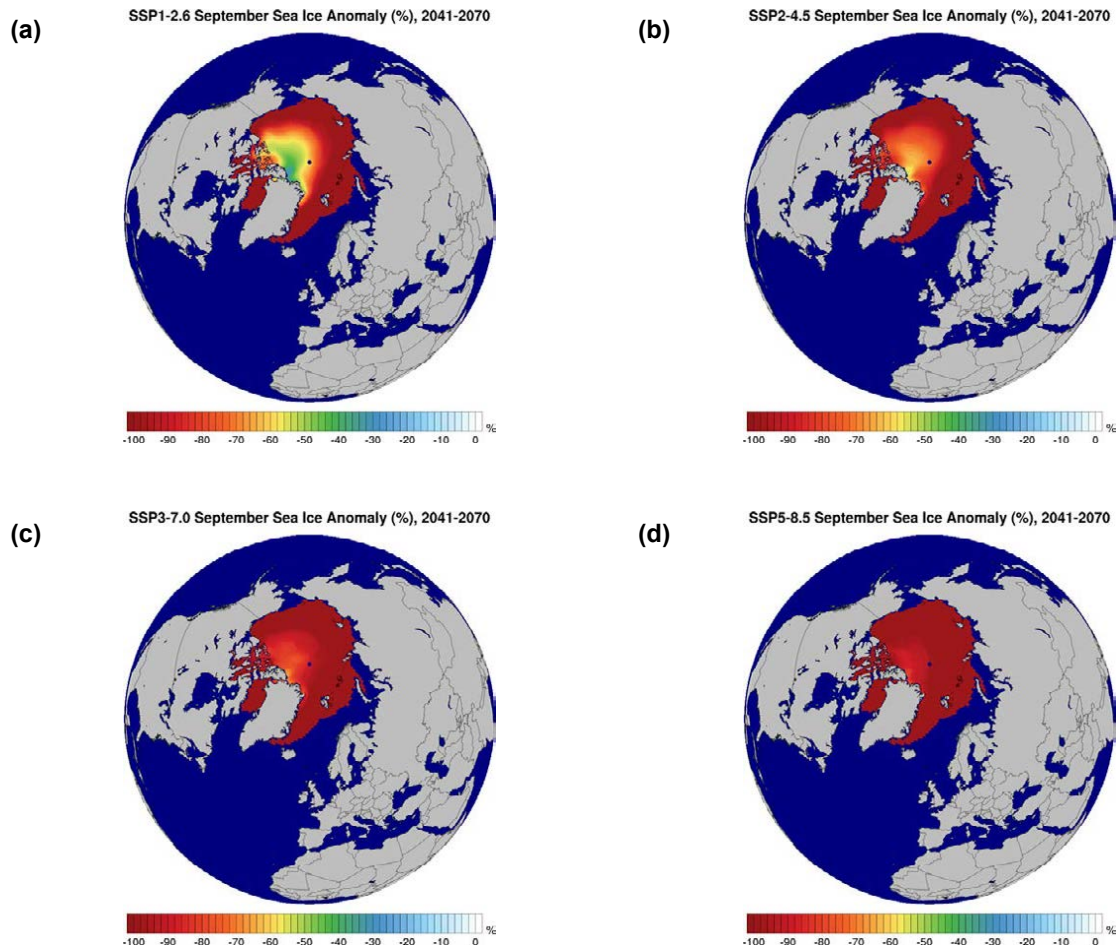


Figure 3.66. Northern Hemisphere September sea ice projections (% change) (2041–2070 vs 1981–2010): (a) SSP1–2.6, (b) SSP2–4.5, (c) SSP3–7.0 and (d) SSP5–8.5. In each case, an average is taken of the ensemble members r6i1p1f1, r9i1p1f1, r11i1p1f1, r13i1p1f1 and r15i1p1f1.

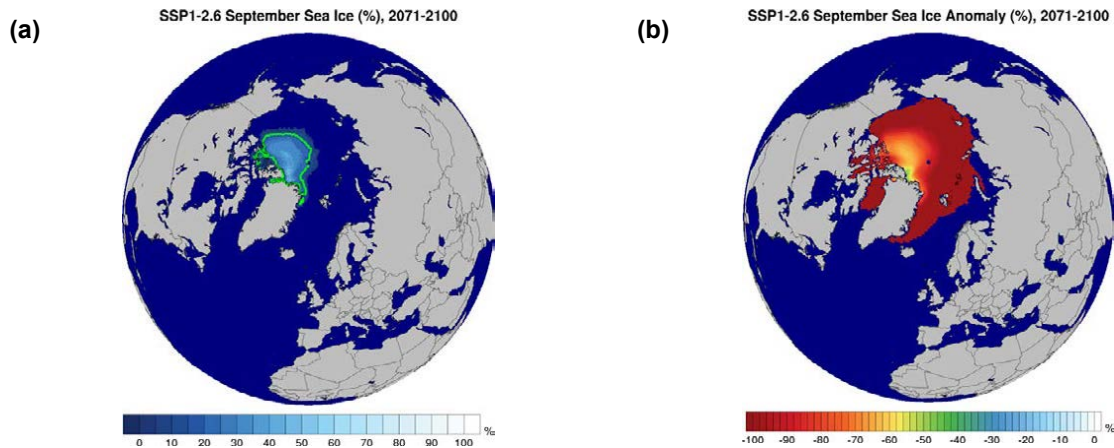


Figure 3.67. Northern Hemisphere September sea ice projections, 2071–2100: (a) SSP1–2.6 sea ice fraction (%) with green line showing the 15% contour line and (b) SSP1–2.6 anomaly relative to 1981–2010 (% change). In each case, an average is taken of the ensemble members r6i1p1f1, r9i1p1f1, r11i1p1f1, r13i1p1f1 and r15i1p1f1.

3.8.2 Southern Hemisphere sea ice projections

Similarly, Southern Hemisphere sea ice fraction projections are presented in Figures 3.68–3.78. In summary, these projections show substantial decreases in sea ice fraction over the full year (Figures 3.68–3.71). By 2071–2100, the Southern Ocean is projected to be nearly ice free during March under SSP1–2.6 and SSP2–4.5 (Figure 3.74) and completely ice free under SSP3–7.0 and SSP5–8.5. Although substantial decreases are projected for the Southern Hemisphere September sea ice extent (Figures 3.75–3.78), the changes are smaller than those in the annual and March projections.

3.8.3 Sea ice projection annual time series

The mean global annual sea ice anomalies (relative to 1981–2010) for all five historical simulations (1850–2014) and 20 SSPs (2015–2100) are presented in Figure 3.79a. The bold lines represent the ensemble means. All ensemble members show a steady decrease in global sea ice from around 2000. By the end of the century, global mean sea ice is projected to decrease by approximately 30%, 50%, 70% and 85% for SSP1–2.6, SSP2–4.5, SSP3–7.0 and SSP5–8.5, respectively. The Northern and Southern Hemisphere annual sea ice anomalies (Figures 3.79b and 3.79c, respectively) are similar to the global trend, although a larger spread between ensemble members is evident in the Southern Hemisphere.

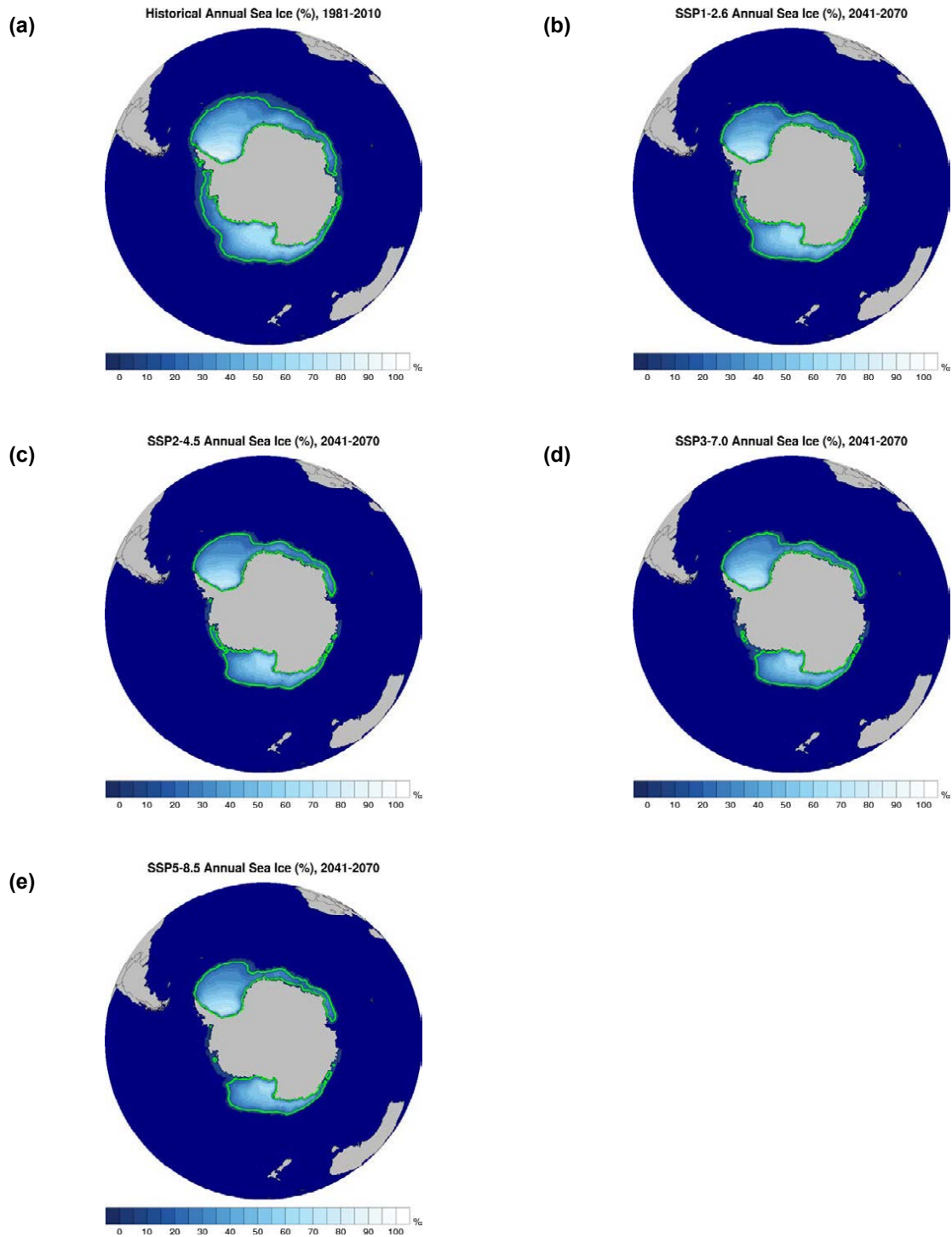


Figure 3.68. Annual mean Southern Hemisphere sea ice fraction (%): (a) historical ensemble for the period 1981–2010 and (b) SSP1–2.6, (c) SSP2–4.5, (d) SSP3–7.0 and (e) SSP5–8.5 for the period 2041–2070. In each case, an average is taken of the ensemble members r6i1p1f1, r9i1p1f1, r11i1p1f1, r13i1p1f1 and r15i1p1f1. The green line shows the 15% contour line of the sea ice fraction.

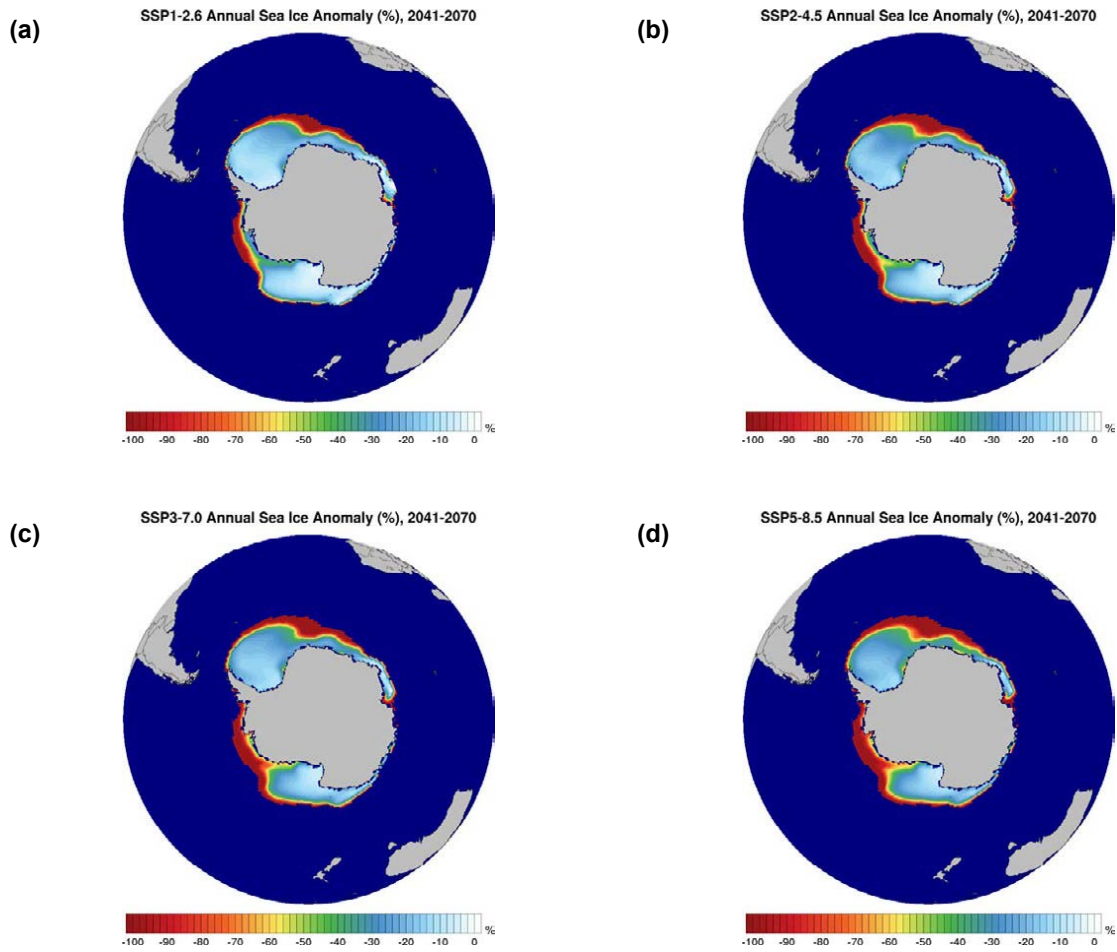


Figure 3.69. Annual Southern Hemisphere sea ice projections (% change) (2041–2070 vs 1981–2010): (a) SSP1–2.6, (b) SSP2–4.5, (c) SSP3–7.0 and (d) SSP5–8.5. In each case, an average is taken of the ensemble members r6i1p1f1, r9i1p1f1, r11i1p1f1, r13i1p1f1 and r15i1p1f1.

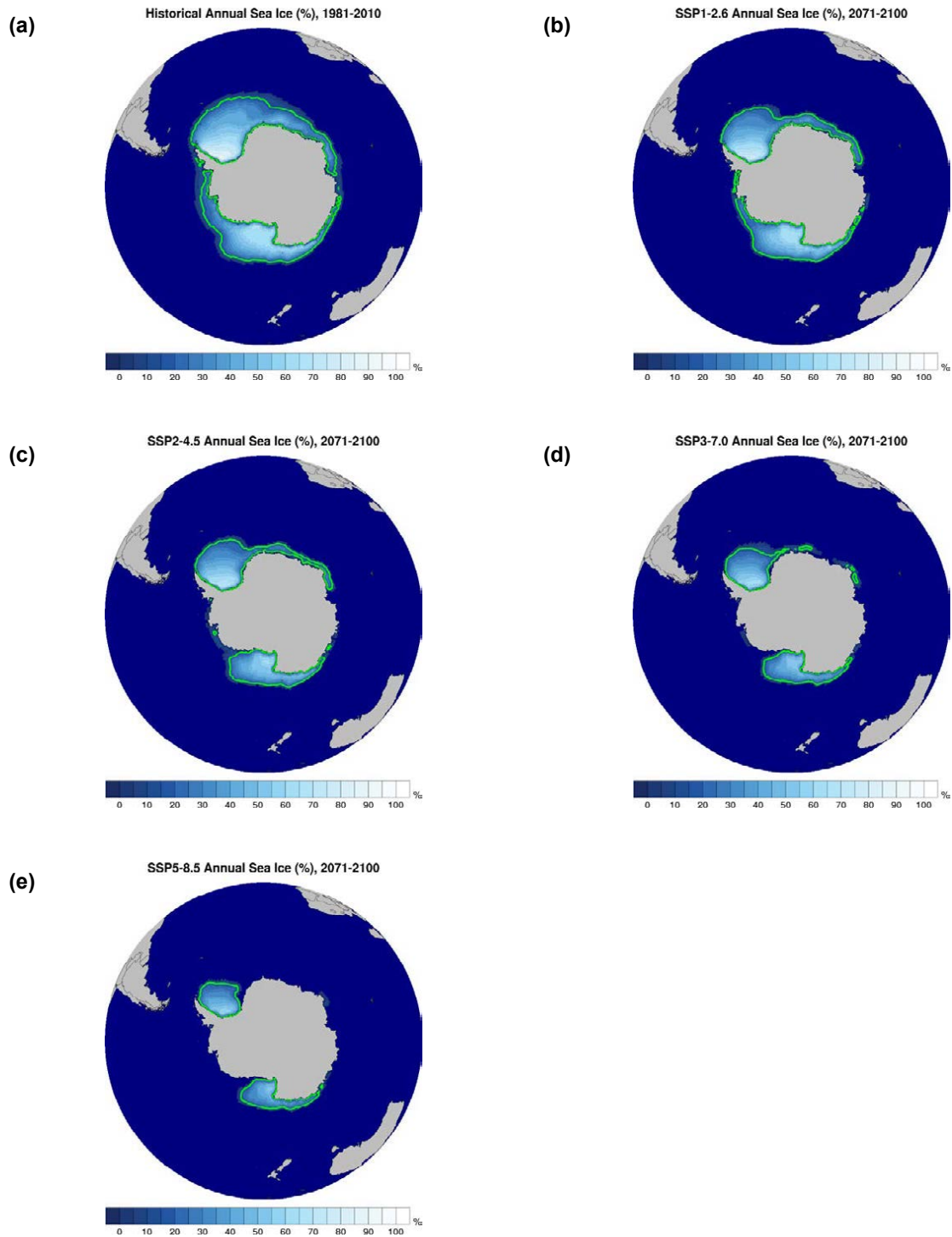


Figure 3.70. Annual mean Southern Hemisphere sea ice fraction (%): (a) historical ensemble for the period 1981–2010 and (b) SSP1–2.6, (c) SSP2–4.5, (d) SSP3–7.0 and (e) SSP5–8.5 for the period 2071–2100. In each case, an average is taken of the ensemble members r6i1p1f1, r9i1p1f1, r11i1p1f1, r13i1p1f1 and r15i1p1f1. The green line shows the 15% contour line of the sea ice fraction.

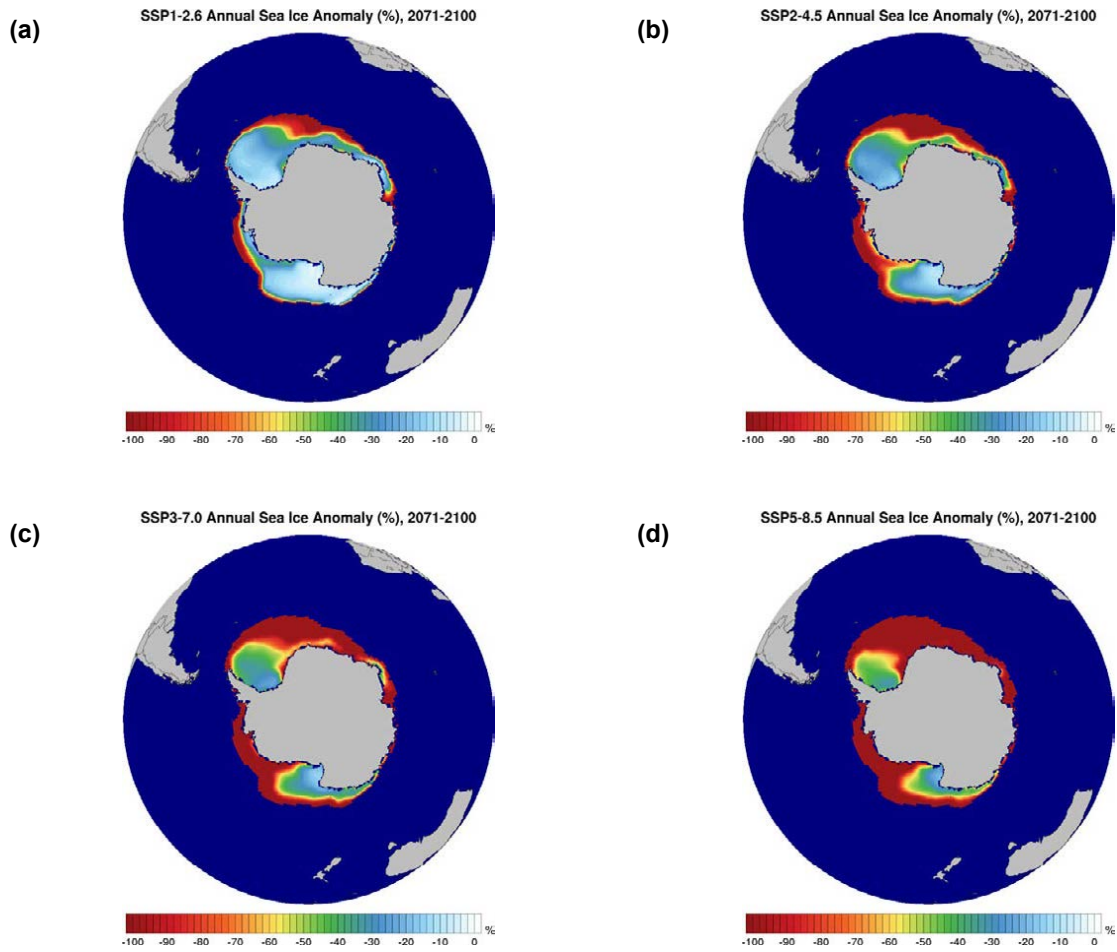


Figure 3.71. Annual Southern Hemisphere sea ice projections (% change) (2071–2100 vs 1981–2010): (a) SSP1–2.6, (b) SSP2–4.5, (c) SSP3–7.0 and (d) SSP5–8.5. In each case, an average is taken of the ensemble members r6i1p1f1, r9i1p1f1, r11i1p1f1, r13i1p1f1 and r15i1p1f1.

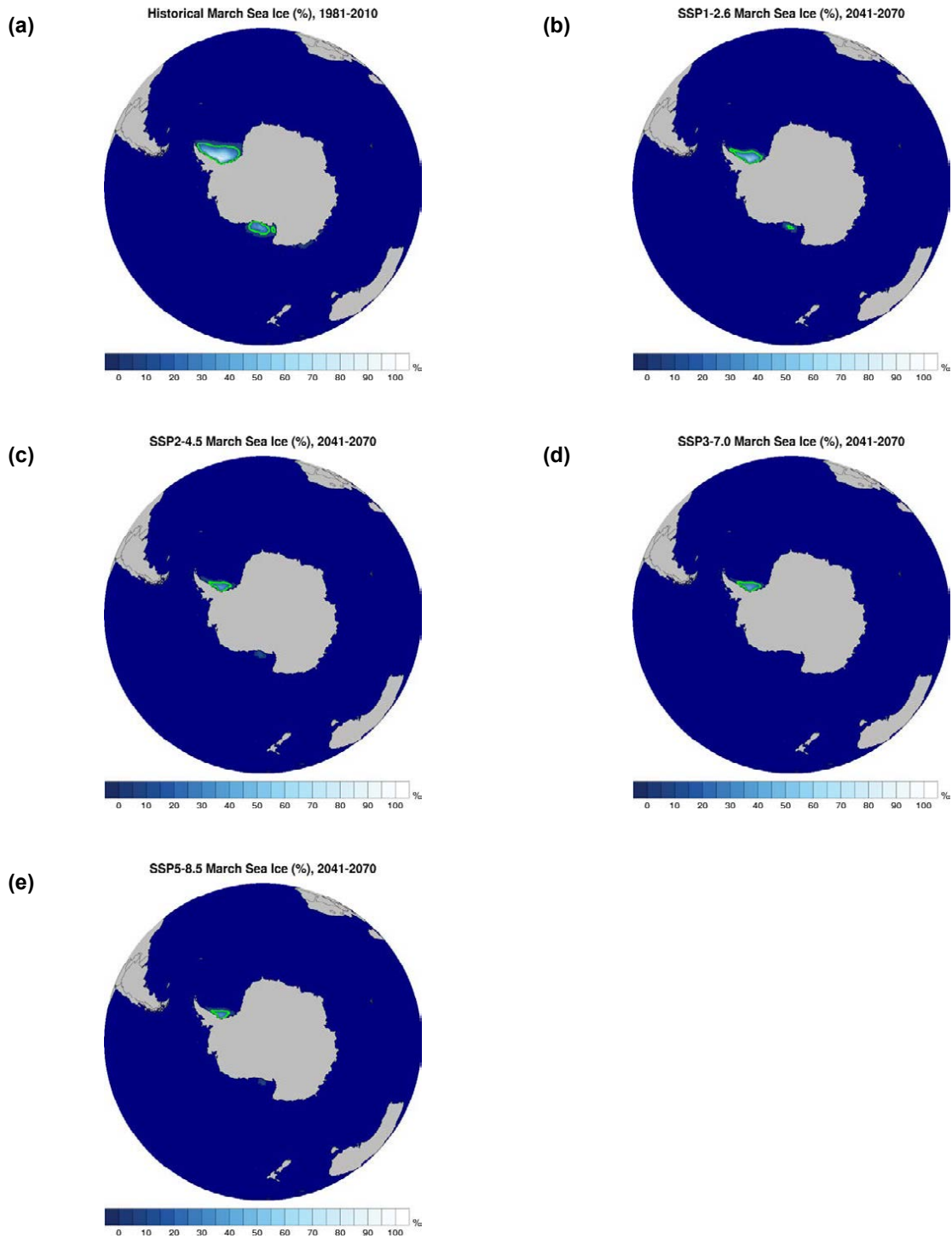


Figure 3.72. Mean Southern Hemisphere March sea ice fraction (%): (a) historical ensemble for the period 1981–2010 and (b) SSP1–2.6, (c) SSP2–4.5, (d) SSP3–7.0 and (e) SSP5–8.5 for the period 2041–2070. In each case, an average is taken of the ensemble members r6i1p1f1, r9i1p1f1, r11i1p1f1, r13i1p1f1 and r15i1p1f1. The green line shows the 15% contour line of sea ice fraction.

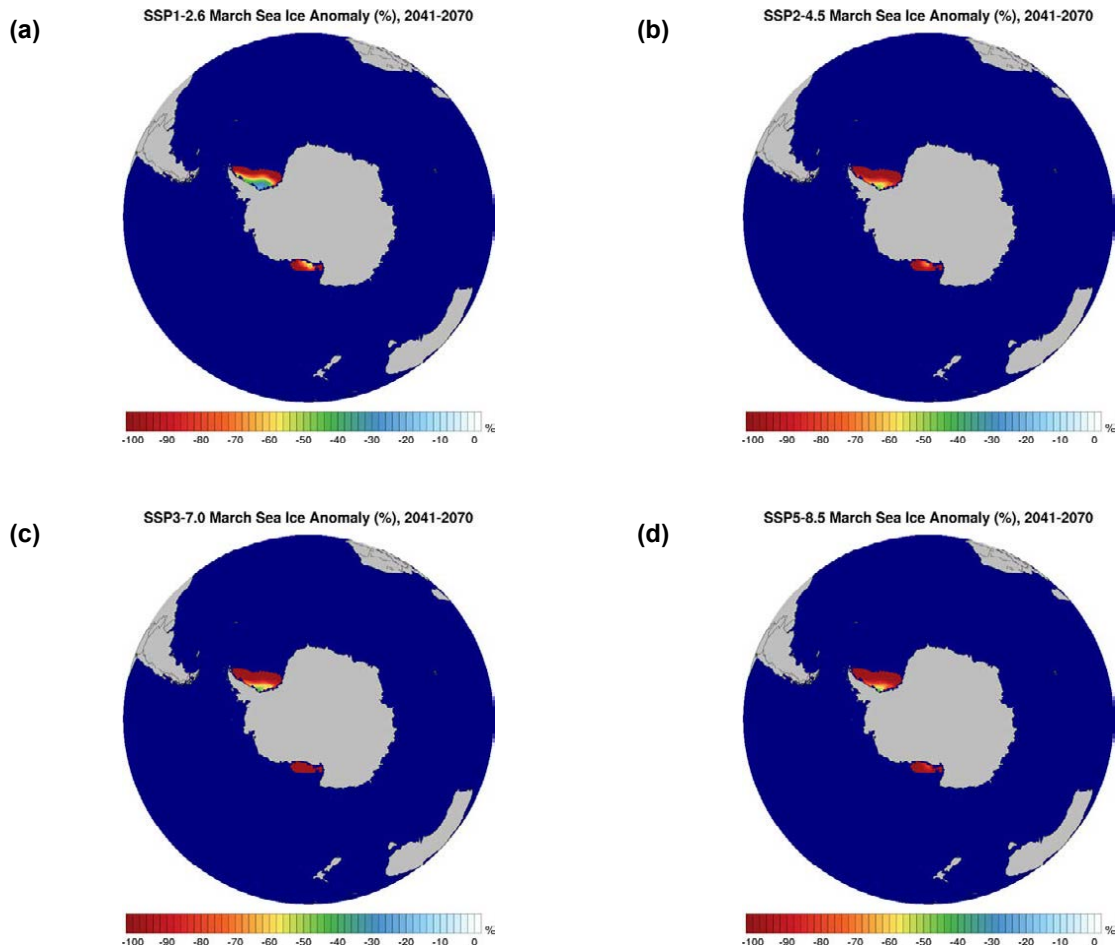


Figure 3.73. Southern Hemisphere March sea ice projections (% change) (2041–2070 vs 1981–2010): (a) SSP1–2.6, (b) SSP2–4.5, (c) SSP3–7.0 and (d) SSP5–8.5. In each case, an average is taken of the ensemble members r6i1p1f1, r9i1p1f1, r11i1p1f1, r13i1p1f1 and r15i1p1f1.

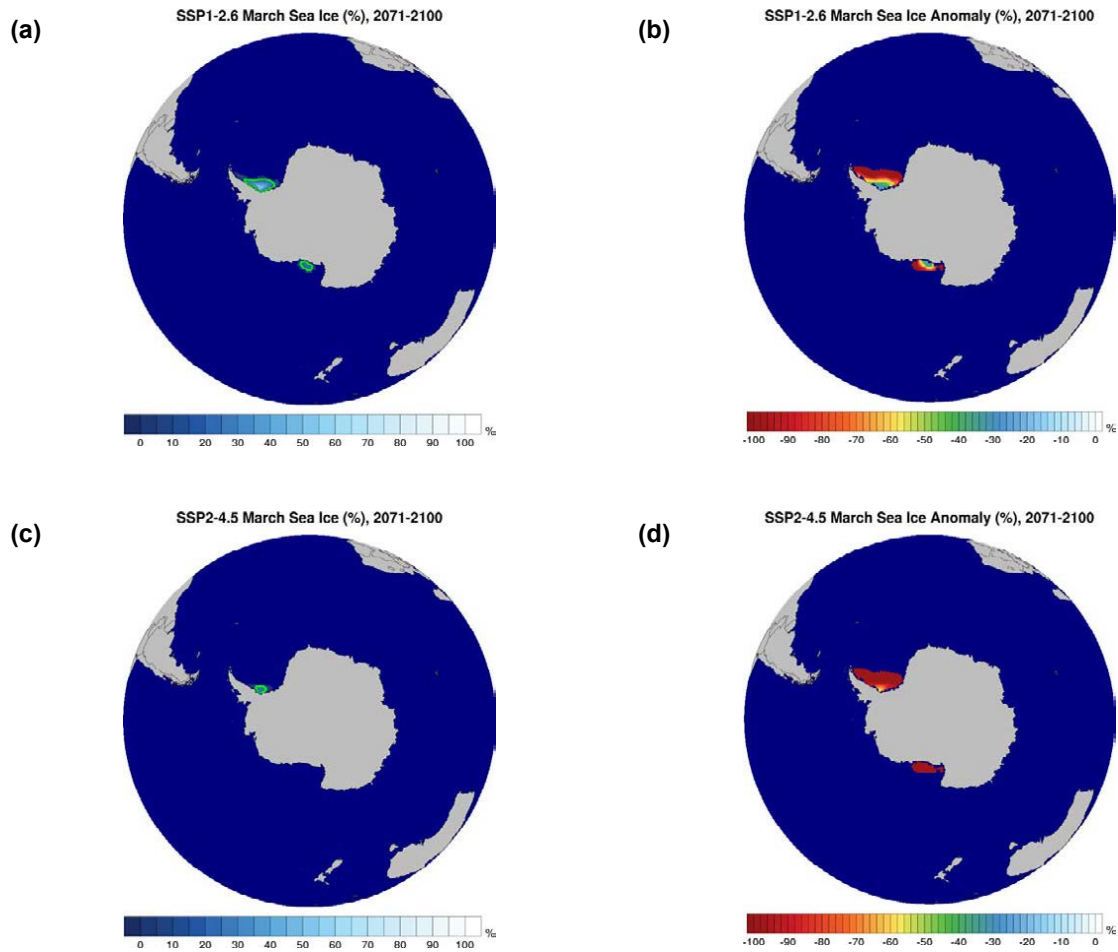


Figure 3.74. Mean Southern Hemisphere March sea ice projections, 2071–2100: (a) SSP1–2.6 sea ice fraction (%) with green line showing the 15% contour line, (b) SSP1–2.6 anomaly relative to 1981–2010 (% change), (c) SSP2–4.5 sea ice fraction (%) with green line showing the 15% contour line, (d) SSP2–4.5 anomaly relative to 1981–2010 (% change). In each case, an average is taken of the ensemble members r6i1p1f1, r9i1p1f1, r11i1p1f1, r13i1p1f1 and r15i1p1f1.

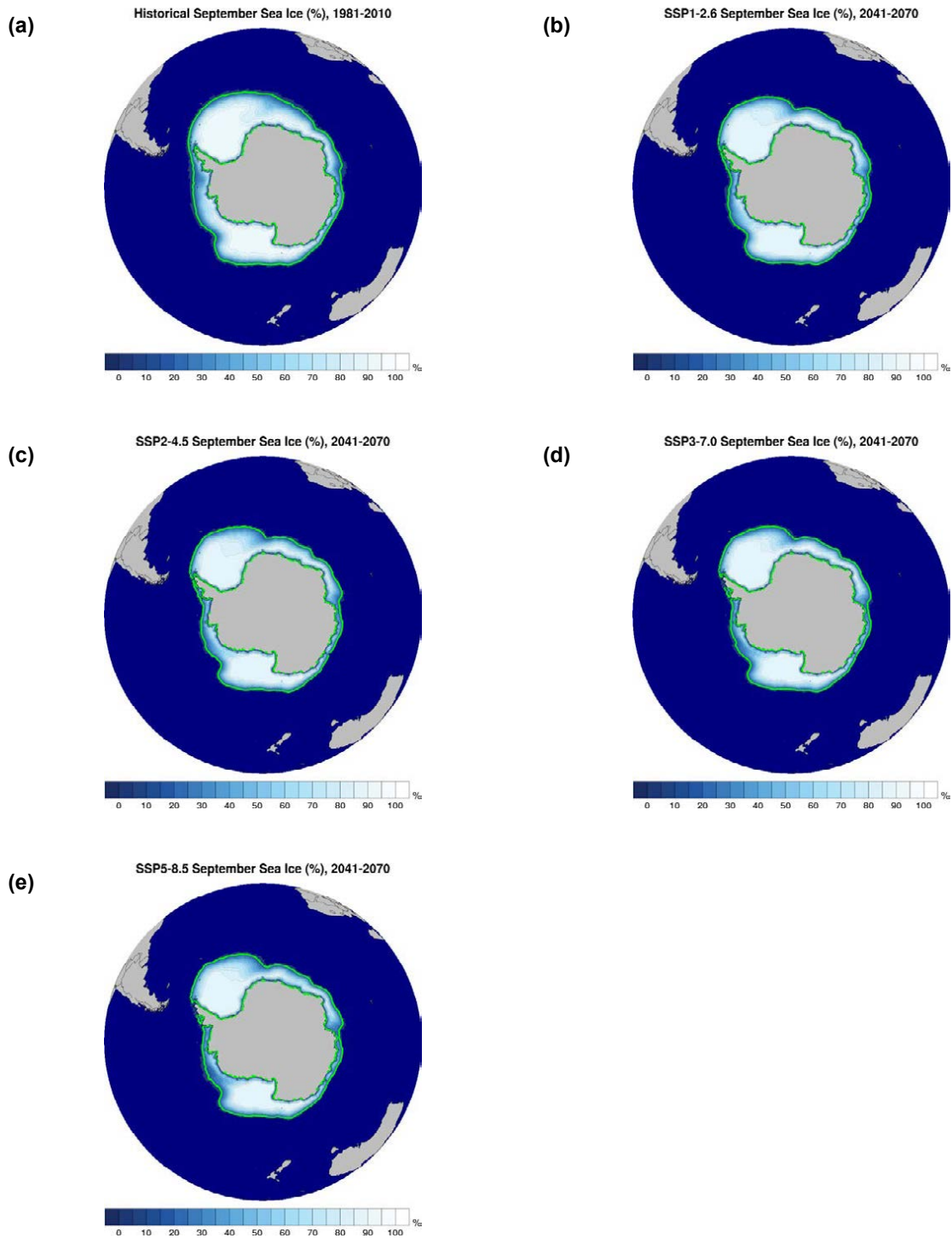


Figure 3.75. Mean Southern Hemisphere September sea ice fraction (%): (a) historical ensemble for the period 1981–2010 and (b) SSP1–2.6, (c) SSP2–4.5, (d) SSP3–7.0 and (e) SSP5–8.5 for the period 2041–2070. In each case, an average is taken of the ensemble members r6i1p1f1, r9i1p1f1, r11i1p1f1, r13i1p1f1 and r15i1p1f1. The green line shows the 15% contour line of sea ice fraction.

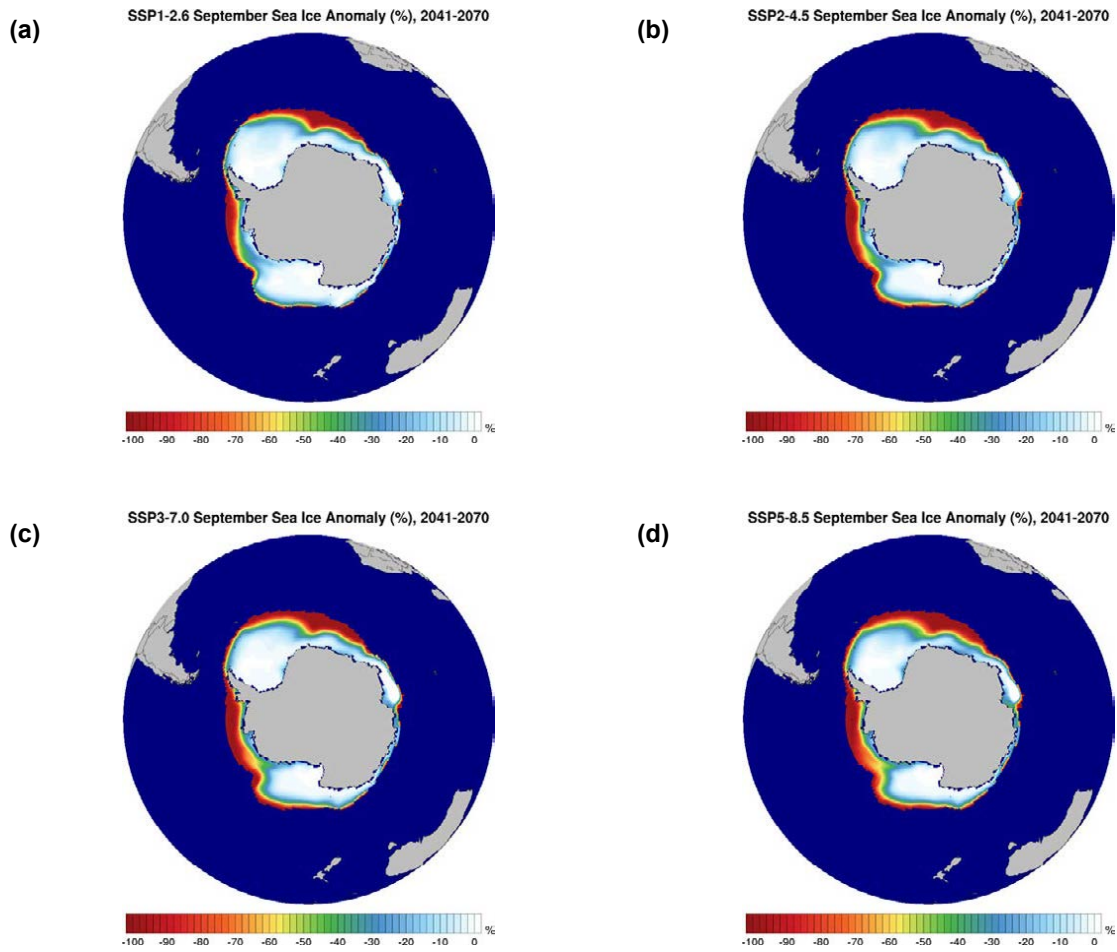


Figure 3.76. Southern Hemisphere September sea ice projections (% change) (2041–2070 vs 1981–2010): (a) SSP1–2.6, (b) SSP2–4.5, (c) SSP3–7.0 and (d) SSP5–8.5. In each case, an average is taken of the ensemble members r6i1p1f1, r9i1p1f1, r11i1p1f1, r13i1p1f1 and r15i1p1f1.

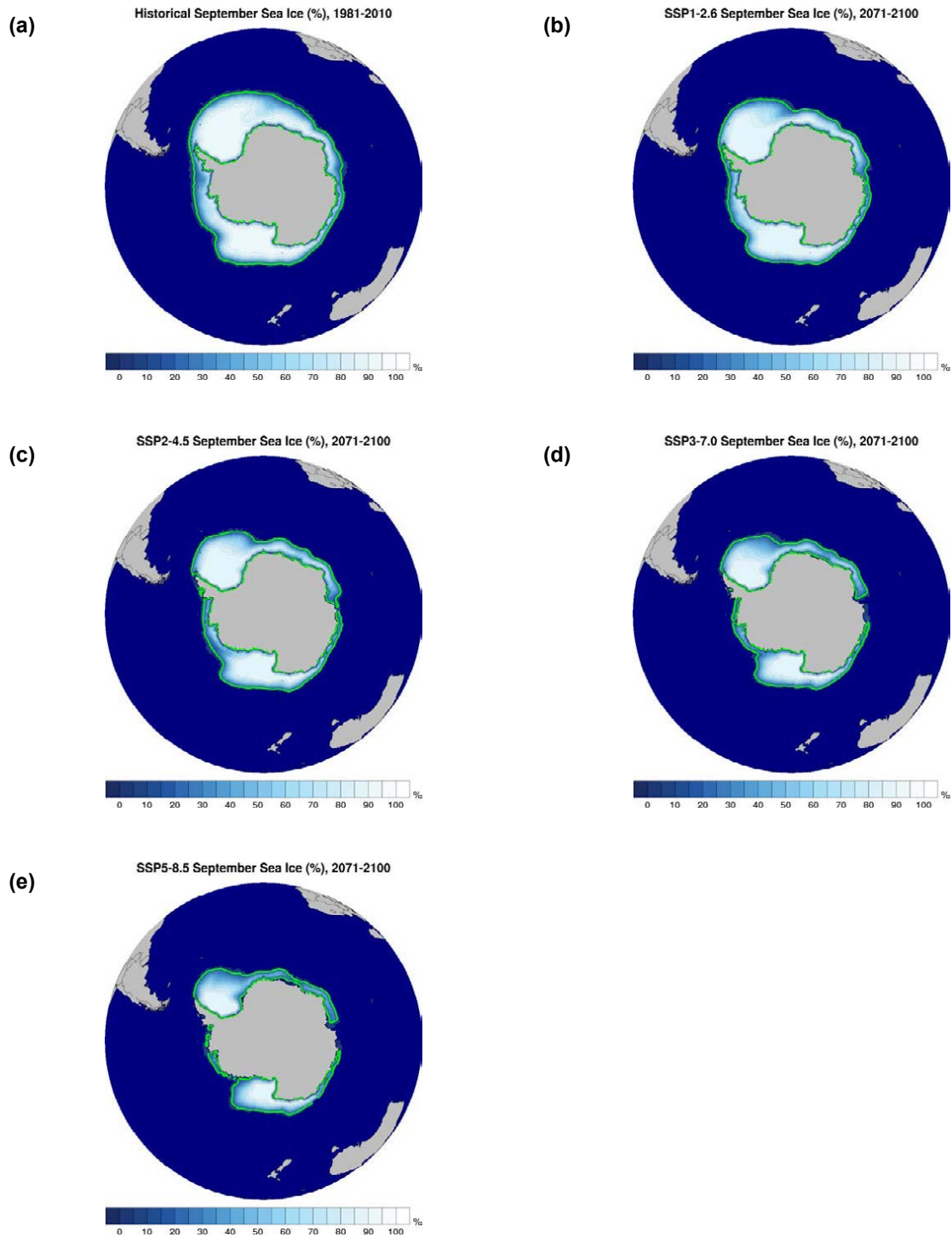


Figure 3.77. Mean Southern Hemisphere September sea ice fraction (%): (a) historical ensemble for the period 1981–2010 and (b) SSP1–2.6, (c) SSP2–4.5, (d) SSP3–7.0 and (e) SSP5–8.5 for the period 2071–2100. In each case, an average is taken of the ensemble members r6i1p1f1, r9i1p1f1, r11i1p1f1, r13i1p1f1 and r15i1p1f1. The green line shows the 15% contour line of sea ice fraction.

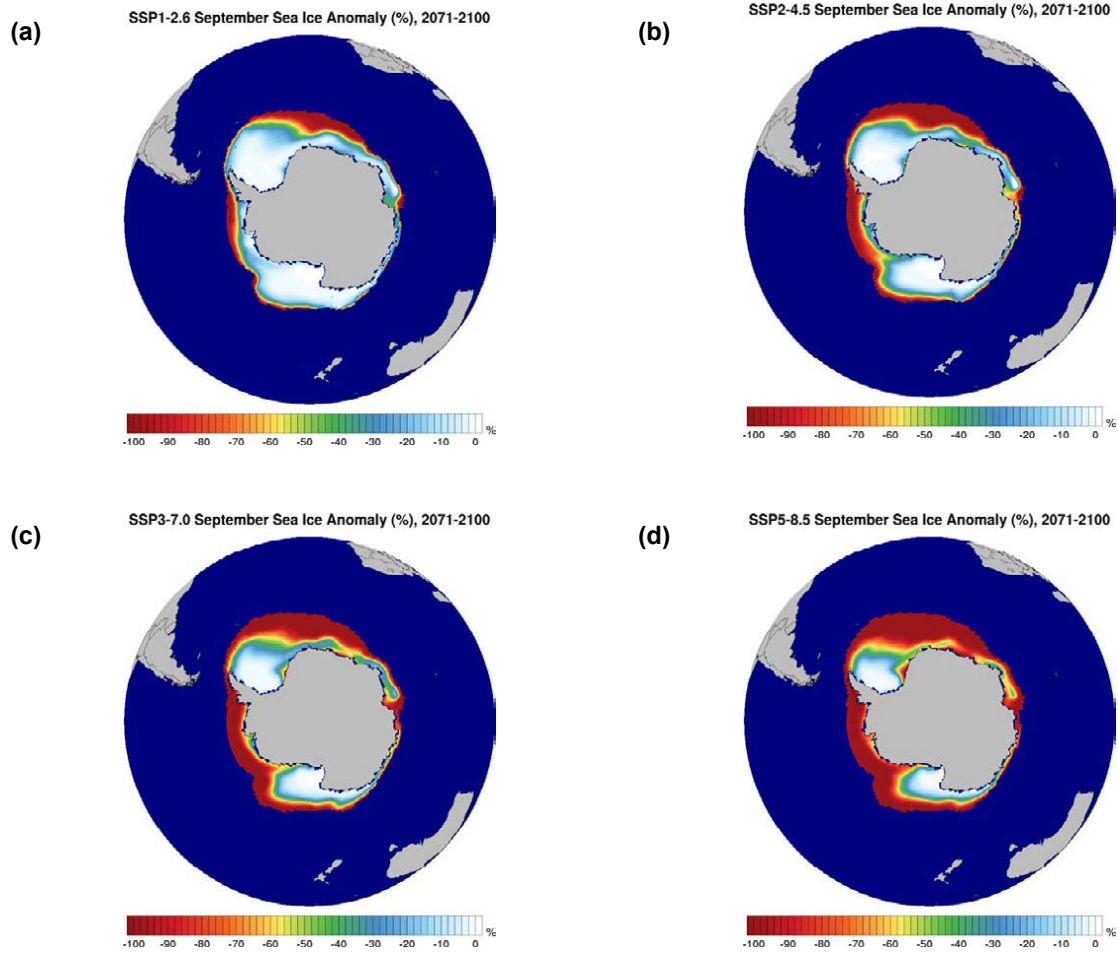


Figure 3.78. Southern Hemisphere September sea ice projections (% change) (2071–2100 vs 1981–2010): (a) SSP1–2.6, (b) SSP2–4.5, (c) SSP3–7.0 and (d) SSP5–8.5. In each case, an average is taken of the ensemble members r6i1p1f1, r9i1p1f1, r11i1p1f1, r13i1p1f1 and r15i1p1f1.

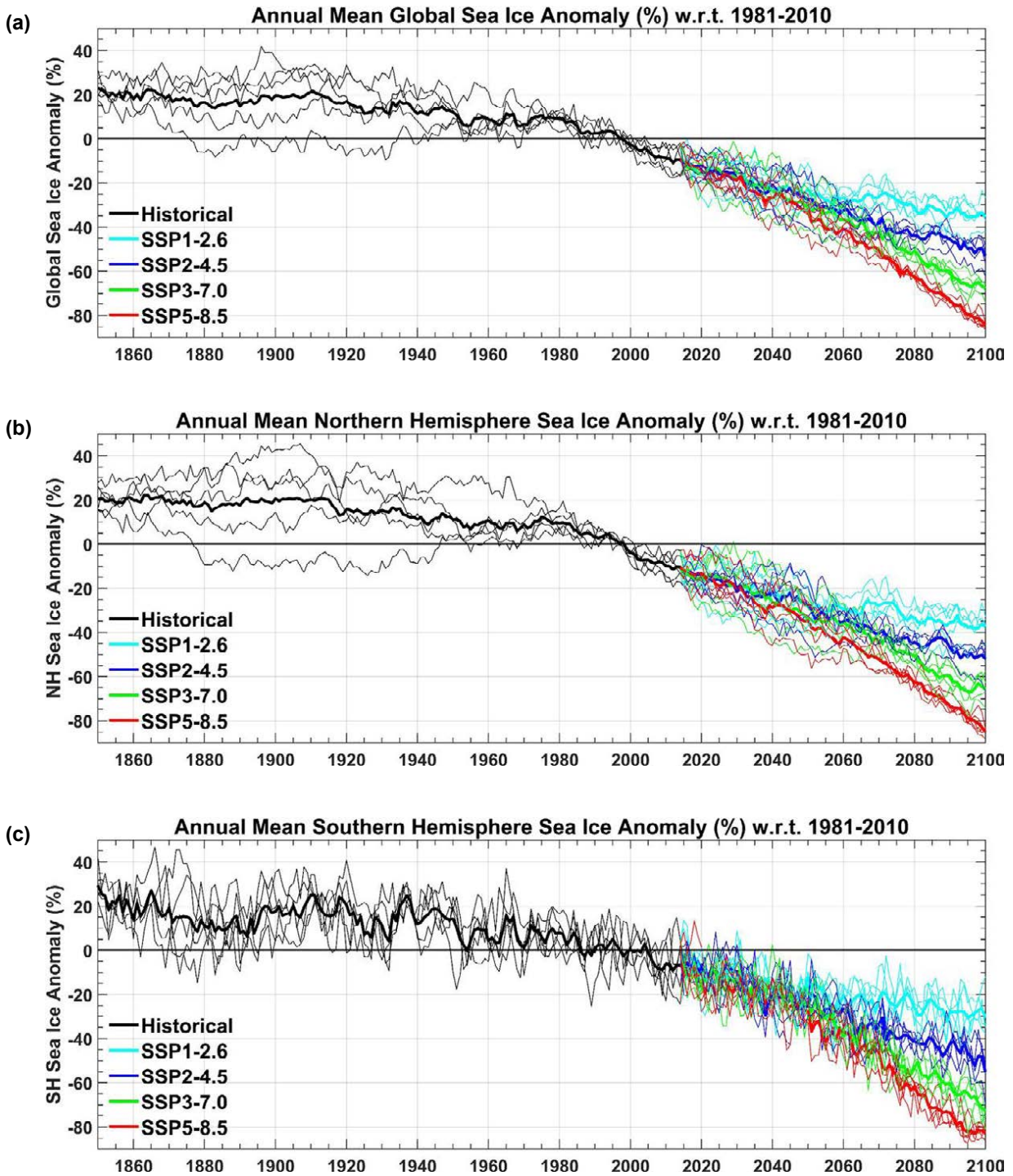


Figure 3.79. Annual sea ice anomalies (% change) with respect to the 30-year period 1981–2010: EC-Earth ensemble members r6i1p1f1, r9i1p1f1, r11i1p1f1, r13i1p1f1 and r15i1p1f1 – (a) global, (b) Northern Hemisphere and (c) Southern Hemisphere. The bold lines represent the ensemble means.

4 Recommendations

The research presented in this report focuses on Ireland's contribution to CMIP6. To date, CMIP6 participation is in the form of EC-Earth DECK CMIP (historical) and ScenarioMIP contributions. Specifically, the following CMIP6 EC-Earth contributions were run:

- five T255L91-ORCA1L75 AOGCM CMIP6 historical simulations, 1850–2014;
- 20 ScenarioMIP simulations: five T255L91-ORCA1L75 AOGCM CMIP6 for all four ScenarioMIP “tier 1” SSPs (SSP1–2.6, SSP2–4.5, SSP3–7.0 and SSP5–8.5).

It is recommended that future national CMIP contributions involve participation in the following MIPs: high-resolution (T511L91-ORCA025L75) HighResMIP and additional historical/ScenarioMIP simulations using the EC-Earth-Veg interactive vegetation configuration. Currently, the authors are managing EC-Earth-Veg contributions, comprising:

- two T255L91-ORCA1L75 EC-Earth-Veg historical simulations, 1850–2014;
- eight ScenarioMIP simulations, 2015–2100: two T255L91-ORCA1L75 EC-Earth-Veg simulations for all four ScenarioMIP “tier 1” SSPs (SSP1–2.6, SSP2–4.5, SSP3–7.0 and SSP5–8.5).

These EC-Earth-Veg simulations are complete. The data are currently being post-processed (“cmorised”) and will be hosted on the ICHEC ESGF node in March 2020. The project team will commence a number of high-resolution experiments in the near future after consultation with the EC-Earth community.

To evaluate the impact of improved models, additional earth system components and increased resolution, it is recommended that a study be undertaken to compare EC-Earth CMIP5 data with CMIP6 data. In particular, the impact on the accuracy of simulated precipitation amounts, extreme events such as heavy rain and high temperature, and storm tracks should be assessed. Preliminary validations, carried out by the EC-Earth community and the project team, confirm that the CMIP6 EC-Earth model outperforms the CMIP5 model in the simulation of the historical climate for the majority of variables analysed. A

detailed analysis of the relative capability of CMIP6 compared with CMIP5 EC-Earth data is an important and necessary next step. This work is currently being carried out by the EC-Earth consortium and the results will be presented in a peer-reviewed publication.

The analysis described in the current report should be extended to include (1) the full ensemble of EC-Earth CMIP6 simulations produced by the consortium and (2) the full CMIP6 dataset produced by the international community. This will be possible as international CMIP6 datasets become available via the ESGF over the coming months. Analysing a large ensemble will allow a robust quantification of climate projection uncertainty and a measure of confidence to be assigned to the projections. Moreover, analysis of a large ensemble will allow the construction of a probability density function of climate projections. Likelihood values can then be assigned to the projected changes. In addition, the validation and climate projection analysis should be extended to include an assessment of sea level rise, extreme events, storm tracks and derived variables, such as frost/ice days, the growing season, drought index, heavy precipitation days and evapotranspiration.

Even with modern supercomputers, running large ensembles of global climate simulations is currently feasible only with horizontal resolutions of ~50 km or coarser (the atmospheric component of the EC-Earth simulations of the current report is limited to ~79-km spatial resolution). As climate fields such as precipitation, wind speed and temperature are closely correlated with the local topography, this is inadequate to simulate the detail and pattern of climate change and its effects on the future climate of Ireland. The RCM method dynamically downscales the coarse information provided by the global models and provides high-resolution information on a subdomain covering Ireland. The computational cost of running the RCM, for a given resolution, is considerably less than that of running a global model. Numerous studies have demonstrated that high-resolution RCMs improve the simulation of fields such as precipitation (Kendon *et al.*, 2012, 2014; Lucas-Picher *et al.*, 2012; Bieniek *et al.*, 2015; Nolan *et al.*, 2017) and

topography-influenced phenomena and extremes with relatively small spatial or short temporal character (Feser *et al.*, 2011; Feser and Barcikowska, 2012; Shkol'nik *et al.*, 2012; Flato *et al.*, 2013). An additional advantage is that the physically based RCMs explicitly resolve more small-scale atmospheric features and provide a better representation of convective precipitation (Rauscher *et al.*, 2010) and extreme precipitation (Kanada *et al.*, 2008). Other examples of the added value of RCMs include improved simulation of near-surface temperatures (Feser, 2006; Di Luca *et al.*, 2016), European storm damage (Donat *et al.*, 2010), strong mesoscale cyclones (Cavicchia and von Storch, 2011), North Atlantic tropical cyclone tracks (Daloz *et al.*, 2015) and near-surface wind speeds (e.g. Kanamaru and Kanamitsu, 2007), particularly in coastal areas with complex topography (Feser *et al.*, 2011; Winterfeldt *et al.*, 2011). The IPCC has concluded that there is “high confidence that downscaling adds value to the simulation of spatial climate detail in regions with highly variable topography (e.g., distinct orography, coastlines) and for mesoscale phenomena and extremes” (Flato *et al.*, 2013). Current RCM research carried out by the project team aims to reduce climate change projection uncertainty and provide sharper estimates of expected climate change in the decades ahead. This is being achieved as follows:

- A large ensemble of high-resolution downscaled simulations will be run using the most up-to-date

RCMs (both standard and coupled atmosphere–ocean–wave models), CMIP6 GCMs and all four “tier-1” SSPs (SSP1–2.6, SSP2–4.5, SSP3–7.0 and SSP5–8.5) for the period 1979–2100.

- Additionally, the accuracy and usefulness of the model predictions will be enhanced by increasing the model resolution (<4 km).
- Furthermore, the RCM work will contribute to the CORDEX project by running the required outer nested domain of the RCM simulations on the Euro-CORDEX domains, conforming to the CORDEX standards and extending the simulation period to 1950–2100.

It should be noted that the EC-Earth ensemble member that was archived for RCM downscaling (r11i1p1f1) was shown to exhibit large biases compared with the other ensemble members in the current report. The biases were particularly evident over the North Atlantic, a region where the boundary data for downscaling over Ireland (and Europe) will be derived. To address this issue, the project team is also archiving model-level data for downscaling from the currently running EC-Earth-Veg ensemble members. Both the r11i1p1f1 and EC-Earth-Veg datasets will be downscaled over the coming months. Furthermore, it is recommended that additional CMIP6 datasets (both EC-Earth datasets and datasets provided by international research groups) are sourced for downscaling.

References

- Aumont, O., Éthé, C., Tagliabue, A., Bopp, L. and Gehlen, M., 2015. PISCES-v2: an ocean biogeochemical model for carbon and ecosystem studies. *Geoscientific Model Development Discussions* 8: 2465–2513.
- Balsamo, G., Viterbo, P., Beljaars, A.C.M., van den Hurk, B.J.J., Hirschi, M., Betts, A.K. and Scipal, K., 2009. A revised hydrology for the ECMWF model: verification from field site to terrestrial water storage and impact in the Integrated Forecast System. *Journal of Hydrometeorology* 10: 623–643. <https://doi.org/10.1175/2008JHM1068.1>.
- Bieniek, P.A., Bhatt, U.S., Walsh, J.E., Rupp, T.S., Zhang, J., Krieger, J.R. and Lader, R., 2015. Dynamical downscaling of ERA-Interim temperature and precipitation for Alaska. *Journal of Applied Meteorology and Climatology* 55: 635–654. <https://doi.org/10.1175/JAMC-D-15-0153.1>.
- C3S (Copernicus Climate Change Service), 2017. ERA5: fifth generation of ECMWF atmospheric reanalyses of the global climate. Copernicus Climate Change Service Climate Data Store (CDS). Available online: <https://confluence.ecmwf.int/display/CKB/ERA5%3A+data+documentation#ERA5:datadocumentation-HowtociteERA5> (accessed 11 February 2020).
- Camargo, S., 2013. Global and regional aspects of tropical cyclone activity in the CMIP5 models. *Journal of Climate* 26: 9880–9902. <https://doi.org/10.1175/JCLI-D-12-00549.1>
- Cavicchia, L. and von Storch, H., 2011. The simulation of medicanes in a high-resolution regional climate model. *Climate Dynamics* 39: 2273–2290.
- Chassignet, E.P. and Marshall, D.P., 2008. Gulf stream separation in numerical ocean models. In Hecht, M. and Hasumi, H. (eds), *Ocean Modelling in an Eddy Regime*, vol. 177. American Geophysical Union, Washington, DC, pp. 39–62.
- Church, J.A., Clark, P.U., Cazenave, A., Gregory, J.M., Jevrejeva, S., Levermann, A., Merrifield, M.A., Milne, G.A., Nerem, R.S., Nunn, P.D. and Payne, A.J., 2013. Sea level change. In Stocker, T.F., Qin, D., Plattner, G.-K., Tignor, M., Allen, S.K., Boschung, J., Nauels, A., Xia, Y., Bex, V. and Midgley, P.M. (eds), *Climate Change 2013: The Physical Science Basis. Contribution of Working Group I to the Fifth Assessment Report of the Intergovernmental Panel on Climate Change*. Cambridge University Press, Cambridge, pp. 1137–1216.
- Cinquini, L., Crichton, D., Mattmann, C., Harney, J., Shipman, G., Wang, F., Ananthakrishnan, R., Miller, N., Denvil, S., Morgan, M. and Pobre, Z., 2014. The Earth System Grid Federation: an open infrastructure for access to distributed geospatial data. *Future Generation Computer Systems* 36: 400–417.
- Daloz, A.S., Camargo, S.J., Kossin, J.P., Emanuel, K., Horn, M., Jonas, J.A., Kim, D., LaRow, T., Lim, Y.K., Patricola, C.M. and Roberts, M., 2015. Cluster analysis of downscaled and explicitly simulated North Atlantic tropical cyclone tracks. *Journal of Climate* 28: 1333–1361.
- DCCAE (Department of Communications, Climate Action and Environment (DCCAE), 2018. *National Adaptation Framework. Planning for a Climate Resilient Ireland*. Available online: <https://dcae.gov.ie/en-ie/climate-action/publications/Documents/10/FINAL%20National%20Adaptation%20Framework-Planning%20for%20a%20Climate%20Resilient%20Ireland.pdf> (accessed 11 February 2020).
- Demory, M.E., Vidale, P.L., Roberts, M.J., Berrisford, P., Strachan, J., Schiemann, R. and Mizielinski, M.S., 2014. The role of horizontal resolution in simulating drivers of the global hydrological cycle. *Climate Dynamics* 42: 2201–2225.
- Di Luca, A., Argüeso, D., Evans, J.P., de Elía, R. and Laprise, R., 2016. Quantifying the overall added value of dynamical downscaling and the contribution from different spatial scales. *Journal of Geophysical Research Atmospheres* 121: 1575–1590. <https://doi.org/10.1002/2015JD024009>.
- Donat, M., Leckebusch, G., Wild, S. and Ulbrich, U., 2010. Benefits and limitations of regional multi-model ensembles for storm loss estimations. *Climate Research* 44: 211–225.
- Ebi, K.L., Hallegatte, S., Kram, T., Arnell, N.W., Carter, T.R., Edmonds, J., Kriegler, E., Mathur, R., O'Neill, B.C., Riahi, K. and Winkler, H., 2014. A new scenario framework for climate change research: background, process, and future directions. *Climatic Change* 122: 363–372.
- ES-DOC (Earth System Documentation), n.d. Earth System Documentation (ES-DOC). Available online: <https://www.earthsystemcog.org/projects/es-doc-models/> (accessed 11 February 2020).
- ESGF-DOCKER, n.d. Contents. Available online: <https://esgf.github.io/esgf-docker/> (accessed 11 February 2020).

- Eyring, V., Bony, S., Meehl, G.A., Senior, C.A., Stevens, B., Stouffer, R.J. and Taylor, K.E., 2015. Overview of the Coupled Model Intercomparison Project Phase 6 (CMIP6) experimental design and organization. *Geoscientific Model Development* 9: 1937–1958.
- Fealy, R., Bruyere, C. and Duffy, C., 2018. *Regional Climate Model Simulations for Ireland for the 21st Century*. Environmental Protection Agency, Johnstown Castle, Ireland.
- Ferraro, R., Waliser, D.E., Gleckler, P., Taylor, K.E. and Eyring, V., 2015. Evolving Obs4MIPs to support phase 6 of the Coupled Model Intercomparison Project (CMIP6). *Bulletin of the American Meteorological Society* 96: ES131–ES133.
- Feser, F., 2006. Enhanced detectability of added value in limited-area model results separated into different spatial scales. *Monthly Weather Review* 134: 2180–2190.
- Feser, F. and Barcikowska, M., 2012. The influence of spectral nudging on typhoon formation in regional climate models. *Environmental Research Letters* 7: 014024.
- Feser, F., Rockel, B., von Storch, H., Winterfeldt, J. and Zahn, M., 2011. Regional climate models add value to global model data: a review and selected examples. *Bulletin of the American Meteorological Society* 92: 1181–1192.
- Flato, G., Marotzke, J., Abiodun, B., Braconnot, P., Chou, S.C., Collins, W., Cox, P., Driouech, F., Emori, S., Eyring, V. and Forest, C. (eds), 2013. *Climate Change 2013: The Physical Science Basis. Contribution of Working Group I to the Fifth Assessment Report of the Intergovernmental Panel on Climate Change*. Cambridge University Press, Cambridge.
- Gleeson, E., McGrath R. and Treanor M., 2013. *Ireland's Climate: The Road Ahead*. Met Éireann, Dublin.
- Haarsma, R.J., Hazeleger, W., Severijns, C., de Vries, H., Sterl, A., Bintanja, R., van Oldenborgh, G.J. and van den Brink, H.W., 2013. More hurricanes to hit Western Europe due to global warming. *Geophysical Research Letters* 40: 1783–1788. <https://doi.org/10.1002/grl.50360>.
- Harris, I.P.D.J., Jones, P.D., Osborn, T.J. and Lister, D.H., 2014. Updated high-resolution grids of monthly climatic observations – the CRU TS3.10 Dataset. *International Journal of Climatology* 34: 623–642.
- Hodges, K.I., Lee, R.W. and Bengtsson, L., 2011. A comparison of extratropical cyclones in recent re-analyses ERA-Interim, NASA MERRA, NCEP CFSR, JRA-25. *Journal of Climate* 24: 4888–4906.
- Huijnen, V., Williams, J.E., van Weele, M., Van Noije, T.P.C., Krol, M.C., Dentener, F.J., Segers, A., Houweling, S., Peters, W., de Laat, J. and Boersma, F., 2010. The global chemistry transport model TM5: description and evaluation of the tropospheric chemistry version 3.0. *Geoscientific Model Development* 3: 445–473.
- IPCC (Intergovernmental Panel on Climate Change), 2013a. Summary for policymakers. In Stocker, T.F., Qin, D., Plattner, G.-K., Tignor, M., Allen, S.K., Boschung, J., Nauels, A., Xia, Y., Bex, V. and Midgley, P.M. (eds), *Climate Change 2013: The Physical Science Basis. Contribution of Working Group I to the Fifth Assessment Report of the Intergovernmental Panel on Climate Change*. Cambridge University Press, Cambridge.
- IPCC (Intergovernmental Panel on Climate Change), 2013b. *Climate Change 2013: The Physical Science Basis. Contribution of Working Group I to the Fifth Assessment Report of the Intergovernmental Panel on Climate Change*. Stocker, T.F., Qin, D., Plattner, G.-K., Tignor, M., Allen, S.K., Boschung, J., Nauels, A., Xia, Y., Bex, V. and Midgley, P.M. (eds). Cambridge University Press, Cambridge.
- IPCC (Intergovernmental Panel on Climate Change), 2013c. Annex I: atlas of global and regional climate projections. van Oldenborgh, G.J., Collins, M., Arblaster, J., Christensen, J.H., Marotzke, J., Power, S.B., Rummukainen, M. and Zhou, T. (eds). In Stocker, T.F., Qin, D., Plattner, G.-K., Tignor, M., Allen, S.K., Boschung, J., Nauels, A., Xia, Y., Bex, V. and Midgley, P.M. (eds), *Climate Change 2013: The Physical Science Basis. Contribution of Working Group I to the Fifth Assessment Report of the Intergovernmental Panel on Climate Change*. Cambridge University Press, Cambridge.
- IPCC (Intergovernmental Panel on Climate Change), 2018. Summary for policymakers. In Masson-Delmotte, V., Zhai, P., Pörtner, H.-O., Roberts, D., Skea, J., Shukla, P.R., Pirani, A., Moufouma-Okia, W., Péan, C., Pidcock, R., Connors, S., Matthews, J.B.R., Chen, Y., Zhou, X., Gomis, M.I., Lonnoy, E., Maycock, T., Tignor, M. and Waterfield, T. (eds), *Global Warming of 1.5°C. An IPCC Special Report on the Impacts of Global Warming of 1.5°C above Pre-industrial Levels and Related Global Greenhouse Gas Emission Pathways, in the Context of Strengthening the Global Response to the Threat of Climate Change, Sustainable Development, and Efforts to Eradicate Poverty*. World Meteorological Organization, Geneva.

- IPCC (Intergovernmental Panel on Climate Change), 2019. Summary for policymakers. In Pörtner, H.-O., Roberts, D.C., Masson-Delmotte, V., Zhai, P., Tignor, M., Poloczanska, E., Mintenbeck, K., Alegría, A., Nicolai, M., Okem, A., Petzold, J., Rama, B. and Weyer, N.M. (eds), *IPCC Special Report on the Ocean and Cryosphere in a Changing Climate*. Available online: https://www.ipcc.ch/site/assets/uploads/sites/3/2019/12/02_SROCC_FM_FINAL.pdf (accessed 1 March 2020).
- Jung, T., Miller, M.J., Palmer, T.N., Towers, P., Wedi, N., Achuthavarier, D., Adams, J.M., Altshuler, E.L., Cash, B.A., Kinter III, J.L. and Marx, L., 2012. High-resolution global climate simulation with the ECMWF model in project Athena: experimental design, model climate, and seasonal forecast skill. *Journal of Climate* 25: 3155–3172.
- Kanada, S., Nakano, M., Hayashi, S., Kato, T., Nakamura, M., Kurihara, K. and Kitoh, A., 2008. Reproducibility of maximum daily precipitation amount over Japan by a high-resolution non-hydrostatic model. *Sola* 4: 105–108.
- Kanamaru, H. and Kanamitsu, M., 2007. Fifty-seven-year California reanalysis downscaling at 10 km (CaRD10). Part II: comparison with North American regional reanalysis. *Journal of Climate* 20: 5572–5592.
- Kendon, E., Roberts, N., Senior, C. and Roberts, M., 2012. Realism of rainfall in a very high-resolution regional climate model. *Journal of Climate* 25: 5791–5806.
- Kendon, E.J., Roberts, N.M., Fowler, H.J., Roberts, M.J., Chan, S.C. and Senior, C.A., 2014. Heavier summer downpours with climate change revealed by weather forecast resolution model. *Nature Climate Change* 4: 570–576.
- Kriegler, E., Edmonds, J., Hallegatte, S., Ebi, K.L., Kram, T., Riahi, K., Winkler, H. and Van Vuuren, D.P., 2014. A new scenario framework for climate change research: the concept of shared climate policy assumptions. *Climatic Change* 122: 401–414.
- Kuwano-Yoshida, A., Minobe, S. and Xie, S.P., 2010. Precipitation response to the gulf stream in an atmospheric GCM. *Journal of Climate* 23: 3676–3698.
- Lucas-Picher, P., Wulff-Nielsen, M., Christensen, J.H., Aðalgeirsdóttir, G., Mottram, R. and Simonsen, S.B., 2012. Very high resolution regional climate model simulations over Greenland: identifying added value. *Journal of Geophysical Research* 117: D02108.
- Madec, G. and the NEMO team, 2008. NEMO ocean engine. Note du Pôle de modélisation de Institut Pierre-Simon Laplace, No. 27. Available online: <https://www.nemo-ocean.eu/doc/> (accessed 13 February 2020).
- Marvel, K., Cook, B.I., Bonfils, C.J.W., Durack, P.J., Smerdon, J.E. and Park Williams, A., 2019. Twentieth-century hydroclimate changes consistent with human influence. *Nature* 569: 59–65.
- Massonnet, F., Ménegoz, M., Acosta, M., Yepes-Arbós, X., Exarchou, E. and Doblas-Reyes, F.J., 2019. Replicability of the EC-Earth3 Earth System Model under a change in computing environment. *Geoscientific Model Development*. <https://doi.org/10.5194/gmd-2019-91>
- Molteni, F., Stockdale, T., Balmaseda, M., Balsamo, G., Buizza, R., Ferranti, L., Magnusson, L., Mogensen, K., Palmer, T. and Vitart, F., 2011. *The New ECMWF Seasonal Forecast System (System 4)*, vol. 49. European Centre for Medium-Range Weather Forecasts, Reading.
- Moss, R.H., Edmonds, J.A., Hibbard, K.A., Manning, M.R., *et al.*, 2010. The next generation of scenarios for climate change research and assessment. *Nature* 463: 747–756
- Nolan, P., 2015. *Ensemble of Regional Climate Model Projections for Ireland*. Environmental Protection Agency, Johnstown Castle, Ireland.
- Nolan, P., Lynch, P. and Sweeney, C., 2014. Simulating the future wind energy resource of Ireland using the COSMO-CLM model. *Wind Energy* 17: 19–37.
- Nolan, P., O’Sullivan, J. and McGrath, R., 2017. Impacts of climate change on mid-twenty-first-century rainfall in Ireland: a high-resolution regional climate model ensemble approach. *International Journal of Climatology* 37: 4347–4363.
- O’Neill, B.C., Kriegler, E., Riahi, K., Ebi, K.L., Hallegatte, S., Carter, T.R., Mathur, R. and van Vuuren, D.P., *et al.*, 2014. A new scenario framework for climate change research: the concept of shared socioeconomic pathways. *Climatic Change* 122: 387–400.
- O’Neill, B.C., Tebaldi, C., van Vuuren, D.P., Eyring, V., Friedlingstein, P., Hurtt, G., Knutti, R., Kriegler, E., Lamarque, J.F., Lowe, J. and Meehl, G.A., 2016. The scenario model intercomparison project (ScenarioMIP) for CMIP6. *Geoscientific Model Development* 9: 3461–3482.
- O’Sullivan J., Sweeney C., Nolan P. and Gleeson E., 2015. A high-resolution, multi-model analysis of Irish temperatures for the mid 21st-century. *International Journal of Climatology* 36: 1256–1267.
- Rauscher, S.A., Coppola, E., Piani, C. and Giorgi, F., 2010. Resolution effects on regional climate model simulations of seasonal precipitation over Europe. *Climate Dynamics* 35: 685–711.

- Riahi, K., Van Vuuren, D.P., Kriegler, E., Edmonds, J., O'Neill, B.C., Fujimori, S., Bauer, N., Calvin, K., Dellink, R., Fricko, O. and Lutz, W., 2017. The shared socioeconomic pathways and their energy, land use, and greenhouse gas emissions implications: an overview. *Global Environmental Change* 42: 153–168.
- Roberts, M.J., Clayton, A., Demory, M.E., Donners, J., Vidale, P.L., Norton, W., Shaffrey, L., Stevens, D.P., Stevens, I., Wood, R.A. and Slingo, J., 2009. Impact of resolution on the tropical pacific circulation in a matrix of coupled models. *Journal of Climate* 22: 2541–2556.
- Rousset, C., Vancoppenolle, M., Madec, G., Fichefet, T., Flavoni, S., Barthélemy, A., Benshila, R., Chanut, J., Lévy, C., Masson, S. and Vivier, F., 2015. The Louvain-la-Neuve sea ice model LIM3. 5: global and regional capabilities. *Geoscientific Model Development* 8: 3403–3441.
- Shaffrey, L., Stevens, I., Norton, W.A., Roberts, M.J., Vidale, P.L., Harle, J.D., Jrrar, A., Stevens, D.P., Woodage, M.J., Demory, M.E. and Donners, J.B.C.D., 2009. UK HiGEM: the new UK High-Resolution Global Environment Model – model description and basic evaluation. *Journal of Climate* 22: 1861–1896.
- Shkol'nik, I., Meleshko, V., Efimov, S. and Stafeeva E., 2012. Changes in climate extremes on the territory of Siberia by the middle of the 21st century: an ensemble forecast based on the MGO regional climate model. *Russian Meteorology and Hydrology* 37: 71–84.
- Sillmann, J., Kharin, V.V., Zhang, X., Zwiers, F.W. and Bronaugh, D., 2013. Climate extremes indices in the CMIP5 multimodel ensemble: part 1. Model evaluation in the present climate. *Journal of Geophysical Research Atmospheres* 118: 1716–1733.
- Small, C. and Nichols, R.J., 2003. A global analysis of human settlement in coastal zones. *Journal of Coastal Research* 19: 584–599.
- Smith, B., Wärlind, D., Arneth, A., Hickler, T., Leadley, P., Siltberg, J. and Zaehle, S., 2014. Implications of incorporating N cycling and N limitations on primary production in an individual-based dynamic vegetation model. *Biogeosciences* 11: 2027–2054.
- Taylor, K.E., Stouffer, R.J. and Meehl, G.A., 2012. An overview of CMIP5 and the experiment design. *Bulletin of the American Meteorological Society* 93: 485–498.
- Taylor, K.E., Juckes, M., Balaji, V., Cinquini, L., Denvil, S., Durack, P.J., Elkington, M., Guilyardi, E., Kharin, S., Lautenschlager, M., Lawrence, B., Nadeau, D. and Stockhause, M., 2018. CMIP6 global attributes, DRS, filenames, directory structure, and CV's. Document version 6.2.7. Available online: <https://goo.gl/v1drZI> (accessed 13 February 2020).
- van Vuuren, D.P., Edmonds, J., Kainuma, M., Riahi, K., Thomson, A., Hibbard, K., Hurtt, G.C., Kram, T., Krey, V., Lamarque, J.F. and Masui, T., 2011. The representative concentration pathways: an overview. *Climatic Change* 109: 5.
- van Vuuren, D.P., Kriegler, E., O'Neill, B.C., Ebi, K.L., Riahi, K., Carter, T.R., Edmonds, J., Hallegatte, S., Kram, T., Mathur, R. and Winkler, H., 2014. A new scenario framework for climate change research: scenario matrix architecture. *Climatic Change* 122: 373–386.
- Vousdoukas, M.I., Mentaschi, L., Voukouvalas, E., Bianchi, A., Dottori F. and Feyen, L., 2018. Climatic and socioeconomic controls of future coastal flood risk in Europe. *Nature Climate Change* 8: 776–780.
- Wehner, M.F., Smith, R.L., Bala, G. and Duffy, P., 2010. The effect of horizontal resolution on simulation of very extreme us precipitation events in a global atmosphere model. *Climate Dynamics* 24: 241–247.
- Winterfeldt, J., Geyer, B. and Weisse, R., 2011. Using QuikSCAT in the added value assessment of dynamically downscaled wind speed. *International Journal of Climatology* 31: 1028–1039.
- WMO (World Meteorological Organization), 2013. *The Global Climate 2001–2010: A Decade of Climate Extremes: Summary Report*. Available online: https://library.wmo.int/doc_num.php?explnum_id=7802 (accessed 11 February 2020).
- Zappa G., Shaffrey, L.C. and Hodges, K.I., 2013. The ability of CMIP5 models to simulate North Atlantic extratropical cyclones. *Journal of Climate* 26: 5379–5396.
- Zhao, M., Held, I.M., Lin, S.J. and Vecchi, G.A., 2009. Simulations of global hurricane climatology, interannual variability, and response to global warming using a 50km resolution GCM. *Journal of Climate* 33: 6653–6678.

Abbreviations

AOGCM	Atmosphere–Ocean General Circulation Model
AR5	Fifth Assessment Report
AR6	Sixth Assessment Report
CMIP	Coupled Model Intercomparison Project
CORDEX	Coordinated Regional Downscaling Experiment
CRU	Climatic Research Unit
DCPP	Decadal Climate Prediction Project
DECK	Diagnostic, Evaluation and Characterization of Klima
DJF	December, January and February
DKRZ	German Climate Computing Centre
ECMWF	European Centre for Medium-Range Weather Forecast
ELPIN	Exclude Land Processes in NEMO
ESGF	Earth System Grid Federation
ESM	Earth system model
GCM	Global climate model
GMSL	Global mean sea level
GSLR	Global sea level rise
HPC	High-performance computing
ICHEC	Irish Centre for High-End Computing
IFS	Integrated Forecast System
IPCC	Intergovernmental Panel on Climate Change
ITCZ	Intertropical Convergence Zone
JJA	June, July and August
KNMI	Royal Netherlands Meteorological Institute
LIM3	Louvain-la-Neuve sea ice model
LPJ-GUESS	Lund-Potsdam-Jena General Ecosystem Simulator
MAE	Mean absolute error
MAM	March, April and May
MIP	Model Intercomparison Project
MSLP	Mean sea level pressure
NEMO	Nucleus for European Modelling of the Ocean
P2P	Peer-to-Peer
PISCES	Pelagic Interactions Scheme for Carbon and Ecosystem Studies
RCM	Regional climate model
RCP	Representative concentration pathway
SON	September, October and November
SSP	Shared socioeconomic pathway
SST	Sea surface temperature
TM5	Tracer Model version 5

AN GHNÍOMHAIREACHT UM CHAOMHNÚ COMHSHAOIL

Tá an Gníomhaireacht um Chaomhnú Comhshaoil (GCC) freagrach as an gcomhshaoil a chaomhnú agus a fheabhsú mar shócmhainn luachmhar do mhuintir na hÉireann. Táimid tiomanta do dhaoine agus don chomhshaoil a chosaint ó éifeachtaí díobhálacha na radaíochta agus an truaillithe.

Is féidir obair na Gníomhaireachta a roinnt ina trí phríomhréimse:

Rialú: Déanaimid córais éifeachtacha rialaithe agus comhlionta comhshaoil a chur i bhfeidhm chun torthaí maithe comhshaoil a sholáthar agus chun díriú orthu siúd nach gcloíonn leis na córais sin.

Eolas: Soláthraimid sonraí, faisnéis agus measúnú comhshaoil atá ar ardchaighdeán, spríodhíre agus tráthúil chun bonn eolais a chur faoin gcinnteoireacht ar gach leibhéal.

Tacaíocht: Bimid ag saothrú i gcomhar le grúpaí eile chun tacú le comhshaoil atá glan, táirgiúil agus cosanta go maith, agus le hiompar a chuirfidh le comhshaoil inbhuanaithe.

Ár bhFreagrachtaí

Ceadúnú

Déanaimid na gníomhaíochtaí seo a leanas a rialú ionas nach ndéanann siad dochar do shláinte an phobail ná don chomhshaoil:

- saoráidí dramhaíola (*m.sh. láithreáin líonta talún, loisceoirí, stáisiúin aistriúcháin dramhaíola*);
- gníomhaíochtaí tionsclaíocha ar scála mór (*m.sh. déantúsaíocht cógaisíochta, déantúsaíocht stroighne, stáisiúin chumhachta*);
- an diantalmhaíocht (*m.sh. muca, éanlaith*);
- úsáid shrianta agus scaoileadh rialaithe Orgánach Géinmhodhnaithe (*OGM*);
- foinsí radaíochta ianúcháin (*m.sh. trealamh x-gha agus radaiteiripe, foinsí tionsclaíocha*);
- áiseanna móra stórála peitрил;
- scardadh dramhuisece;
- gníomhaíochtaí dumpála ar farraige.

Forfheidhmiú Náisiúnta i leith Cúrsaí Comhshaoil

- Clár náisiúnta iniúchtaí agus cigireachtaí a dhéanamh gach bliain ar shaoráidí a bhfuil ceadúnas ón nGníomhaireacht acu.
- Maoirseacht a dhéanamh ar fhreagrachtaí cosanta comhshaoil na n-údarás áitiúil.
- Caighdeán an uisce óil, arna sholáthar ag soláthraithe uisce phoiblí, a mhaoirsiú.
- Obair le húdarás áitiúla agus le gníomhaireachtaí eile chun dul i ngleic le coireanna comhshaoil trí chomhordú a dhéanamh ar líonra forfheidhmiúcháin náisiúnta, trí dhírú ar chiontóirí, agus trí mhaoirsiú a dhéanamh ar leasúchán.
- Cur i bhfeidhm rialachán ar nós na Rialachán um Dhramhthrealamh Leictreach agus Leictreonach (DTLL), um Shrian ar Shubstaintí Guaiseacha agus na Rialachán um rialú ar shubstaintí a ídionn an ciseal ózóin.
- An dlí a chur orthu siúd a bhriseann dlí an chomhshaoil agus a dhéanann dochar don chomhshaoil.

Bainistíocht Uisce

- Monatóireacht agus tuairisciú a dhéanamh ar cháilíocht aibhneacha, lochanna, uisce idirchriosacha agus cósta na hÉireann, agus screamhuisec; leibhéal uisce agus sruthanna aibhneacha a thomhas.
- Comhordú náisiúnta agus maoirsiú a dhéanamh ar an gCreat-Treoir Uisce.
- Monatóireacht agus tuairisciú a dhéanamh ar Cháilíocht an Uisce Snámha.

Monatóireacht, Anailís agus Tuairisciú ar an gComhshaoil

- Monatóireacht a dhéanamh ar cháilíocht an aeir agus Treoir an AE maidir le hAer Glan don Eoraip (CAFÉ) a chur chun feidhme.
- Tuairisciú neamhspleách le cabhrú le cinnteoireacht an rialtais náisiúnta agus na n-údarás áitiúil (*m.sh. tuairisciú tréimhsiúil ar staid Chomhshaoil na hÉireann agus Tuarascálacha ar Tháscairí*).

Rialú Astaíochtaí na nGás Ceaptha Teasa in Éirinn

- Fardail agus réamh-mheastacháin na hÉireann maidir le gáis ceaptha teasa a ullmhú.
- An Treoir maidir le Trádáil Astaíochtaí a chur chun feidhme i gcomhar breis agus 100 de na táirgeoirí dé-ocsaíde carbóin is mó in Éirinn.

Taighde agus Forbairt Comhshaoil

- Taighde comhshaoil a chistiú chun brúnna a shainathint, bonn eolais a chur faoi bheartais, agus réitigh a sholáthar i réimsí na haeráide, an uisce agus na hinbhuanaitheachta.

Measúnacht Straitéiseach Timpeallachta

- Measúnacht a dhéanamh ar thionchar pleananna agus clár beartaithe ar an gcomhshaoil in Éirinn (*m.sh. mórphleananna forbartha*).

Cosaint Raideolaíoch

- Monatóireacht a dhéanamh ar leibhéal radaíochta, measúnacht a dhéanamh ar nochtadh mhuintir na hÉireann don radaíocht ianúcháin.
- Cabhrú le pleananna náisiúnta a fhorbairt le haghaidh éigeandálaí ag eascairt as tairmí núicléacha.
- Monatóireacht a dhéanamh ar fhorbairtí thar lear a bhaineann le saoráidí núicléacha agus leis an tsábháilteacht raideolaíochta.
- Sainseirbhísí cosanta ar an radaíocht a sholáthar, nó maoirsiú a dhéanamh ar sholáthar na seirbhísí sin.

Treoir, Faisnéis Inrochtana agus Oideachas

- Comhairle agus treoir a chur ar fáil d'earnáil na tionsclaíochta agus don phobal maidir le hábhair a bhaineann le caomhnú an chomhshaoil agus leis an gcosaint raideolaíoch.
- Faisnéis thráthúil ar an gcomhshaoil ar a bhfuil fáil éasca a chur ar fáil chun rannpháirtíocht an phobail a spreagadh sa chinnteoireacht i ndáil leis an gcomhshaoil (*m.sh. Timpeall an Tí, léarscáileanna radóin*).
- Comhairle a chur ar fáil don Rialtas maidir le hábhair a bhaineann leis an tsábháilteacht raideolaíoch agus le cúrsaí práinnfhreagartha.
- Plean Náisiúnta Bainistíochta Dramhaíola Guaisí a fhorbairt chun dramhaíl ghuaiseach a chosaint agus a bhainistiú.

Múscailt Feasachta agus Athrú Iompraíochta

- Feasacht chomhshaoil níos fearr a ghiniúint agus dul i bhfeidhm ar athrú iompraíochta dearfach trí thacú le gnóthais, le pobail agus le teaghlaigh a bheith níos éifeachtúla ar acmhainní.
- Tástáil le haghaidh radóin a chur chun cinn i dtithe agus in ionaid oibre, agus gníomhartha leasúcháin a spreagadh nuair is gá.

Bainistíocht agus struchtúr na Gníomhaireachta um Chaomhnú Comhshaoil

Tá an ghníomhaíocht á bainistiú ag Bord Iáinimseartha, ar a bhfuil Ard-Stiúrthóir agus cúigear Stiúrthóirí. Déantar an obair ar fud cúig cinn d'Oifigí:

- An Oifig um Inmharthanacht Comhshaoil
- An Oifig Forfheidhmithe i leith cúrsaí Comhshaoil
- An Oifig um Fianaise is Measúnú
- Oifig um Chosaint Radaíochta agus Monatóireachta Comhshaoil
- An Oifig Cumarsáide agus Seirbhísí Corparáideacha

Tá Coiste Comhairleach ag an nGníomhaireacht le cabhrú léi. Tá dáréag comhaltáí air agus tagann siad le chéile go rialta le plé a dhéanamh ar ábhair inní agus le comhairle a chur ar an mBord.

Authors: Paul Nolan and Alastair McKinstry

This report provides an overview of future global climate projections as simulated by the EC-Earth Earth system model. In total, five historical (1850–2014) and 20 simulations of future climate across a full range of emissions pathways (2015–2100) were run and analysed. Model-level data were archived allowing for regional downscaling using regional climate models. The simulations comprise Ireland's contribution to the Coupled Model Intercomparison Project (phase 6) (CMIP6) and will be included for assessment in the United Nations Intergovernmental Panel on Climate Change (IPCC) Sixth Assessment (AR6) reports.

Identifying Pressures

It is now accepted beyond doubt that historical and future greenhouse gas emissions and changing land use had and will have a significant effect on the Earth's climate. The IPCC Fifth Assessment (AR5) report concluded that "warming of the climate system is unequivocal, and since the 1950s, many of the observed changes are unprecedented over decades to millennia". Furthermore, it is extremely likely (95–100% probability) that human influence was the dominant cause of global warming between 1951 and 2010. The United Nations has declared that the world experienced more unprecedented high-impact climate extremes in the first decade of the 21st century than in any previous decade. Understanding of the potential for additional climate change needs to be continually refined, improved and updated to reflect the best available science and emerging understanding of global social and economic development and exploit the advances in information technologies.

Informing Policy

Accurate climate projections, produced by climate models, can assist policymakers to plan for and adapt to the adverse effects of climate change. The EC-Earth CMIP6 data, produced as part of this report, provide sharper and more accurate projections of the future global climate and will lead to a better understanding

not only of the physical climate system but also of the climate impact on societies. The EC-Earth data will assist in addressing all three of the CMIP6 broad scientific questions and a number of the grand challenges of the World Climate Research Programme. The datasets will enhance the overall understanding of anthropogenic climate change on a global scale and will assist in presenting a case for a follow on to national targets, such as the United Nations COP21 Paris Agreement. This study ensures that Ireland remains at the forefront of global climate change research and continues its involvement with the Coordinated Regional Climate Downscaling Experiment (CORDEX) and CMIP6 and IPCC AR6 reports.

Developing Solutions

All CMIP6 EC-Earth data were published on the Irish Centre for High-End Computing (ICHEC) Earth System Grid Federation (ESGF) node. ESGF is an international collaboration between climate centres with a mission to support CMIP6 and future IPCC assessments. The data produced as part of the current report will be analysed by the international research community for inclusion in the upcoming IPCC AR6 reports. In addition, the EC-Earth simulation data will be used as a basis for more focused regional climate impact studies, such as national downscaling projects and the international CORDEX research community.